

## Natural Swarms in 3.99 Dimensions

Andrea Cavagna,<sup>1,2</sup> Luca Di Carlo,<sup>2,1</sup> Irene Giardina,<sup>2,1,3</sup> Tomás S. Grigera,<sup>4,5,6</sup>  
Stefania Melillo,<sup>1,2</sup> Leonardo Parisi,<sup>1,2</sup> Giulia Pisegna,<sup>2,1</sup> and Mattia Scandolo<sup>2,1</sup>

<sup>1</sup>*Istituto Sistemi Complessi, Consiglio Nazionale delle Ricerche, 00185 Rome, Italy*

<sup>2</sup>*Dipartimento di Fisica, Università Sapienza, 00185 Rome, Italy*

<sup>3</sup>*INFN, Unità di Roma 1, 00185 Rome, Italy*

<sup>4</sup>*Instituto de Física de Líquidos y Sistemas Biológicos CONICET - Universidad Nacional de La Plata, La Plata, Argentina*

<sup>5</sup>*CCT CONICET La Plata, Consejo Nacional de Investigaciones Científicas y Técnicas, Argentina*

<sup>6</sup>*Departamento de Física, Facultad de Ciencias Exactas, Universidad Nacional de La Plata, Argentina*

The dynamical critical exponent  $z$  of natural swarms of insects is calculated using the renormalization group to order  $\epsilon = 4 - d$ . A novel fixed point emerges, where both off-equilibrium activity and mode-coupling inertial interactions are relevant. In three dimensions the critical exponent at the new fixed point is  $z = 1.3$ , in fair agreement with experiments.

Collective behaviour is found in a startling variety of biological systems, across a range of spatial and temporal scales, from clusters of bacteria and colonies of cells, up to insect swarms, bird flocks, and vertebrate groups [1]. A unifying ingredient, which also provides a connection to statistical physics, is the presence of strong correlations: experiments in bird flocks [2], fish schools [3], mammal herds [4], insect swarms [5], bacterial clusters [6, 7] and proteins [8] have found that the correlation length,  $\xi$ , is significantly larger than the microscopic scales. In some instances,  $\xi$  scales with the system's size, giving rise to scale-free correlations [2, 7, 9]. Strikingly, another key hallmark of statistical physics, namely dynamic scaling [10, 11], has been verified in the case of natural swarms of insects [12]. Dynamic scaling is noteworthy, as it entangles spatial and temporal relaxation into one simple law, known as *critical slowing down* [11]: the collective relaxation time scales as a power of the correlation length,  $\tau \sim \xi^z$ , thus defining the dynamical critical exponent,  $z$ .

Within statistical physics, strong correlations and scaling laws are the two stepping stones leading to the Renormalization Group (RG): when we coarse-grain short-wavelength fluctuations, the parameters of different models flow towards one common fixed point ruling their large-scale behaviour. RG fixed points therefore organise into few universality classes the macroscopic behaviour of strongly correlated systems, thus providing parameter-free predictions of the critical exponents [13]. Biology is vastly more complex than physics, but the widespread presence of strong correlations and the validity of scaling laws can hardly be considered a coincidence, and they rather call for an exploration of the correlation-scaling-RG path also in collective biological systems. Note that we do not need a system strictly at a second-order critical point to pursue this program; what is essential is that the finite-size biological system is correlated over distances much larger than the microscopic scale.

The renormalization group is becoming increasingly used in the broader field of active matter [14]. The pioneering hydrodynamic theory of Toner and Tu [15, 16] has been studied through the RG both in the polarised phase [17, 18] and near ordering [19–21], with applications in

systems with nematic or polar order [22–24], and motility-induced phase separation [25, 26]. RG has also been employed to study violations of the fluctuation-dissipation theorem and entropy production in scalar active models [27], active membranes [28], bacterial chemotaxis [29] and cellular growth [30]. Direct comparisons with experiments are few, though: the critical exponent of giant number fluctuations in  $d = 2$  [16, 31] was confirmed in experiments on vibrated polar disks [32]; other RG exponents have been checked in numerical simulations [33–36]. Comparisons with biological experiments are even scarcer. Experiments studying giant number fluctuations in swimming filamentous bacteria displaying long-range nematic order [37] found an exponent in disagreement with RG predictions of active nematic [23] and polar [18] systems. To the best of our knowledge, there is yet no successful test of an RG prediction against experiments on living active matter.

Here we apply the renormalization group to the dynamics of insect swarms. Swarms of midges in the field are near-critical, strongly correlated systems [9], obeying dynamic scaling [12] with an experimental exponent  $z_{\text{exp}}$  in the interval [1.0, 1.3], significantly smaller than the naive value  $z = 2$  of equilibrium overdamped dynamics [38]. Critical exponents do not depend on inessential details and when they do change – because of some new key ingredient – they do not change much. Thus the discrepancy in this case indicates that fundamental new physics is required. Although critical slowing down is not merely a dispersion relation, smaller  $z$  anyway indicates that fluctuations are more swiftly transported across the system. Hence, the effort to find new ingredients to match theory with experiments in natural swarms must look for more efficient mechanisms of information transfer. Activity is the first obvious candidate, as it allows fluctuations to propagate not only thanks to the inter-individual interaction, but also through the self-propelled motion of the individuals<sup>1</sup>. Indeed, the first step towards bridging the gap between experiments and theory was

<sup>1</sup> This is the off-equilibrium mechanism discovered by Toner and Tu,

the incompressible active matter study of Chen, Toner, and Lee [19], where a near-critical RG analysis found that activity lowers  $z$  from 2 to 1.7, a result valid also for compressible systems as long as density fluctuations are weak [40]. This is a step in the right direction, although the chasm with the experimental exponent remains significant. The second mechanism known to give faster information propagation is inertia. Behavioural inertia in the velocity alignment was first introduced to explain linear information transfer in bird flocks [41, 42], but experiments found clear evidence of inertial alignment also in natural swarms [12], indicating the existence of a coupling between velocity and the generator of its rotations, i.e. the spin [42]. At equilibrium, this type of mode-coupling interaction is known to decrease  $z$  from 2 to 1.5 [43], supporting the idea that inertia may also contribute to correcting  $z$  in the right direction. Overall, this scenario suggests that the *combined* effect of activity *and* inertia may account for the small experimental exponent  $z$ . Here, we perform an RG study of such theory, and find  $z = 1.3$ , a value closer to the experimental exponent than any previous theoretical determination. We remark that this is a parameter-free prediction, with no experimental input beyond the information that both activity and inertia are relevant.

A hydrodynamic theory of active matter with inertial mode-coupling interactions requires three fields: velocity, density, and spin [44, 45], and at least ten non-linear vertices, making an RG calculation completely out of reach. To make progress, following [19] we eliminate density fluctuations by imposing incompressibility,  $\nabla \cdot \mathbf{v}(\mathbf{x}, t) = 0$ , a reasonable assumption given that numerical evidence [40] indicates that compressible active systems conform to the incompressible critical exponents as long as density fluctuations are weak and no phase separation occurs. To make explicit the role of the microscopic particles speed,  $v_0$ , we will use the polarization field  $\boldsymbol{\psi}(\mathbf{x}, t) = \mathbf{v}(\mathbf{x}, t)/v_0$ . Having  $v_0$  as an explicit parameter is useful to take the zero-activity limit,  $v_0 \rightarrow 0$ , and compare with equilibrium calculations [38, 46]. The generator of rotations of  $\boldsymbol{\psi}(\mathbf{x}, t)$  is the spin,  $\mathbf{s}(\mathbf{x}, t)$ . In  $d = 3$  the spin is a vector; however, incompressibility requires  $\boldsymbol{\psi}$  to have the same dimension as space, and because RG entails an expansion in powers of  $\epsilon = 4 - d$ , we need a generic  $d$ -dimensional spin, which is a  $d \times d$  antisymmetric tensor. Mode-coupling interaction is described by the Poisson bracket [38],

$$\{s_{\alpha\beta}(\mathbf{x}), \psi_\gamma(\mathbf{x}')\} = 2g \mathbb{I}_{\alpha\beta\gamma\rho} \psi_\rho(\mathbf{x}) \delta^{(d)}(\mathbf{x} - \mathbf{x}'), \quad (1)$$

where  $g$  is the coupling constant regulating the rotational symmetry, while  $\mathbb{I}_{\alpha\beta\gamma\nu} = (\delta_{\alpha\gamma}\delta_{\beta\nu} - \delta_{\alpha\nu}\delta_{\beta\gamma})/2$  is the identity in the space of  $s_{\alpha\beta}$ .

The dynamical field theory we study combines the off-equilibrium hydrodynamic approach to active matter of

Toner and Tu [15, 16, 19], with the conservative mode-coupling structure used to describe superfluid helium and quantum antiferromagnets (Models E and G of [38]), and it thus represents the coarse-grained hydrodynamic theory of microscopic inertial active dynamics [42]. The equations of motion are given by,

$$D_t \psi_\alpha = -\Gamma \frac{\delta \mathcal{H}}{\delta \psi_\alpha} + g \psi_\beta \frac{\delta \mathcal{H}}{\delta s_{\alpha\beta}} - \partial_\alpha \mathcal{P} + \theta_\alpha, \quad (2)$$

$$D_t s_{\alpha\beta} = -\Lambda_{\alpha\beta\gamma\nu} \frac{\delta \mathcal{H}}{\delta s_{\gamma\nu}} + 2g \mathbb{I}_{\alpha\beta\gamma\nu} \psi_\gamma \frac{\delta \mathcal{H}}{\delta \psi_\nu} + \zeta_{\alpha\beta}, \quad (3)$$

where the material derivatives are,

$$\begin{aligned} D_t \psi_\alpha &= \partial_t \psi_\alpha + \gamma_v v_0 \psi_\nu \partial_\nu \psi_\alpha, \\ D_t s_{\alpha\beta} &= \partial_t s_{\alpha\beta} + \gamma_s v_0 \psi_\nu \partial_\nu s_{\alpha\beta}. \end{aligned} \quad (4)$$

Activity breaks Galilean invariance [16], so that the couplings  $\gamma_v$  and  $\gamma_s$  can be different from 1 and from each other. At the r.h.s there are the derivatives of the Landau-Ginzburg coarse-grained Hamiltonian [15],

$$\mathcal{H} = \int d^d x \left[ \frac{1}{2} \partial_\beta \psi_\alpha \partial_\beta \psi_\alpha + \frac{r}{2} \psi^2 + \frac{u}{4} \psi^4 + \frac{1}{2} s^2 \right].$$

The  $\boldsymbol{\psi}$ -dependent part of  $\mathcal{H}$  is the classic  $O(n)$  alignment interaction, while the ‘kinetic’ term  $s^2$  means that the spin has a purely dynamical role without effects on the statics [38]. The off-diagonal derivatives of  $\mathcal{H}$  in (2)-(3) are the non-dissipative mode-coupling terms, which characterise inertial dynamics [42]: instead of acting directly on the local polarization, the social alignment force  $\delta \mathcal{H}/\delta \boldsymbol{\psi}$  acts on the spin, which in turns rotates  $\boldsymbol{\psi}$ . The diagonal derivatives represent the dissipative terms, regulated by the kinetic coefficients  $\Gamma$  and  $\Lambda$ . The pressure  $\mathcal{P}$  enforces incompressibility, which in  $k$ -space translates into  $k_\alpha \psi_\alpha = 0$ , or  $P_{\alpha\beta}^\perp \psi_\beta = \psi_\alpha$ , with  $P_{\alpha\beta}^\perp = \delta_{\alpha\beta} - k_\alpha k_\beta / k^2$ . To respect this constraint, one must project the equation for  $\boldsymbol{\psi}$  and its noise correlator in Fourier space [19, 47],

$$\langle \theta_\alpha(\mathbf{k}, t) \theta_\beta(\mathbf{k}', t') \rangle = (2\pi)^d 2\tilde{\Gamma} P_{\alpha\beta}^\perp \delta^{(d)}(\mathbf{k} - \mathbf{k}') \delta(t - t')$$

where  $\tilde{\Gamma} \neq \Gamma$  out of equilibrium. The interaction between projected polarization and spin produces anisotropic corrections to  $\Lambda$  [46], so it is convenient to assume an anisotropic form from the outset,

$$\Lambda_{\alpha\beta\gamma\nu} = \left( \lambda^\perp \mathbb{P}_{\alpha\beta\gamma\nu}^\perp + \lambda^\parallel (\mathbb{I} - \mathbb{P}^\perp)_{\alpha\beta\gamma\nu} \right) k^2, \quad (5)$$

where  $\mathbb{P}_{\alpha\beta\gamma\nu}^\perp$  is the projector in the antisymmetric space [46], while the  $k^2$  factor preserves the conservation of the total spin encoded in the Poisson structure [38]; we will consider later the effects of adding a non-conservative (i.e.  $k$  independent) spin dissipation to  $\Lambda$ . Finally, the spin noise has correlator,

$$\langle \zeta_{\alpha\beta}(\mathbf{k}, t) \zeta_{\gamma\nu}(\mathbf{k}', t') \rangle = (2\pi)^d 4\tilde{\Lambda}_{\alpha\beta\gamma\nu} \delta^{(d)}(\mathbf{k} - \mathbf{k}') \delta(t - t')$$

where  $\tilde{\Lambda}$  has the same tensorial form as  $\Lambda$ , although out of equilibrium  $\lambda^{\perp, \parallel} \neq \tilde{\lambda}^{\perp, \parallel}$ .

---

responsible for stabilising long-range order in the Vicsek model [39], giving rise to an ordering transition even in  $d = 2$  [15].

Within an RG calculation it is always possible to find a set of effective parameters and couplings that are independent of the field dimensions and upon which physical predictions uniquely depend. The effective parameters for (2)-(3) are (we set the cutoff to 1 to simplify the notation),

$$w = \frac{\Gamma}{\lambda^{\parallel}}, \quad x = \frac{\lambda^{\perp}}{\lambda^{\parallel}}, \quad \theta^{\perp} = \frac{\tilde{\Gamma}\lambda^{\perp}}{\Gamma\tilde{\lambda}^{\perp}}, \quad \theta^{\parallel} = \frac{\tilde{\Gamma}\lambda^{\parallel}}{\Gamma\tilde{\lambda}^{\parallel}}, \quad (6)$$

where  $\theta^{\perp,\parallel} \neq 1$  if the system is out-of-equilibrium. The effective couplings regulating activity are,

$$c_v = v_0 \frac{\gamma_v}{\Gamma} \sqrt{\frac{\tilde{\Gamma}}{\Gamma}}, \quad c_s = v_0 \frac{\gamma_s}{\lambda^{\parallel}} \sqrt{\frac{\tilde{\Gamma}}{\Gamma}}, \quad (7)$$

which vanish for  $v_0 \rightarrow 0$ , thus giving the equilibrium limit of the theory [46]. Finally, the effective mode-coupling and ferromagnetic coupling constants are,

$$f = \frac{\tilde{\lambda}^{\parallel} g^2}{\lambda^{\parallel 2} \Gamma}, \quad \tilde{u} = \frac{\tilde{\Gamma}}{\Gamma} u. \quad (8)$$

The scaling dimension of all effective couplings, (7)-(8), is proportional to  $4 - d$ , indicating that the – static and dynamic – upper critical dimension is  $d_c = 4$ , and that an expansion in powers of  $\epsilon = 4 - d$  is appropriate. We perform a momentum-shell [13] RG analysis of the equations of motion in the near-critical regime ( $r = 0$ ); the  $\epsilon$ -expansion produces 65 Feynman diagrams at one-loop, describing the flow of the effective parameters and couplings. The full calculation – which is admittedly strenuous – is described in details in the Supplementary Information. A rich fixed-point structure emerges (Fig. 1):

*i)* The trivial fixed point has both activity and mode-coupling equal to zero,  $c_v^* = c_s^* = f^* = 0$  (black square), which at one loop gives the naive value of the dynamical critical exponent,  $z = 2$ ; it corresponds to the *overdamped equilibrium* case of classical ferromagnets, where both spin and self-propulsion are absent (more precisely, the incompressibility constraint leads to a theory for ferromagnets with dipolar interactions [48]).

*ii)* The *underdamped equilibrium* fixed point (blue diamond) has nonzero mode-coupling but no activity,  $f^* \neq 0, c_v^* = c_s^* = 0$ . This fixed point has  $z = 1.5$  in  $d = 3$  and it describes the equilibrium physics of superfluids and quantum antiferromagnets (Models E and G of [38]); in this case incompressibility becomes a solenoidal constraint on the primary field [46].

*iii)* Conversely, the *overdamped off-equilibrium* fixed point (green triangle) has zero mode-coupling, but nonzero activity,  $f^* = 0, c_v^* \neq 0$ , giving  $z = 1.7$  in  $d = 3$ , and it describes near-critical incompressible active matter for which inertial effects (and therefore the spin) are irrelevant, as described by Chen, Toner, and Lee in [19].

*iv)* Finally, we find a novel *underdamped off-equilibrium* fixed point (red circle), where *both* activity *and* inertial mode-coupling interaction are non-zero,  $c_v^* \neq 0, c_s^* \neq 0, f^* \neq 0$ . As we expected, the combined effect of activity

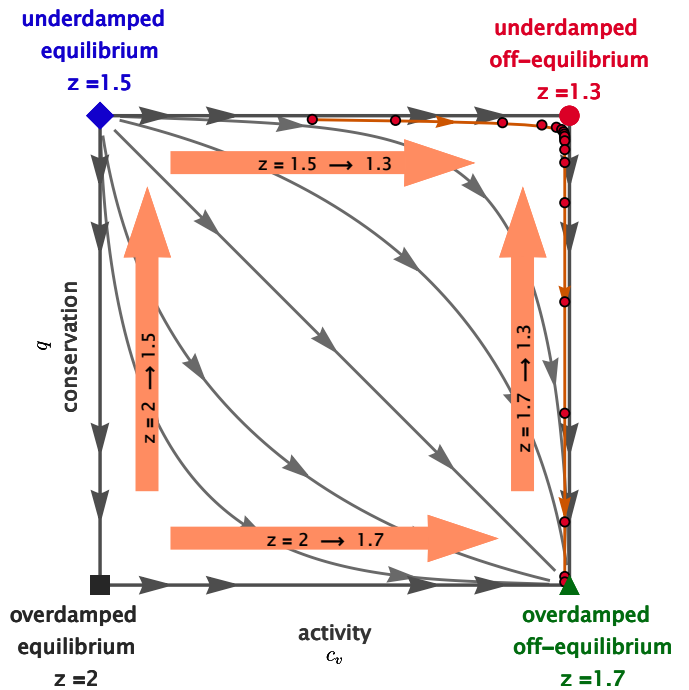


FIG. 1. **RG flow and effects of activity and conservation.** Grey arrows indicate the RG flow in the activity-conservation plane. The new underdamped off-equilibrium fixed point (red circle) is stable against the underdamped equilibrium fixed point, but unstable against the overdamped off-equilibrium one. However, when dissipation is sufficiently low, a crossover makes the RG flow linger around the new fixed point for many coarse-graining iterations (small red circles), implying that this fixed point can rule the large scale dynamics of finite-size systems. Orange arrows indicate the effects of activity and conservation on the value of the dynamical critical exponent: while both separately contribute to decrease  $z$ , it is only their combined effect that brings the critical exponent close to the experimental value.

and inertia lowers significantly the dynamical critical exponent, and we find  $z = 1.3$  in  $d = 3$ . This fixed point describes near-critical active matter in which inertial effects are relevant.

In order to understand why  $z = 1.3$  applies to finite-size natural swarms, we must study the stability of the fixed points, and to do so we need to introduce friction. So far our theory conserved the total spin, thanks to the Poisson mode-coupling structure and to the factor  $k^2$  in the spin kinetic coefficient, eq.(5). Perfect spin conservation, however, is not realistic in the biophysical context, and one expects some non-conservative spin dissipation to be present [42]; this can be introduced by adding a  $k$ -independent friction  $\eta$  to the spin kinetic coefficient (5), namely,  $(\lambda^{\parallel} + \lambda^{\perp})k^2 \rightarrow (\lambda^{\parallel} + \lambda^{\perp})k^2 + \eta$ . The ratio between conservative kinetic coefficient and non-conservative friction naturally generates a *conservation length scale*,  $\mathcal{R} = \sqrt{\lambda^{\parallel}/\eta}$ , which is larger the smaller is friction, and whose meaning is clear: fluctuations with scale shorter than  $\mathcal{R}$  obey a conservative dynamics, while beyond  $\mathcal{R}$

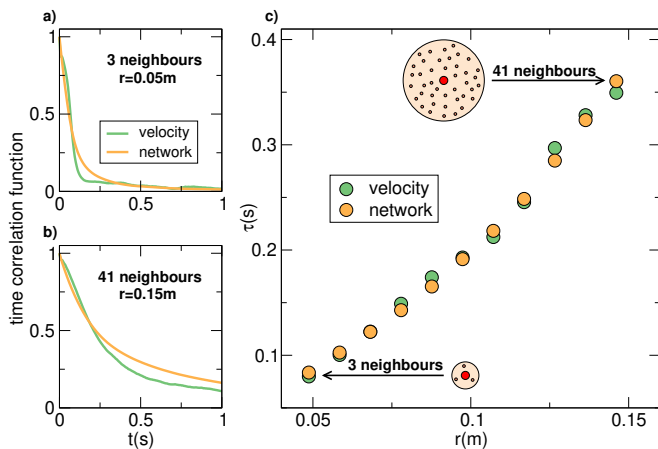


FIG. 2. **Swarms are strongly active.** **a, b:** Network correlation (yellow) and velocity correlation (green) as a function of time, at two different spatial scales  $r$ . The network correlation measures the fraction of neighbours remaining within a region of size  $r$  around a given individual, after a time  $t$  (see SI-Section II, for details); it therefore quantifies how quickly the interaction network rearranges on a given spatial scale. The two values of  $r$  considered correspond to neighbourhoods with - on average - 3 individuals and 41 individuals. **c:** Characteristic time of network and velocity correlation vs.  $r$  in the range  $[0.05m, 0.15m]$ , an interval within which the metric interaction range of real swarms certainly belongs to [5]. Results show that network rearrangement occurs on the same timescale as velocity relaxation both locally and for neighbourhoods containing many individuals. Data are from event 20150924\_ACQ2, with  $N = 781$  individuals (SI-Table 1).

dissipation dominates (both  $\lambda^{\parallel}$  and  $\lambda^{\perp}$  have finite RG limits – see SI-Section ID 1 – hence we could use either to define  $\mathcal{R}$ ). The RG dimension of  $\eta$  is positive (see SI-Section ID 3), so that friction grows along the RG flow; hence, in the asymptotic limit  $\mathcal{R}$  shrinks to zero and fluctuations are overdamped over all scales. To represent this flow on a diagram it is convenient to introduce the reduced conservative coupling,  $q \equiv f \mathcal{R}^2 / (1 + \mathcal{R}^2)$ , where  $f$  is the conservative coupling constant, eq.(8): when  $\mathcal{R} = \infty$  (i.e.  $\eta = 0$ ), one has  $q = f$ , corresponding to conserved underdamped dynamics; conversely, when either  $\mathcal{R} = 0$  (i.e.  $\eta \rightarrow \infty$ ) or  $f = 0$ , one has  $q = 0$ , corresponding to non-conserved overdamped dynamics. The RG flow drives  $q \rightarrow 0$ , hence both underdamped fixed points (blue diamond and red circle in Fig. 1) are unstable against dissipation. Moreover, the activity coupling constant,  $c_v$ , defined in (7), has positive RG dimension too (see SI-Section ID 1), hence the equilibrium fixed points (black square and blue diamond in Fig. 1) are unstable against activity: any nonzero microscopic speed,  $v_0$ , drives the RG flow towards active dynamics. In conclusion, both dissipation and activity are relevant, hence the only asymptotically stable fixed point is the overdamped active one (green triangle in Fig. 1).

The *asymptotic* RG limit, though, does not necessarily describe what happens in *finite-size* systems. Depending

on the initial RG values of the coupling constants, that is on their physical experimental values, the RG trajectory may remain trapped for many iterations in the vicinity of a mixed-stability fixed point, giving rise to a crossover with important finite-size implications [49]. How strong we expect dissipation and activity to be in natural swarms? The sharply inertial shape of the dynamic correlation functions (see Figure 3 of [12]) constitutes solid experimental evidence that effective friction in natural swarms is *weak*. On the other hand, in Fig. 2 we show that the rewiring of the interaction network in swarms occurs on the same time-scale as velocity relaxation; hence, activity is *strong*. Weak friction and strong activity imply that the RG flow starts *close* to underdamped line, but *far* from the equilibrium line, so that the first RG iterations rapidly lead the system in the vicinity of the underdamped off-equilibrium fixed point, lingering there for many RG iterations, before flowing to the overdamped off-equilibrium fixed point (red dots in Fig. 1). The crucial point is the following: if by the ‘time’ the RG iterations leave the critical region, the flow is still in the neighbourhood of the conservative fixed point, then the dynamics is ruled by  $z = 1.3$ . Let us see how this works.

The RG flow of the correlation length is always given by,  $\xi_l = \xi_{l-1}/b = \xi/b^l$ ; on the other hand, the conservation length scale acquires an anomalous dimension equal to  $z/2$  (see SI-Section ID 3), hence  $\mathcal{R}_l = \mathcal{R}_{l-1}/b^{z/2} = \mathcal{R}/(b^l)^{z/2}$ , where  $\xi$  and  $\mathcal{R}$  are the physical values of these quantities; we can combine these relations obtaining,  $\mathcal{R}_l = (\xi_l/\xi)^{z/2} \mathcal{R}$ . The system is off-criticality once the correlation length has been reduced to  $\xi_l \sim 1$ ; besides, vicinity to the underdamped fixed point requires  $q_l \sim f_l$ , namely  $\mathcal{R}_l \gg 1$ . We therefore find that for  $\xi \ll \mathcal{R}^{2/z}$ , critical slowing down is governed by  $z = 1.3$ . The system’s size  $L$  is an upper limit for the correlation length, hence if  $L \ll \mathcal{R}^{2/z}$ , *all* critical fluctuations are ruled by the conservative fixed point; by recalling that  $\mathcal{R} \sim 1/\sqrt{\eta}$ , we obtain that whenever the physical friction and the system’s size are small enough to satisfy,  $\eta L^z \ll 1$ , the dynamic critical exponent is  $z = 1.3$ . Note that, since activity lowers  $z$  from 1.5 to 1.3, the domain of conservative dynamics is *larger* in the off-equilibrium case than in the equilibrium one. Remarkably, instead of destroying the Poisson structure, off-equilibrium activity in fact *protects it against dissipation*, expanding the regime of conservative dynamics with respect to equilibrium.

The dynamical critical exponent in natural swarms was first measured in [12], giving  $1.0 < z_{\text{exp}} < 1.3$ . Here we added 8 swarming events to our original dataset, notably including a new swarm of 780 individuals (the largest swarm of [12] had  $N = 278$ ). For each of the 38 swarms we measure the relaxation time,  $\tau$ , and the correlation length,  $\xi$  as in [12]. To estimate a confidence window for  $z_{\text{exp}}$  we use a resampling method, by fitting the relation  $\log \tau = z \log \xi$  to a very large number of randomly drawn subsets containing half the data (see Fig. 3); in this way we obtain the confidence window  $1.04 \leq z_{\text{exp}} \leq 1.28$  at  $1\text{-}\sigma$ ,  $0.92 \leq z_{\text{exp}} \leq 1.40$  at  $2\text{-}\sigma$ , and  $0.80 \leq z_{\text{exp}} \leq 1.52$  at  $3\text{-}\sigma$ . Fig. 3

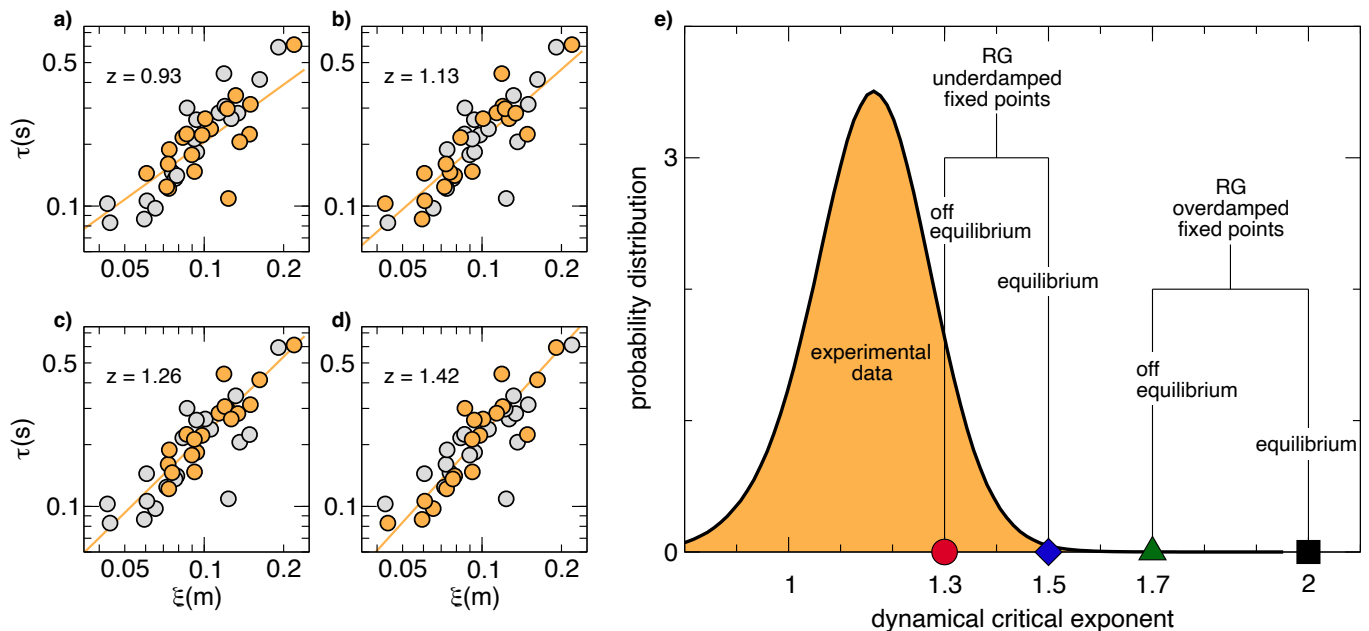


FIG. 3. **Experimental data vs theoretical RG predictions.** a–d: We measured the correlation length and relaxation time in 38 swarming events, whose detailed properties we report in Table 1 in the SI. To obtain an estimate of the experimental distribution of the critical exponent, we use a resampling method: we randomly select  $10^7$  subsets with half the number of points, and in each subset we determine  $z$  as the slope of the linear fit of  $\log \tau$  vs  $\log \xi$ . In panels a–d we report four such subsets (yellow points), with their relative linear fit in log-log scale. e: Experimental distribution of the dynamical critical exponent from the resampling method. The novel underdamped off-equilibrium fixed point,  $z = 1.3$  (red circle), where both activity and inertia are relevant, is the theoretical prediction with the best agreement with the experimental data.

shows that the novel active mode-coupling fixed point,  $z = 1.3$ , is by far the most consistent with experiments. In fact, considering that the inertial equilibrium fixed point ( $z = 1.5$ ) is not a plausible description of the strongly active dynamics of natural swarms, the only realistic prediction prior to the present calculation was the overdamped active value,  $z = 1.7$ , compared to which the new exponent  $z = 1.3$  is a major step forward. The agreement with experiments might further improve by going beyond first order in the  $\epsilon$ -expansion and by allowing some mild density fluctuations, using the method of [50].

The fact that our result has been obtained through the calculation of Feynman diagrams is crucial, no matter how hopelessly technical this statement sounds. The RG rests on two keystones: rescaling of space and time, and coarse-graining of the short-wavelength (UV) degrees of freedom, which impacts on the long-wavelength (IR) physics. UV-IR coupling is the most profound aspect of the RG, as it produces *anomalous* scaling dimensions of the parameters. In some cases, the coarse-graining step is trivial, so that UV and IR modes remain decoupled; when

that happens RG is mere dimensional analysis, producing critical exponents that are a combination of the naive dimensions.<sup>2</sup> Within the  $\epsilon$ -expansion, the hallmark of the UV-IR coupling is the emergence of nonzero diagrams that correct the scaling dimensions, yielding non-trivial critical exponents.<sup>3</sup> This is the case of the present calculation, which therefore tests the core idea of the RG, namely that integrating out the short-scale details impacts on the large-scale behaviour by introducing *anomalies* in the dimensions of the physical quantities. To our knowledge, this is the first time in the context of living active matter that the UV-IR coupling gives a theoretical exponent consistent with experiments. This result supports the idea that the renormalization group, with its most fruitful consequence – universality – may have an incisive impact also in biology.

This work was supported by ERC Advanced Grant RG.BIO (n.785932) to AC. TSG was supported by grants from CONICET, ANPCyT and UNLP (Argentina). We thank E. Branchini, F. Cecconi, M. Cencini and V. Skultety for discussions.

<sup>2</sup> For example, the naive dynamical exponent  $z = 2$  results from dimensional analysis of overdamped dynamics,  $\partial_t \psi = \Gamma \partial_x^2 \psi$ , which – in absence of renormalization of the kinetic coefficient  $\Gamma$  – simply leads to the dimensional relation,  $x \sim t^{1/2}$ .

<sup>3</sup> In some cases the UV-IR coupling exists, but symmetries set some constraints on the scaling dimensions that can thus be worked out without actually calculating the (nonzero) Feynman diagrams; when that happens, RG still gives non-trivial exponents [16].

- [1] D. J. Sumpter, *Collective animal behavior* (Princeton University Press, 2010).
- [2] A. Cavagna, A. Cimorelli, I. Giardina, G. Parisi, R. Santagati, F. Stefanini, and M. Viale, *Proceedings of the National Academy of Sciences* **107**, 11865 (2010).
- [3] A. Strandburg-Peshkin, C. R. Twomey, N. W. Bode, A. B. Kao, Y. Katz, C. C. Ioannou, S. B. Rosenthal, C. J. Torney, H. S. Wu, S. A. Levin, *et al.*, *Current Biology* **23**, R709 (2013).
- [4] F. Ginelli, F. Peruani, M.-H. Pillot, H. Chaté, G. Theraulaz, and R. Bon, *Proceedings of the National Academy of Sciences* **112**, 12729 (2015).
- [5] A. Attanasi, A. Cavagna, L. Del Castello, I. Giardina, S. Melillo, L. Parisi, O. Pohl, B. Rossaro, E. Shen, E. Silvestri, and M. Viale, *PLOS Computational Biology* **10**, 1 (2014).
- [6] C. Dombrowski, L. Cisneros, S. Chatkaew, R. E. Goldstein, and J. O. Kessler, *Physical review letters* **93**, 098103 (2004).
- [7] H. P. Zhang, A. Be'er, E.-L. Florin, and H. L. Swinney, *Proceedings of the National Academy of Sciences* **107**, 13626 (2010).
- [8] Q.-Y. Tang, Y.-Y. Zhang, J. Wang, W. Wang, and D. R. Chialvo, *Physical review letters* **118**, 088102 (2017).
- [9] A. Attanasi, A. Cavagna, L. Del Castello, I. Giardina, S. Melillo, L. Parisi, O. Pohl, B. Rossaro, E. Shen, E. Silvestri, and M. Viale, *Phys. Rev. Lett.* **113**, 238102 (2014).
- [10] R. A. Ferrell, N. Menyhard, H. Schmidt, F. Schwabl, and P. Szépfalusy, *Phys. Rev. Lett.* **18**, 891 (1967).
- [11] B. I. Halperin and P. C. Hohenberg, *Phys. Rev.* **177**, 952 (1969).
- [12] A. Cavagna, D. Conti, C. Creato, L. Del Castello, I. Giardina, T. S. Grigera, S. Melillo, L. Parisi, and M. Viale, *Nature Physics* **13**, 914 (2017).
- [13] K. G. Wilson and J. Kogut, *Physics Reports* **12**, 75 (1974).
- [14] M. C. Marchetti, J. F. Joanny, S. Ramaswamy, T. B. Liverpool, J. Prost, M. Rao, and R. A. Simha, *Rev. Mod. Phys.* **85**, 1143 (2013).
- [15] J. Toner and Y. Tu, *Phys. Rev. Lett.* **75**, 4326 (1995).
- [16] J. Toner and Y. Tu, *Phys. Rev. E* **58**, 4828 (1998).
- [17] B. Mahault, F. Ginelli, and H. Chaté, *Phys. Rev. Lett.* **123**, 218001 (2019).
- [18] J. Toner, *The Journal of Chemical Physics* **150**, 154120 (2019), <https://doi.org/10.1063/1.5081742>.
- [19] L. Chen, J. Toner, and C. F. Lee, *New Journal of Physics* **17**, 042002 (2015).
- [20] V. Škultéty, i. c. v. Birnšteinová, T. Lučivjanský, and J. Honkonen, *Phys. Rev. E* **102**, 032616 (2020).
- [21] V. Holubec, D. Geiss, S. A. M. Loos, K. Kroy, and F. Cichos, *Finite-size scaling at the edge of disorder in a time-delay vicsek model* (2021), arXiv:2107.06059 [cond-mat.soft].
- [22] S. Mishra, R. A. Simha, and S. Ramaswamy, *Journal of Statistical Mechanics: Theory and Experiment* **2010**, P02003 (2010).
- [23] S. Ramaswamy, *Annual Review of Condensed Matter Physics* **1**, 323 (2010).
- [24] J. Toner, Y. Tu, and S. Ramaswamy, *Annals of Physics* **318**, 170 (2005).
- [25] F. Caballero, C. Nardini, and M. E. Cates, *Journal of Statistical Mechanics: Theory and Experiment* **2018**, 123208 (2018).
- [26] C. Maggi, N. Gnan, M. Paoluzzi, E. Zaccarelli, and A. Crisanti, *Critical active dynamics is captured by a colored-noise driven field theory* (2021), arXiv:2108.13971 [cond-mat.soft].
- [27] F. Caballero and M. E. Cates, *Phys. Rev. Lett.* **124**, 240604 (2020).
- [28] F. Cagnetta, V. Skultety, M. R. Evans, and D. Marenduzzo, *Universal properties of active membranes* (2021), arXiv:2104.06764 [cond-mat.stat-mech].
- [29] S. Mahdisoltani, R. B. A. Zinati, C. Duclut, A. Gambassi, and R. Golestanian, *Phys. Rev. Research* **3**, 013100 (2021).
- [30] A. Gelimson and R. Golestanian, *Phys. Rev. Lett.* **114**, 028101 (2015).
- [31] J. Toner, *The Journal of chemical physics* **150**, 154120 (2019).
- [32] J. Deseigne, O. Dauchot, and H. Chaté, *Phys. Rev. Lett.* **105**, 098001 (2010).
- [33] Y. Tu, J. Toner, and M. Ulm, *Phys. Rev. Lett.* **80**, 4819 (1998).
- [34] H. Chaté, F. Ginelli, G. Grégoire, and F. Raynaud, *Phys. Rev. E* **77**, 046113 (2008).
- [35] F. Ginelli, F. Peruani, M. Bär, and H. Chaté, *Phys. Rev. Lett.* **104**, 184502 (2010).
- [36] A. Doostmohammadi, T. N. Shendruk, K. Thijssen, and J. M. Yeomans, *Nature Communications* **8**, 15326 (2017).
- [37] D. Nishiguchi, K. H. Nagai, H. Chaté, and M. Sano, *Phys. Rev. E* **95**, 020601 (2017).
- [38] P. C. Hohenberg and B. I. Halperin, *Rev. Mod. Phys.* **49**, 435 (1977).
- [39] T. Vicsek, A. Czirók, E. Ben-Jacob, I. Cohen, and O. Shochet, *Phys. Rev. Lett.* **75**, 1226 (1995).
- [40] A. Cavagna, L. Di Carlo, I. Giardina, T. S. Grigera, and G. Pisegna, *Phys. Rev. Research* **3**, 013210 (2021).
- [41] A. Attanasi, A. Cavagna, L. Del Castello, I. Giardina, T. S. Grigera, A. Jelić, S. Melillo, L. Parisi, O. Pohl, E. Shen, and M. Viale, *Nature Physics* **10**, 691 (2014).
- [42] A. Cavagna, L. Del Castello, I. Giardina, T. Grigera, A. Jelic, S. Melillo, T. Mora, L. Parisi, E. Silvestri, M. Viale, *et al.*, *Journal of Statistical Physics* **158**, 601 (2015).
- [43] B. Halperin, P. Hohenberg, and E. Siggia, *Physical Review B* **13**, 1299 (1976).
- [44] A. Cavagna, I. Giardina, T. S. Grigera, A. Jelic, D. Levine, S. Ramaswamy, and M. Viale, *Physical Review Letters* **114**, 218101 (2015).
- [45] X. Yang and M. C. Marchetti, *Physical Review Letters* **115**, 258101 (2015).
- [46] A. Cavagna, L. D. Carlo, I. Giardina, T. Grigera, G. Pisegna, and M. Scandolo, arXiv:2103.10914 (2021).
- [47] D. Forster, D. R. Nelson, and M. J. Stephen, *Phys. Rev. A* **16**, 732 (1977).
- [48] A. D. Bruce and A. Aharony, *Phys. Rev. B* **10**, 2078 (1974).
- [49] A. Cavagna, L. Di Carlo, I. Giardina, L. Grandinetti, T. S. Grigera, and G. Pisegna, *Phys. Rev. Lett.* **123**, 268001 (2019).
- [50] J. Toner, *Physical Review Letters* **108**, 088102 (2012).

## Supplementary Information: Natural Swarms in 3.99 Dimensions

### I. THE RENORMALIZATION GROUP CALCULATION

The calculation we are going to describe here is the final point of a rather long trajectory, so that it may be useful for the reader to keep in mind the map of the main works leading to the present result. The hydrodynamic theory originally developed by Toner and Tu for flocks [1], can also be applied to swarms when studied in its critical phase; this was done in the incompressible case in [2], which is our starting point for the active incompressible non-inertial branch of our theory. The crossover between the non-active (equilibrium) fixed point to the active (off-equilibrium) fixed point in this theory was studied in [3], where it was also established that the results of the incompressible RG calculation agree perfectly well with simulations of the compressible model, provided that density fluctuations are mild (no phase separation). The experimental evidence of an inertial coupling between velocity and spin, and therefore of the need to go beyond Toner-Tu theory, was first found for flocks in [4] and later for swarms in [5]; the microscopic model of active self-propelled particles obeying such inertial mode-coupling dynamics is the Inertial Spin Model (ISM), which is defined in detail in [6]; the Vicsek model [7] is the overdamped limit of the ISM [6]: when spin dissipation is very large compared to inertia, the spin becomes irrelevant and one reduces to a theory for just one degree of freedom, the velocity. A discussion of the connections between Vicsek model, Toner and Tu theory and the ISM can be found in [8].

The path from the microscopic inertial active model (the ISM) to the relative coarse-grained dynamical field theory that we study here has required some intermediate steps. First, the equilibrium version (i.e. fixed network, or non-active) of the ISM has a field-theoretical benchmark in Model E (planar case) and Model G (3d case), according to the classic Halperin-Hohenberg classification of dynamical critical phenomena [9]; these equilibrium models are really a fundamental starting point for understanding the inertial mode-coupling dynamics of a primary field coupled to the generator of its rotations. These equilibrium non-active models have perfect conservation of the spin - namely zero dissipation - which is unlikely to be exactly true in biological systems, hence in [10, 11] we studied the effect of dissipation at equilibrium on this kind of theories, finding that for finite-size systems the conservative fixed point of the mode-coupling theories is still relevant. Finally, we assessed (again at equilibrium) how to impose the incompressibility constraint (which is a solenoidal constraint on a fixed network) on a theory where there is inertial coupling between primary field and spin in [12]. The present calculation finally analyses the active out-of-equilibrium incompressible case in presence of inertial mode-coupling between velocity and spin.

#### A. Derivation of the equations of motion

##### 1. Describing activity: the Toner and Tu theory in the incompressible case

The starting point of our field-theoretical description is given by the hydrodynamic theory developed by Toner and Tu [1], representing the minimal description of an active system with rotational invariance. This theory represents the hydrodynamic counterpart of the Vicsek model (VM) [7], although it should in general describe any model which shares the same symmetries and conservation laws. The VM describes the dynamics of a collection of self-propelled particles with fixed speed  $v_0$ , whose velocities interact through a dynamic alignment as in equilibrium XY or Heisenberg models. The continuous theory of Toner and Tu represents a sort of moving ferromagnet, combining activity with Model A dynamics  $\partial_t \mathbf{v} = -\delta_{\mathbf{v}} \mathcal{H} + \boldsymbol{\theta}$  [9], with  $\mathcal{H}$  being the Landau-Ginzburg free-energy. This makes the Toner and Tu theory fall into the class of overdamped Langevin equations, in which the *social* force  $\delta_{\mathbf{v}} \mathcal{H}$  acts directly on the time-evolution of the order parameter. In the incompressible limit - see SI-Section IA 4 - the equation of motion for the velocity field in the near-critical Toner and Tu theory is given by [2],

$$\partial_t \mathbf{v} + \gamma_v (\mathbf{v} \cdot \nabla) \mathbf{v} = \Gamma \nabla^2 \mathbf{v} - (m + Jv^2) \mathbf{v} - \nabla \mathcal{P} + \boldsymbol{\theta} . \quad (9)$$

where on the l.h.s. we can recognise the material derivative  $D_t \mathbf{v} = \partial_t \mathbf{v} + \gamma_v (\mathbf{v} \cdot \nabla) \mathbf{v}$ . Since the active force breaks Galilean invariance [13], the coefficient  $\gamma_v$  needs not to be equal to unity. On the r.h.s. we have the alignment force  $\nabla^2 \mathbf{v}$ , the active force coming from a Landau potential, the pressure and a gaussian white noise of variance  $2\bar{\Gamma}$ . An RG analysis of Eq. (9) near criticality predicts at one loop a dynamic critical exponent of  $z = 1.7$  in  $d = 3$  dimensions [2].

When  $\gamma_v = 0$ , namely in absence of advection, equilibrium Model A's critical behaviour is recovered, with the dynamic exponent being  $z = 2$  at one-loop. A crossover thus occurs between the equilibrium and the off-equilibrium critical behaviour [3]. The microscopic parameter controlling this crossover is the microscopic speed  $v_0$ ; to see this it is convenient to work with the coarse-grained orientation field  $\boldsymbol{\psi}$  (or local polarization) rather than with the velocity

field  $\mathbf{v}$ . In models as the VM, in which each individual has the same speed  $v_0$ , the connection between these two fields is simply given by,

$$\mathbf{v}(\mathbf{x}, t) = v_0 \boldsymbol{\psi}(\mathbf{x}, t) . \quad (10)$$

Written in terms of the field  $\boldsymbol{\psi}$ , equation (9) becomes,

$$\partial_t \boldsymbol{\psi} + v_0 \gamma_v (\boldsymbol{\psi} \cdot \nabla) \boldsymbol{\psi} = \Gamma \nabla^2 \boldsymbol{\psi} - \left( m + J \psi^2 \right) \boldsymbol{\psi} - \nabla \mathcal{P} + \boldsymbol{\theta} , \quad (11)$$

in which the explicit dependence of the advection term on the microscopic parameter  $v_0$  clarifies the mechanism underlying the crossover between equilibrium Model A and off-equilibrium theory [3].

## 2. Restoring inertia: equilibrium mode-coupling dynamics

Experimental evidence about swarms' temporal correlation function shows that an inertial structure, absent in the incompressible Toner and Tu theory, is needed to describe natural swarms [5]. This is confirmed by the discrepancies between the experimental value of the dynamic critical exponent  $z$ , found to be between 1.0 and 1.3 in natural swarms, and the theoretical prediction of  $z = 1.7$  of the Toner and Tu incompressible theory in  $d = 3$  [2]. As proposed in [4] for the case of flocks, restoring inertia can be done by recognizing that, although Eq. (9) is invariant under rotations, there is no trace of a conservation law associated with this symmetry. However, according to Noether's theorem, when a theory is invariant under a given symmetry, the generator of this symmetry is conserved. The presence of conservation laws heavily affects the critical properties of a system, leading to completely different dynamic behaviours. Since Toner and Tu theory is built to be invariant under rotational symmetry, our aim is to couple (9) with the conservation law associated with the rotational invariance, in order to restore inertial behaviour.

From the microscopic perspective, restoring inertia, namely going from the Vicsek model to the Inertial Spin Model (ISM), implies that the aligning force does not act directly on  $\partial_t \mathbf{v}$ , but is mediated by the generator of rotational symmetry. In the ISM the state of each individual is defined by 3 degrees of freedom: position  $\mathbf{x}$ , velocity  $\mathbf{v}$  (both present also in the Vicsek Model) and a new variable  $\mathbf{s}$  that is the conjugate momenta of the phase of  $\mathbf{v}$ . This new variable, in analogy with quantum mechanics, has been called spin since it represents the generator of rotations in the *internal* space of the velocities. It must not be confused with angular momentum, which is the generator of rotations in positions' space. The spin of an individual is proportional to the curvature of its trajectory, namely to the inverse of its radius of curvature: all individuals sharing the same spin undergo equal radius turns rather than parallel-path turns [4]. Spin-velocity coupling in the ISM allows to obtain an equation for the velocity with a dynamics that is second-order in time, namely *inertial* [6].

When shifting our attention to hydrodynamics, inertia can be restored by coupling the velocity field with the spin field [10]. The global conservation of the spin allows it to fluctuate on space-time-scales comparable with those of critical fluctuations, thus making spin-velocity couplings relevant in the RG sense. To simplify the discussion, we will first discuss the effects of restoring inertia in absence of activity, namely at equilibrium. At equilibrium, a mode-coupling interaction between an order parameter  $\boldsymbol{\psi}$  and its spin  $\mathbf{s}$  arises from their Poisson-bracket relation [9],

$$\left\{ s_{\alpha\beta}(\mathbf{x}), \psi_\gamma(\mathbf{x}') \right\} = 2g \mathbb{I}_{\alpha\beta\gamma\nu} \psi_\nu(\mathbf{x}) \delta(\mathbf{x} - \mathbf{x}') , \quad (12)$$

which encodes the fact that  $\mathbf{s}$  is the generator of rotations of  $\boldsymbol{\psi}$ . In general, when the order parameter is a  $n$ -dimensional vector, the generator of its rotations  $\mathbf{s}$  is a  $n \times n$  anti-symmetric tensor [14]. The tensor  $\mathbb{I}$  represents the identity in the space of  $s_{\alpha\beta}$ , and it is given by,

$$\mathbb{I}_{\alpha\beta\gamma\nu} = \frac{\delta_{\alpha\gamma} \delta_{\beta\nu} - \delta_{\alpha\nu} \delta_{\beta\gamma}}{2} , \quad (13)$$

with the factor  $\frac{1}{2}$  ensuring that  $\mathbb{I}_{\alpha\beta\gamma\nu} s_{\gamma\nu} = s_{\alpha\beta}$  and  $\mathbb{I}_{\alpha\beta\sigma\tau} \mathbb{I}_{\sigma\tau\gamma\nu} = \mathbb{I}_{\alpha\beta\gamma\nu}$ .

We work here with an order parameter of generic dimension  $n$ , although in the physical case we have  $n = 3$ . This choice might seem inconvenient at first glance. When  $n = 3$ , the spin  $\mathbf{s}$  can be written as a 3-dimensional vector, lightening the tensorial structure and reducing the number of indices (this comes from the fact that when  $n = 3$ , the plane on which the rotation occurs can be uniquely identified by the vector orthogonal to it, while this does not happen when  $n \neq 3$ ). However, there is a reason other than self-harm for which we prefer working with a tensorial spin rather than a vectorial one. In the active inertial case, which will be investigated in the following sections, the order parameter  $\boldsymbol{\psi}$  is linked to the velocity  $\mathbf{v}$  through the relation  $\mathbf{v} = v_0 \boldsymbol{\psi}$  (Eq. (10)). This makes both  $\mathbf{v}$  and  $\boldsymbol{\psi}$  have the same dimension  $d$  of space. Although the physical case is given by  $n = d = 3$ , the RG perturbative expansion is

performed by expanding  $d$  near the upper critical dimension  $d_c = 4$ . Hence, when activity is at play, one is forced to work with an order parameter of dimension  $n = d \sim d_c$  to correctly perform the RG perturbative expansion. The spin associated with an  $n$ -dimensional order parameter, in generic dimension  $n$ , is represented by a  $n \times n$  anti-symmetric tensor rather than a vector. Therefore, since in the present work we are interested in combining the effects of activity and mode-coupling, we will need to work with this more generic form.

The equilibrium dynamics of a near-critical system in which  $\mathbf{s}$  is conserved, known as Model G in the physical case of a three dimensional order parameter ( $n = 3$ ) [9] and generalized by the Sasvari-Schwabl-Szepfalusy (SSS) model in  $n$  dimensions [14, 15], can be constructed following the classic Mori-Zwanzig formalism [16, 17] and it is given by,

$$\partial_t \psi_\alpha = -\Gamma \frac{\delta \mathcal{H}}{\delta \psi_\alpha} + g \psi_\beta \frac{\delta \mathcal{H}}{\delta s_{\alpha\beta}} + \theta_\alpha, \quad (14)$$

$$\partial_t s_{\alpha\beta} = -\Lambda_{\alpha\beta\gamma\nu} \frac{\delta \mathcal{H}}{\delta s_{\gamma\nu}} + 2g \mathbb{I}_{\alpha\beta\gamma\nu} \psi_\gamma \frac{\delta \mathcal{H}}{\delta \psi_\nu} + \zeta_{\alpha\beta} \quad (15)$$

Here the free-energy functional  $\mathcal{H}$  is chosen to take the usual Landau-Ginzburg form for the critical field  $\psi$  while it is gaussian for the spin field (we set to 1 the inertia, which does not get any renormalization),

$$\mathcal{H} = \int d^d x \left[ \frac{1}{2} \psi_\alpha \left( -\nabla^2 + r \right) \psi_\alpha + \frac{u}{4} (\psi_\alpha \psi_\alpha)^2 + \frac{1}{4} s_{\alpha\beta} s_{\alpha\beta} \right]. \quad (16)$$

The square gradient enforces local alignment of the order parameter  $\psi$ , while  $r\psi^2 + u\psi^4$  is the modulus' confining potential. At mean-field level, when  $r < 0$  the ground state exhibits symmetry breaking and an ordered phase is observed, while for  $r > 0$  the ground state is given by the disordered state with zero mean polarization.

Inertia is restored thanks to the presence of mode-coupling interactions that encode the conservative nature of the dynamics, arising as a consequence of the Poisson-bracket relation (12). The term  $\partial_t s \sim g\psi\delta_\psi\mathcal{H}$  represents the action of the *force* on the dynamics of the spin, rather than directly on the order parameter. The indirect action of this force on the dynamics of  $\psi$  is guaranteed by the term  $\partial_t \psi \sim g\psi\delta_s\mathcal{H}$ , which expresses the rotation of  $\psi$  induced by the conservation of  $\mathbf{s}$ . This mode-coupling restores an *underdamped* structure of the equations of motion, thus allowing to describe an inertial behaviour. On the other hand, the terms  $\partial_t \psi = -\Gamma\delta_\psi\mathcal{H}$  and  $\partial_t s \sim -\Lambda\delta_s\mathcal{H}$  represent dynamic relaxations, giving rise to the diffusion and transport phenomenology typical of stochastic statistical systems. These dissipative terms are thus complemented by the white Gaussian noises  $\theta$  and  $\zeta$ , whose variances are given by Einstein relations when the system is at equilibrium. The dissipative constant (or kinetic coefficient)  $\Gamma$  rules the relaxation of the order parameter and it is a crucial player in determining the dynamic exponent  $z$  since it fixes the time-scale on which relaxation occurs. Similarly, the kinetic tensor  $\Lambda_{\alpha\beta\gamma\nu}$  rules the relaxation of the spin. When the total spin is conserved, the tensor  $\Lambda$  must be proportional to  $\nabla^2$  [9], and in the isotropic theory it takes the form,

$$\Lambda_{\alpha\beta\gamma\nu} = -\mathbb{I}_{\alpha\beta\gamma\nu} \lambda \nabla^2. \quad (17)$$

An RG analysis of this field theory shows that the critical dynamic exponent is given by  $z = \frac{d}{2}$  [9, 15, 18], which reduces to  $z = 1.5$  in  $d = 3$ .

In general, we do not expect biological systems to have exactly conserved spin, and therefore it is reasonable to assume that a dissipative,  $k$ -independent, term  $\eta\mathbb{I}_{\alpha\beta\gamma\nu}$  is also present into  $\Lambda_{\alpha\beta\gamma\nu}$ . Although from a purely hydrodynamic perspective - i.e. at long wavelengths and long times - the existence of a spin dissipation  $\eta$  would make the field  $\mathbf{s}$  a fast mode that can be dropped from the hydrodynamic description [9], it was shown in [10, 11] that this is not the case for finite-size systems. When the size of the system is finite, crossover phenomena that are usually ignored in the hydrodynamic limit may become relevant. In the present case, if the dissipation is weak  $\eta \ll \lambda^{\perp/\parallel}$ , the system undergoes an RG crossover between the conservative regime of Model G ( $\eta = 0$ ) and the fully overdamped dissipative case of Model A ( $\eta \neq 0$ ). Below a certain crossover length-scale  $L_c$  determined by the extent of dissipation, i.e. for modes with wavevector  $k \gg L_c^{-1}$ , the critical dynamics has a conservative nature as if  $\eta = 0$ , with  $z = 1.5$  [10, 11]. On the other hand, on length-scales larger than  $L_c$ ,  $k \ll L_c^{-1}$ , the dissipation overcomes and the dissipative result of Model A is recovered.

Natural swarms, in particular, definitively have a finite size. The largest swarm of which we have experimental data has *only*  $\sim 800$  individuals, while many swarms have less than 100 individuals (see Table I of SI-Section II). Moreover, in natural swarms, the spin dissipation must be small enough to keep the system in its underdamped phase, as otherwise the temporal correlation functions of the theory would not reproduce the experimental ones [5]. This means having a crossover length-scale  $L_c$  larger than the system's size so that experimentally one observes the conservative dynamics at all the accessible scales [10]. For this reason, we study the hydrodynamic field theory in the case in which the global spin is conserved, deriving the hydrodynamic theory at  $\eta = 0$ . We shall come back to the crossover between conservative and dissipative dynamics of the off equilibrium theory in SI-Section ID 3, to give a quantitative estimation of the scaling of  $L_c$  in terms of the dissipation  $\eta$ .

### 3. Putting together activity and inertial dynamics

Inspired by this equilibrium dynamic structure, we build the off-equilibrium theory describing inertial active matter by adding a term  $g\boldsymbol{\psi} \times \delta_s \mathcal{H}$  to the active field theory (11), identifying the rotation of  $\boldsymbol{\psi}$  induced by the conservation of  $\mathbf{s}$ . The dynamics for  $\mathbf{s}$  is instead constructed starting from Eq. (15), with advection added through the minimal substitution  $\partial_t \rightarrow \mathcal{D}_t = \partial_t + \gamma_s \mathbf{v} \cdot \nabla$ , encoding the fact that also the spin field is transported by the velocity. Here  $\gamma_s$  is not necessary equal to 1 since Galilean invariance is violated. Thus, the resulting equations of motion take the following form:

$$\partial_t \psi_\alpha + v_0 \gamma_v (\psi_\nu \partial_\nu) \psi_\alpha = -\Gamma \frac{\delta \mathcal{H}}{\delta \psi_\alpha} + g \psi_\beta \frac{\delta \mathcal{H}}{\delta s_{\alpha\beta}} - \partial_\alpha \mathcal{P} + \theta_\alpha, \quad (18)$$

$$\partial_t s_{\alpha\beta} + v_0 \gamma_s (\psi_\nu \partial_\nu) s_{\alpha\beta} = -\Lambda_{\alpha\beta\gamma\nu} \frac{\delta \mathcal{H}}{\delta s_{\gamma\nu}} + 2g \mathbb{I}_{\alpha\beta\gamma\nu} \psi_\gamma \frac{\delta \mathcal{H}}{\delta \psi_\nu} + \zeta_{\alpha\beta} \quad (19)$$

The theory will be studied in the incompressible case, therefore we omit all terms incompatible with this constraint, such as - for example - the two non-standard advective terms  $\mathbf{v} (\nabla \cdot \mathbf{v})$  and  $\nabla v^2$  arising in the compressible Toner and Tu theory as a consequence of the absence of Galilean invariance [13]. Incompressibility, however, does not forbid the presence of non-standard advection terms in the equation of motion for the spin and indeed we will demonstrate in SI-Section IC 4 that the RG does generate two of these terms, namely,

$$V_{\alpha\beta}^{\text{adv},1} = v_0 \mu_1 \gamma_s \partial_\nu (s_{\alpha\nu} \psi_\beta - s_{\beta\nu} \psi_\alpha), \quad (20)$$

$$V_{\alpha\beta}^{\text{adv},2} = v_0 \mu_2 \gamma_s \left[ \partial_\alpha (\psi_\nu s_{\nu\beta}) - \partial_\beta (\psi_\nu s_{\nu\alpha}) \right]. \quad (21)$$

Moreover, we will demonstrate that the RG also generates two of these anomalous mode-coupling terms in the equation of the spin (see SI-Section IC 4),

$$V_{\alpha\beta}^{\text{mc},1} = \phi_1 g \left[ \partial_\alpha (\psi_\nu \partial_\nu \psi_\beta) - \partial_\beta (\psi_\nu \partial_\nu \psi_\alpha) \right], \quad (22)$$

$$V_{\alpha\beta}^{\text{mc},2} = \phi_2 g \partial_\nu \left[ \psi_\nu (\partial_\alpha \psi_\beta - \partial_\beta \psi_\alpha) \right]. \quad (23)$$

Crucially, each one of these anomalous terms is the divergence of a current, implying that the RG does not generate non-conserved ( $k$ -independent) spin dissipation: the conservation of the total spin, hallmark of the mode-coupling theories [9], is preserved even out of equilibrium. The novel vertices are accompanied by four new dimensionless couplings  $\mu_1, \mu_2, \phi_1, \phi_2$ .

Some other terms might change the results we find in the present work. It is the case of linear couplings between spin and velocity in [19], which near criticality take the form  $\partial_t \psi_\alpha \sim \partial_\beta s_{\alpha\beta}$  and  $\partial_t s_{\alpha\beta} \sim \nabla^2 (\partial_\alpha \psi_\beta - \partial_\beta \psi_\alpha)$ . These terms modify the structure of linearized hydrodynamic equations, allowing the presence of propagators and correlation functions that mix the fields  $\mathbf{s}$  and  $\boldsymbol{\psi}$ . However, if such terms were included, the number of diagrams (which are not few even in the present calculation) would inevitably become enormous and impossible to manage. Moreover, the presence of these new linear terms does not modify the dynamic critical exponent  $z$  of the linear theory, while the presence of advection or inertial mode-coupling alone has a great impact on it. Therefore, the presence of these additional linear terms is expected only to perturb the effect of non-linear interactions on the critical exponents. Hence, we decide to focus on the study of spin-velocity couplings due to non-linear interactions only by working on the sub-manifold of the parameter space where such linear terms are not present. Because we find highly non-trivial results even in the case in which these linear terms are ignored, we believe that including them from the beginning could only slightly improve the results we find here.

The resulting equations of motion therefore become,

$$\partial_t \psi_\alpha + v_0 \gamma_v (\psi_\nu \partial_\nu) \psi_\alpha = -\Gamma \frac{\delta \mathcal{H}}{\delta \psi_\alpha} + g \psi_\beta \frac{\delta \mathcal{H}}{\delta s_{\alpha\beta}} - \partial_\alpha \mathcal{P} + \theta_\alpha, \quad (24)$$

$$\begin{aligned} & \partial_t s_{\alpha\beta} + v_0 \gamma_s (\psi_\nu \partial_\nu) s_{\alpha\beta} + v_0 \mu_1 \gamma_s \partial_\nu (s_{\alpha\nu} \psi_\beta - s_{\beta\nu} \psi_\alpha) + v_0 \mu_2 \gamma_s \left[ \partial_\alpha (\psi_\nu s_{\nu\beta}) - \partial_\beta (\psi_\nu s_{\nu\alpha}) \right] = \\ & = -\Lambda_{\alpha\beta\gamma\nu} \frac{\delta \mathcal{H}}{\delta s_{\gamma\nu}} + 2g \mathbb{I}_{\alpha\beta\gamma\nu} \psi_\gamma \frac{\delta \mathcal{H}}{\delta \psi_\nu} + \phi_1 g \left[ \partial_\alpha (\psi_\nu \partial_\nu \psi_\beta) - \partial_\beta (\psi_\nu \partial_\nu \psi_\alpha) \right] + \phi_2 g \partial_\nu \left[ \psi_\nu (\partial_\alpha \psi_\beta - \partial_\beta \psi_\alpha) \right] + \zeta_{\alpha\beta} \quad (25) \end{aligned}$$

In principle, these equations should be coupled to an additional equation for the density field  $\rho$ . However, as we will discuss in SI-Section IA 4, we can get rid of the density field by studying incompressible systems. Moreover, due to anisotropic effects caused by requiring the system to be incompressible, the kinetic tensor  $\Lambda$  in (17) will have two different diffusive coefficients  $\lambda^\perp \neq \lambda^\parallel$  for the longitudinal and transverse modes of  $\mathbf{s}$  [12].

Although the system we are dealing with is out of equilibrium, it is possible to identify the truly non-equilibrium dynamic terms from those arising from a free-energy functional  $\mathcal{H}$  that would survive also in the equilibrium limit  $v_0 \rightarrow 0$ . In this limit, the theory resembles the dynamical structure of Model G [9], therefore (14), (15) can be viewed as given by the merging of this equilibrium model [9] with Navier-Stokes equation [20]. The latter takes into account the active motion of particles, as it happens for the Toner and Tu theory.

Because the system is out of equilibrium, Einstein relations between the kinetic coefficients and the corresponding noise variances are not expected to hold. Therefore,  $\boldsymbol{\theta}$  and  $\boldsymbol{\zeta}$  of Eq. (24), (25) are white gaussian noises with zero mean  $\langle \boldsymbol{\theta} \rangle = \langle \boldsymbol{\zeta} \rangle = 0$  and variance given by

$$\langle \theta_\alpha(\mathbf{x}, t) \theta_\beta(\mathbf{x}', t') \rangle = 2\tilde{\Gamma} \delta_{\alpha\beta} \delta(\mathbf{x} - \mathbf{x}') \delta(t - t') , \quad (26)$$

$$\langle \zeta_{\alpha\beta}(\mathbf{x}, t) \zeta_{\gamma\nu}(\mathbf{x}', t') \rangle = -4\tilde{\Lambda}_{\alpha\beta\gamma\nu} \nabla^2 \delta(\mathbf{x} - \mathbf{x}') \delta(t - t') , \quad (27)$$

where  $\tilde{\Gamma} \neq \Gamma$  and the amplitude  $\tilde{\Lambda}$  to take the same form of  $\Lambda$  but with  $\tilde{\lambda}^\perp \neq \lambda^\perp$  and  $\tilde{\lambda}^\parallel \neq \lambda^\parallel$ .

All the other terms, which cannot be written as derivatives of a free energy functional, represent genuinely off-equilibrium interactions; these are advection and anomalous terms, which all occur as a consequence of the fact that individuals are not fixed on a network. As we already said, the couplings of the advective terms  $\gamma_v$  and  $\gamma_s$  need not be equal to 1 nor to each other, due to the absence of Galilean invariance [13]. Together with these active terms, we added also a pressure force  $-\partial_\alpha \mathcal{P}$  to (24), as it happens in Navier-Stokes, as well as in Toner-Tu equations.

#### 4. Enforcing incompressibility

In an active system, individuals are not fixed on a lattice but are free to move, allowing fluctuations in the local number density to arise. When the total number of individuals is conserved, these fluctuations occur on large space and time-scales, making the local density  $\rho(\mathbf{x}, t)$  one of the slow-modes characterizing the hydrodynamic behaviour of the system [9]. The time-evolution of the coarse-grained density field is thus given by the continuity equation,

$$\partial_t \rho + v_0 \nabla \cdot (\rho \boldsymbol{\psi}) = 0 , \quad (28)$$

where  $v_0 \boldsymbol{\psi} = \mathbf{v}$  is the velocity field. When considering systems with effective alignment interactions, the presence of density fluctuations plays a crucial role in determining the phenomenology of the ordering transition. While in equilibrium ferromagnetic systems the transition is known to be continuous, things radically change when activity is added [21–23]. The presence of density fluctuations generates instabilities when the transition is approached from the ordered state, thus leading to a discontinuous transition from finite to zero polarization. On the contrary, a continuous transition has been shown to arise if density fluctuations are suppressed [2].

In *small* systems the transition may acquire a continuous phenomenology as a consequence of finite-size effects [22], with density fluctuations not being strong enough to destabilize the second-order transition typical of equilibrium models [7]. Natural swarms have been shown to exhibit static and dynamic scaling laws typical of systems near to a continuous transition [5, 24], thus suggesting density fluctuations are not strong in determining the collective state, and that a continuous phenomenology approach can be used to model them. This is achieved by requiring a homogenous and constant density in eq (28), namely  $\rho(\mathbf{x}, t) = \rho_0$ , thus dropping it from the hydrodynamic description. Moreover, not only this provides a more realistic reference to the natural system, but it also decreases the technical intricacy of the RG calculation to a level that can be managed. Therefore, in the present work, we shall get rid of density fluctuations and study the theory at fixed density, namely assuming the system to be incompressible.

In an incompressible system Eq. (28) becomes a constraint on the field  $\mathbf{v}$  and, consequently, on the polarization  $\boldsymbol{\psi}$ :

$$\nabla \cdot \boldsymbol{\psi} = 0 \quad (29)$$

In Fourier-space this constraint translates into the following two equivalent statements,

$$k_\alpha \psi_\alpha(\mathbf{k}) = 0 \quad , \quad P_{\alpha\beta}^\perp(\mathbf{k}) \psi_\beta(\mathbf{k}) = \psi_\alpha(\mathbf{k}) , \quad (30)$$

where we have defined an object which is rather central to this calculation, namely the operator that projects  $\boldsymbol{\psi}$  onto the subspace orthogonal to  $\mathbf{k}$ ,

$$P_{\alpha\beta}^\perp(\mathbf{k}) = \delta_{\alpha\beta} - \frac{k_\alpha k_\beta}{k^2} \quad (31)$$

and where,

$$\psi_\alpha(\mathbf{x}) = \int_{\mathbf{k}} e^{i\mathbf{x}\cdot\mathbf{k}} \psi_\alpha(\mathbf{k}) . \quad (32)$$

Here and in the following, we will use the notation,

$$\int_{\mathbf{k}} = \int_{|\mathbf{k}| < \Lambda} \frac{d^d k}{(2\pi)^d} \quad (33)$$

where  $\Lambda$  is the ultraviolet cutoff of the theory, of the order of the inverse of the microscopic inter-particle distance. Summation over greek letter indices is understood.

In order to enforce incompressibility in equations (24) and (25), two steps are necessary. The first one is rather intuitive, and it consists in projecting the equation of motion for  $\psi$  (24) onto the subspace transverse to  $\mathbf{k}$ , which is a standard procedure [2, 20]; this is equivalent to say that the pressure term  $\partial_\alpha \mathcal{P}$  enforces the constraint. The second step is less intuitive and it has been discovered in the equilibrium limit  $v_0 \rightarrow 0$  [12]: the presence of a solenoidal constraint on the order parameter  $\psi$  requires to project also the *force*  $\delta_\psi \mathcal{H}$  that appears in the mode-coupling term of equation (25) [12]. This second projection leads to the presence of an additional non-linear interaction in the equation of motion for  $\mathbf{s}$ , the so-called DYNAMIC-Static (DYS) vertex, first found in [12],

$$\partial_t s_{\alpha\beta}(\mathbf{k}) \sim 2\kappa \mathbb{I}_{\alpha\beta\gamma\nu} \int_{\mathbf{q}, \mathbf{p}, \mathbf{h}} \psi_\gamma(\mathbf{q}) P_{\nu\rho}(\mathbf{q}) \psi_\sigma(\mathbf{p}) \psi_\sigma(\mathbf{h}) \psi_\rho(\mathbf{k} - \mathbf{q} - \mathbf{p} - \mathbf{h}) . \quad (34)$$

This vertex mixes the effects of the dynamic mode-coupling term and the static ferromagnetic  $\psi^4$  interaction. At equilibrium the coupling constant  $\kappa$  must obey the relation  $\kappa = gu$ , a crucial result that allows the equilibrium theory to be closed under renormalization [12]. However, off-equilibrium effects may lead to a violation of the relation between  $\kappa$ ,  $g$  and  $u$  meaning that, in general, one can have,

$$\kappa \neq gu \quad (35)$$

We shall demonstrate that at the new off-equilibrium inertial fixed point,  $u$  and  $g$  remain finite, while  $\kappa$  vanishes. For this reason, in the main text, we omitted altogether the DYS interaction in the equations of motion to facilitate reading. However, in the actual calculation described here, this interaction will be kept for two reasons. First, it allows maintaining a connection with the equilibrium theory of [12], in particular, recovering the same result as in equilibrium when  $v_0 \rightarrow 0$  is an important consistency check in such a complicated calculation. Secondly, the presence of this vertex is crucial for an additional reason: the high dimensionality of the parameter space (13 dimensions) and the intricate form of the  $\beta$ -functions will not allow us to find analytically the RG fixed point. To perform a successful numerical integration of the RG flow equations, the initial condition will be chosen in a region of the parameters space close to the equilibrium theory with solenoidal constraint. For the RG flow to go smoothly from the equilibrium to the off-equilibrium novel fixed point, it is technically crucial to keep this DYS interaction in the calculation, even though it eventually flows to zero at the new RG fixed point. In other words, although the DYS vertex is not relevant at the novel fixed point so that it does not contribute to the new value of the dynamical critical exponent, it is technically relevant to *find* the new fixed point in the far too vast parameters space.

### 5. The equations of motion of incompressible inertial active swarms

Incompressibility implies that the field  $\psi$  is only allowed to fluctuate in the direction perpendicular to  $\mathbf{k}$ , thus generating an anisotropic behaviour of the field  $\mathbf{s}$  that acquires two different relaxation rates for its longitudinal and transverse components with respect to  $\mathbf{k}$  [12]. Therefore the tensor  $\Lambda_{\alpha\beta\gamma\nu}$ , and consequently also  $\tilde{\Lambda}$ , takes the form,

$$\Lambda_{\alpha\beta\gamma\nu} = \left( \lambda^\perp \mathbb{P}_{\alpha\beta\gamma\nu}^\perp + \lambda^\parallel (\mathbb{I} - \mathbb{P}^\perp)_{\alpha\beta\gamma\nu} \right) k^2 , \quad (36)$$

where  $\mathbb{P}_{\alpha\beta\gamma\nu}^\perp$  is the projection operator in the anti-symmetric space of  $\mathbf{s}$  [12], which in  $k$ -space is given by

$$\mathbb{P}_{\alpha\beta\gamma\nu}^\perp(\mathbf{k}) = \mathbb{I}_{\alpha\beta\gamma\nu} - \mathbb{I}_{\alpha\beta\sigma\tau} P_{\sigma\gamma}^\perp(\mathbf{k}) P_{\tau\nu}^\perp(\mathbf{k}) , \quad (37)$$

and we recall that,

$$\mathbb{I}_{\alpha\beta\gamma\nu} = \frac{\delta_{\alpha\gamma}\delta_{\beta\nu} - \delta_{\alpha\nu}\delta_{\beta\gamma}}{2} . \quad (38)$$

After symmetrizing terms containing powers of the same field, the incompressible equations of motion in  $k$ -space, finally become,

$$\begin{aligned} \partial_t \psi_\alpha(\mathbf{k}, t) + \left(k^2 \Gamma + m\right) \psi_\alpha(\mathbf{k}, t) &= \theta_\alpha - v_0 \frac{i\gamma_\nu}{2} P_{\alpha\beta\gamma}(\mathbf{k}) \int_{\mathbf{q}} \psi_\beta(\mathbf{q}, t) \psi_\gamma(\mathbf{k} - \mathbf{q}, t) \\ &\quad - \frac{J}{3} Q_{\alpha\beta\gamma\nu}(\mathbf{k}) \int_{\mathbf{q}, \mathbf{h}} \psi_\beta(\mathbf{q}, t) \psi_\gamma(\mathbf{h}, t) \psi_\nu(\mathbf{k} - \mathbf{q} - \mathbf{h}, t) \\ &\quad + g P_{\alpha\rho}^\perp(\mathbf{k}) \mathbb{I}_{\rho\beta\gamma\nu} \int_{\mathbf{q}} \psi_\beta(\mathbf{k} - \mathbf{q}, t) s_{\gamma\nu}(\mathbf{q}, t) , \end{aligned} \quad (39)$$

$$\begin{aligned} \partial_t s_{\alpha\beta}(\mathbf{k}, t) + \Lambda_{\alpha\beta\gamma\nu} s_{\gamma\nu}(\mathbf{k}, t) &= \zeta_{\alpha\beta} - v_0 i \gamma_s \mathbb{I}_{\alpha\beta\gamma\nu} k_\rho \int_{\mathbf{q}} s_{\gamma\nu}(\mathbf{q}, t) \psi_\rho(\mathbf{k} - \mathbf{q}, t) \\ &\quad - 2 v_0 i \mu_1 \gamma_s \mathbb{I}_{\alpha\beta\rho\eta} \mathbb{I}_{\rho\tau\gamma\nu} k_\tau \int_{\mathbf{q}} s_{\gamma\nu}(\mathbf{q}, t) \psi_\eta(\mathbf{k} - \mathbf{q}, t) \\ &\quad - 2 v_0 i \mu_2 \gamma_s \mathbb{I}_{\alpha\beta\rho\sigma} \mathbb{I}_{\rho\eta\gamma\nu} k_\sigma \int_{\mathbf{q}} s_{\gamma\nu}(\mathbf{q}, t) \psi_\eta(\mathbf{k} - \mathbf{q}, t) \\ &\quad + 2 g \mathbb{I}_{\alpha\beta\gamma\nu} \int_{\mathbf{q}} \mathbf{k} \cdot \mathbf{q} \psi_\gamma(-\mathbf{q} + \mathbf{k}/2, t) \psi_\nu(\mathbf{q} + \mathbf{k}/2, t) \\ &\quad + 2 \Phi_1 g \mathbb{I}_{\alpha\beta\rho\sigma} \mathbb{I}_{\rho\tau\gamma\nu} \int_{\mathbf{q}} k_\sigma q_\tau \psi_\gamma(-\mathbf{q} + \mathbf{k}/2, t) \psi_\nu(\mathbf{q} + \mathbf{k}/2, t) \\ &\quad + 2 \Phi_2 g \mathbb{I}_{\alpha\beta\rho\sigma} \mathbb{I}_{\rho\tau\gamma\nu} \int_{\mathbf{q}} k_\tau q_\sigma \psi_\gamma(-\mathbf{q} + \mathbf{k}/2, t) \psi_\nu(\mathbf{q} + \mathbf{k}/2, t) \\ &\quad + \frac{\kappa}{6} \int_{\mathbf{q}, \mathbf{h}, \mathbf{p}} K_{\alpha\beta\gamma\nu\sigma\tau}(\mathbf{k}, \mathbf{q}, \mathbf{h}, \mathbf{p}, \mathbf{k} - \mathbf{q} - \mathbf{h} - \mathbf{p}) \times \\ &\quad \times \psi_\gamma(\mathbf{q}, t) \psi_\nu(\mathbf{h}, t) \psi_\sigma(\mathbf{p}, t) \psi_\tau(\mathbf{k} - \mathbf{q} - \mathbf{h} - \mathbf{p}, t) , \end{aligned} \quad (40)$$

where the following tensors were introduced,

$$P_{\alpha\beta\gamma}(\mathbf{k}) = k_\beta P_{\alpha\gamma}^\perp(\mathbf{k}) + k_\gamma P_{\alpha\beta}^\perp(\mathbf{k}) , \quad (41)$$

$$Q_{\alpha\beta\gamma\nu}(\mathbf{k}) = P_{\alpha\beta}^\perp(\mathbf{k}) \delta_{\gamma\nu} + P_{\alpha\gamma}^\perp(\mathbf{k}) \delta_{\beta\nu} + P_{\alpha\nu}^\perp(\mathbf{k}) \delta_{\beta\gamma} , \quad (42)$$

$$\begin{aligned} K_{\alpha\beta\gamma\nu\sigma\tau}(\mathbf{k}, \mathbf{p}_1, \mathbf{p}_2, \mathbf{p}_3, \mathbf{p}_4) &= \mathbb{I}_{\alpha\beta\gamma\rho} Q_{\rho\nu\sigma\tau}(\mathbf{k} - \mathbf{p}_1) + \mathbb{I}_{\alpha\beta\nu\rho} Q_{\rho\gamma\sigma\tau}(\mathbf{k} - \mathbf{p}_2) + \\ &\quad + \mathbb{I}_{\alpha\beta\sigma\rho} Q_{\rho\gamma\nu\tau}(\mathbf{k} - \mathbf{p}_3) + \mathbb{I}_{\alpha\beta\tau\rho} Q_{\rho\gamma\nu\sigma}(\mathbf{k} - \mathbf{p}_4) , \end{aligned} \quad (43)$$

and the noises have correlations,

$$\langle \theta_\alpha(\mathbf{k}, t) \theta_\beta(\mathbf{k}', t') \rangle = 2 (2\pi)^d \tilde{\Gamma} P_{\alpha\beta}^\perp(\mathbf{k}) \delta^{(d)}(\mathbf{k} + \mathbf{k}') \delta(t - t') , \quad (44)$$

$$\langle \zeta_{\alpha\beta}(\mathbf{k}, t) \zeta_{\gamma\nu}(\mathbf{k}', t') \rangle = 4 (2\pi)^d \tilde{\Lambda}_{\alpha\beta\gamma\nu}(\mathbf{k}) \delta^{(d)}(\mathbf{k} + \mathbf{k}') \delta(t - t') , \quad (45)$$

Finally, to simplify the notation, in (39), (40) the following reduced parameters have been defined,

$$J = \Gamma u \quad \Phi_1 = -2(\phi_1 + \phi_2) , \quad (46)$$

$$m = \Gamma r \quad \Phi_2 = -2\phi_2 . \quad (47)$$

## B. Setting up the stage for the diagrammatic expansion

### 1. The Martin-Siggia-Rose-Janssen-De Dominicis action

In order to employ RG to study the critical dynamics of our model we follow the method proposed by Martin, Siggia, Rose [25], Janssen [26] and De Dominicis [27]. The Martin-Siggia-Rose-Janssen-De Dominicis (MSRJD) formalism

allows to describe the behaviour of fields evolving according to stochastic differential equations in terms of a field theory formulated using path integrals. The dynamic behaviour of the field  $\phi$ , defined by the following Ito stochastic differential equation,

$$\mathcal{F}[\phi] - \theta = 0 \quad (48)$$

is reproduced by the field-theoretical action  $\mathcal{S}$  given by,

$$\mathcal{S}[\phi, \hat{\phi}] = \int d\mathbf{x} dt \hat{\phi}_\alpha \mathcal{F}_\alpha[\phi] - \hat{\phi}_\alpha L_{\alpha\beta} \hat{\phi}_\beta \quad (49)$$

Here  $\mathcal{F}$  is the deterministic evolution operator,  $\theta$  a white gaussian noise with variance  $2L_{\alpha\beta}$ . The introduction of the hatted field  $\hat{\phi}$  in the action is the price that has to be paid to exploit the path integral formulation, using the standard rules of static renormalization and writing the perturbative series in terms of Feynman diagrams. The field theoretical description reproduces the stochastic dynamics in the sense that, for a given observable  $\mathcal{O}[\phi]$ ,

$$\langle \mathcal{O} \rangle = \langle \mathcal{O} \rangle_S \quad (50)$$

where  $\langle \mathcal{O} \rangle$  is the average value of  $\mathcal{O}$  over all possible realizations of the noise  $\theta$ , while

$$\langle \mathcal{O} \rangle_S = \frac{1}{\mathcal{Z}} \int \mathcal{D}\phi \int \mathcal{D}\hat{\phi} \mathcal{O}[\phi] e^{-\mathcal{S}[\phi, \hat{\phi}]} \quad (51)$$

Thanks to this equivalence, the critical dynamics can be investigated by studying the action  $\mathcal{S}$  through RG techniques. The gaussian part of the action  $\mathcal{S}$  derives from the linear dynamics, namely the linear part of the operator  $\mathcal{F}$ , while the interactions derive from non-linear terms. Within this formalism, an external source  $\mathbf{h}$  introduced in the dynamical equation of  $\phi$  is coupled to  $\hat{\psi}$  in the effective action. Therefore, the response function, known also as Green function or propagator, can be written as,

$$\frac{\delta \langle \phi_\alpha(\mathbf{x}, t) \rangle}{\delta h_\beta(\mathbf{x}', t')} = \langle \phi_\alpha(\mathbf{x}, t) \hat{\phi}_\beta(\mathbf{x}', t') \rangle \quad (52)$$

For this reason,  $\hat{\phi}$  takes the name ‘response field’.

The MSRDJ action  $\mathcal{S}$  for the stochastic equations (39) and (40) depends upon four fields:  $\psi$ ,  $\hat{\psi}$ ,  $\mathbf{s}$  and  $\hat{\mathbf{s}}$ . The action can be split in the following terms,

$$\mathcal{S}[\psi, \hat{\psi}, \mathbf{s}, \hat{\mathbf{s}}] = \mathcal{S}_{0,\psi}[\psi, \hat{\psi}] + \mathcal{S}_{0,\mathbf{s}}[\mathbf{s}, \hat{\mathbf{s}}] + \mathcal{S}_I[\psi, \hat{\psi}, \mathbf{s}, \hat{\mathbf{s}}] \quad (53)$$

where  $\mathcal{S}_{0,\psi}$  and  $\mathcal{S}_{0,\mathbf{s}}$  are the gaussian parts of the action, respectively coming from the linear dynamic terms of the equations of motion of  $\psi$  and  $\mathbf{s}$ , while  $\mathcal{S}_I$  is the interacting part. From Eq. (49) we have,

$$\mathcal{S}_{0,\psi}[\psi, \hat{\psi}] = \int_{\tilde{\mathbf{k}}} \hat{\psi}_\alpha(-\tilde{\mathbf{k}}) \left[ -i\omega + \Gamma k^2 + m \right] \psi_\alpha(\tilde{\mathbf{k}}) - \tilde{\Gamma} \hat{\psi}_\alpha(-\tilde{\mathbf{k}}) P_{\alpha\beta}^\perp(\mathbf{k}) \hat{\psi}_\beta(\tilde{\mathbf{k}}) \quad (54)$$

$$\mathcal{S}_{0,\mathbf{s}}[\mathbf{s}, \hat{\mathbf{s}}] = \frac{1}{2} \int_{\tilde{\mathbf{k}}} \hat{\mathbf{s}}_{\alpha\beta}(-\tilde{\mathbf{k}}) \left[ -i\omega \mathbb{I}_{\alpha\beta\gamma\nu} + \Lambda_{\alpha\beta\gamma\nu} \right] s_{\gamma\nu}(\tilde{\mathbf{k}}) - \hat{\mathbf{s}}_{\alpha\beta}(-\tilde{\mathbf{k}}) \tilde{\Lambda}_{\alpha\beta\gamma\nu} \hat{\mathbf{s}}_{\gamma\nu}(\tilde{\mathbf{k}}) \quad (55)$$

$$\begin{aligned} \mathcal{S}_I[\psi, \hat{\psi}, \mathbf{s}, \hat{\mathbf{s}}] = & -g \int_{\tilde{\mathbf{k}}, \tilde{\mathbf{q}}} \hat{\psi}_\alpha(-\tilde{\mathbf{k}}) P_{\alpha\rho}^\perp(\mathbf{k}) \mathbb{I}_{\rho\beta\gamma\nu} \psi_\beta(\tilde{\mathbf{k}} - \tilde{\mathbf{q}}) s_{\gamma\nu}(\tilde{\mathbf{q}}) + \\ & -g \mathbb{I}_{\alpha\beta\rho\sigma} \mathbb{I}_{\rho\tau\gamma\nu} \int_{\tilde{\mathbf{k}}, \tilde{\mathbf{q}}} \hat{\mathbf{s}}_{\alpha\beta}(-\tilde{\mathbf{k}}) [\mathbf{k} \cdot \mathbf{q} \delta_{\sigma\tau} + \Phi_1 k_\sigma q_\tau + \Phi_2 q_\sigma k_\tau] \psi_\gamma(-\tilde{\mathbf{q}} + \tilde{\mathbf{k}}/2) \psi_\nu(\tilde{\mathbf{q}} + \tilde{\mathbf{k}}/2) - \\ & + v_0 \frac{i\gamma_\nu}{2} \int_{\tilde{\mathbf{k}}, \tilde{\mathbf{q}}} \hat{\psi}_\alpha(-\tilde{\mathbf{k}}) P_{\alpha\beta\gamma}(\mathbf{k}) \psi_\beta(\tilde{\mathbf{q}}) \psi_\gamma(\tilde{\mathbf{k}} - \tilde{\mathbf{q}}) - \\ & + v_0 \frac{i\gamma_s}{2} \mathbb{I}_{\alpha\beta\rho\sigma} \mathbb{I}_{\rho\tau\gamma\nu} \int_{\tilde{\mathbf{k}}, \tilde{\mathbf{q}}} \hat{\mathbf{s}}_{\alpha\beta}(-\tilde{\mathbf{k}}) [k_\eta \delta_{\sigma\tau} + 2\mu_1 k_\tau \delta_{\sigma\eta} + 2\mu_2 k_\sigma \delta_{\tau\eta}] s_{\gamma\nu}(\tilde{\mathbf{q}}) \psi_\eta(\tilde{\mathbf{k}} - \tilde{\mathbf{q}}) - \\ & + \frac{J}{3} \int_{\tilde{\mathbf{k}}, \tilde{\mathbf{q}}, \tilde{\mathbf{h}}} \hat{\psi}_\alpha(-\tilde{\mathbf{k}}) Q_{\alpha\beta\gamma\nu}(\mathbf{k}) \psi_\beta(\tilde{\mathbf{q}}) \psi_\gamma(\tilde{\mathbf{h}}) \psi_\nu(\tilde{\mathbf{k}} - \tilde{\mathbf{q}} - \tilde{\mathbf{h}}) + \\ & - \frac{\kappa}{12} \int_{\tilde{\mathbf{k}}, \tilde{\mathbf{q}}, \tilde{\mathbf{h}}, \tilde{\mathbf{p}}} \hat{\mathbf{s}}_{\alpha\beta}(-\tilde{\mathbf{k}}) K_{\alpha\beta\gamma\nu\sigma\tau}(\mathbf{k}, \mathbf{q}, \mathbf{h}, \mathbf{p}, \mathbf{k} - \mathbf{q} - \mathbf{h} - \mathbf{p}) \psi_\gamma(\tilde{\mathbf{q}}) \psi_\nu(\tilde{\mathbf{h}}) \psi_\sigma(\tilde{\mathbf{p}}) \psi_\tau(\tilde{\mathbf{k}} - \tilde{\mathbf{q}} - \tilde{\mathbf{h}} - \tilde{\mathbf{p}}) \end{aligned} \quad (56)$$

We wrote the effective action in  $k$  and  $\omega$  space, where the generic field  $\phi$  is given by

$$\phi(\mathbf{x}, t) = \int_{\tilde{\mathbf{k}}} e^{i(\mathbf{x} \cdot \tilde{\mathbf{k}} - t\omega)} \phi(\tilde{\mathbf{k}}), \quad (57)$$

with  $\tilde{\mathbf{k}} = (\mathbf{k}, \omega)$  and,

$$\int_{\tilde{\mathbf{k}}} = \int_{|\mathbf{k}| < \Lambda} \frac{d^d k}{(2\pi)^d} \int_{-\infty}^{\infty} \frac{d\omega}{2\pi}. \quad (58)$$

Notice that there is no cutoff in the frequency  $\omega$ .

## 2. Free theory: propagators and correlation functions

The starting point to build the perturbative expansion of the equations of motion is the free theory, obtained by setting to zero all the dynamic non-linear couplings, namely  $g$ ,  $\gamma_v$ ,  $\gamma_s$ ,  $J$  and  $\kappa$ . From the gaussian part of the action, given by Eqs. (54) and (55), we can derive the expressions for the bare propagators and correlation functions for the effective field theory, which are the same as Model G with solenoidal constraint [12], and are given by,

$$\langle \psi_\alpha(\tilde{\mathbf{k}}) \hat{\psi}_\beta(\tilde{\mathbf{q}}) \rangle_0 = \mathbb{G}_{\alpha\beta}^{0,\psi}(\tilde{\mathbf{k}}) \hat{\delta}(\tilde{\mathbf{k}} + \tilde{\mathbf{q}}), \quad \langle s_{\alpha\beta}(\tilde{\mathbf{k}}) \hat{s}_{\gamma\nu}(\tilde{\mathbf{q}}) \rangle_0 = \mathbb{G}_{\alpha\beta\gamma\nu}^{0,s}(\tilde{\mathbf{k}}) \hat{\delta}(\tilde{\mathbf{k}} + \tilde{\mathbf{q}}), \quad (59)$$

$$\langle \psi_\alpha(\tilde{\mathbf{k}}) \psi_\beta(\tilde{\mathbf{q}}) \rangle_0 = \mathbb{C}_{\alpha\beta}^{0,\psi}(\tilde{\mathbf{k}}) \hat{\delta}(\tilde{\mathbf{k}} + \tilde{\mathbf{q}}), \quad \langle s_{\alpha\beta}(\tilde{\mathbf{k}}) s_{\gamma\nu}(\tilde{\mathbf{q}}) \rangle_0 = \mathbb{C}_{\alpha\beta\gamma\nu}^{0,s}(\tilde{\mathbf{k}}) \hat{\delta}(\tilde{\mathbf{k}} + \tilde{\mathbf{q}}), \quad (60)$$

where  $\hat{\delta}(\tilde{\mathbf{h}}) = (2\pi)^{d+1} \delta^{(d)}(\mathbf{h}) \delta(\omega_h)$ . The subscripted zeros on thermal averages indicate that they are computed within the non-interacting theory. The tensors  $\mathbb{G}$  and  $\mathbb{C}$  are given by,

$$\mathbb{G}_{\alpha\beta}^{0,\psi}(\tilde{\mathbf{k}}) = G_{0,\psi}(\tilde{\mathbf{k}}) \delta_{\alpha\beta} \quad (61)$$

$$\mathbb{C}_{\alpha\beta}^{0,\psi}(\tilde{\mathbf{k}}) = C_{0,\psi}(\tilde{\mathbf{k}}) P_{\alpha\beta}^\perp(\mathbf{k}) \quad (62)$$

$$\mathbb{G}_{\alpha\beta\gamma\nu}^{0,s}(\tilde{\mathbf{k}}) = G_{0,s}^\perp(\tilde{\mathbf{k}}) \mathbb{P}_{\alpha\beta\gamma\nu}^\perp(\mathbf{k}) + G_{0,s}^\parallel(\tilde{\mathbf{k}}) (\mathbb{I} - \mathbb{P}^\perp)_{\alpha\beta\gamma\nu}(\mathbf{k}) \quad (63)$$

$$\mathbb{C}_{\alpha\beta\gamma\nu}^{0,s}(\tilde{\mathbf{k}}) = C_{0,s}^\perp(\tilde{\mathbf{k}}) \mathbb{P}_{\alpha\beta\gamma\nu}^\perp(\mathbf{k}) + C_{0,s}^\parallel(\tilde{\mathbf{k}}) (\mathbb{I} - \mathbb{P}^\perp)_{\alpha\beta\gamma\nu}(\mathbf{k}) \quad (64)$$

In Eq. (61), (63), (62) and (64) we have,

$$G_{0,\psi}(\mathbf{k}, \omega) = \frac{1}{-i\omega + \Gamma k^2 + m} \quad C_{0,\psi}(\mathbf{k}, \omega) = \frac{2\tilde{\Gamma}}{\omega^2 + (m + \Gamma k^2)^2} \quad (65)$$

$$G_{0,s}^\perp(\mathbf{k}, \omega) = \frac{2}{-i\omega + \lambda^\perp k^2} \quad C_{0,s}^\perp(\mathbf{k}, \omega) = \frac{4\tilde{\lambda}^\perp k^2}{\omega^2 + (\lambda^\perp k^2)^2} \quad (66)$$

$$G_{0,s}^\parallel(\mathbf{k}, \omega) = \frac{2}{-i\omega + \lambda^\parallel k^2} \quad C_{0,s}^\parallel(\mathbf{k}, \omega) = \frac{4\tilde{\lambda}^\parallel k^2}{\omega^2 + (\lambda^\parallel k^2)^2} \quad (67)$$

In the diagrammatic framework, the fields  $\psi$  and  $\hat{\psi}$  are represented with a solid line, while the fields  $s$  and  $\hat{s}$  are represented with wavy lines. Bare propagators and correlation functions thus take the following graphical representation

$$\langle \psi_\alpha \hat{\psi}_\beta \rangle_0 = \text{solid line with arrow} \quad \langle s_{\alpha\beta} \hat{s}_{\gamma\nu} \rangle_0 = \text{wavy line with arrow} \quad (68)$$

$$\langle \psi_\alpha \psi_\beta \rangle_0 = \text{solid line} \quad \langle s_{\alpha\beta} s_{\gamma\nu} \rangle_0 = \text{wavy line} \quad (69)$$

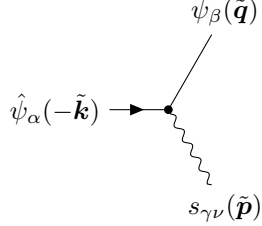
where the arrows in the propagators always point in the direction of the response field.

## 3. Non-linear terms: the vertices

The six terms that compose  $\mathcal{S}_I$  represent the non-linear interactions in the equations of motion. Each interaction involves one response field, identifying the equation of motion in which the corresponding non-linearity appears:  $\hat{\psi}$  if the vertex comes from a non-linearity in the equation of  $\psi$ ,  $\hat{s}$  if it comes from a non-linearity in the equation of  $s$  In

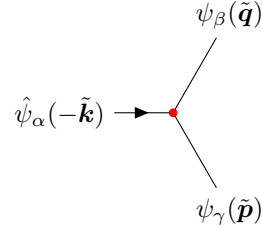
the diagrammatic framework, these interactions are graphically represented by vertices, in which different lines merge, each representing one of the fields involved in the interaction. We remind that full lines represent  $\hat{\psi}$  and  $\psi$  fields, while wavy lines represent  $\hat{s}$  and  $s$  fields. Moreover, an *entering* arrow is used to identify the leg representing the response field. We shall choose vertices to have opposed signs with respect to the interactions; the convenience of this choice is that vertices play a crucial role in building Feynman diagrams, which come from the expansion of  $\exp(-\mathcal{S})$ .

The first vertex involving  $\hat{\psi}$  represents the mode coupling non-linearity proportional to the dynamic coupling  $g$ ,



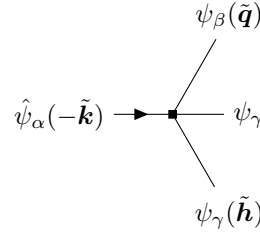
$$= gP_{\alpha\rho}^\perp(\mathbf{k})\mathbb{I}_{\rho\beta\gamma\nu}\hat{\delta}(\tilde{\mathbf{k}} - \tilde{\mathbf{q}} - \tilde{\mathbf{p}}), \quad (70)$$

The second interaction involving  $\hat{\psi}$  is the self-propulsion (or advection) interaction coming from the convective derivative in the equation of motion. This vertex is proportional to  $v_0\gamma_\nu$ , and it vanishes when the microscopic speed does. Graphically, this interaction is represented by



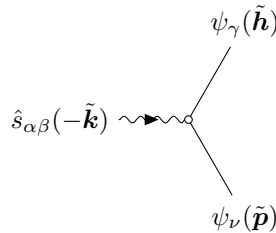
$$= -v_0\frac{i\gamma_\nu}{2}P_{\alpha\beta\nu}(\mathbf{k})\hat{\delta}(\tilde{\mathbf{k}} - \tilde{\mathbf{q}} - \tilde{\mathbf{p}}), \quad (71)$$

The third vertex involving  $\hat{\psi}$  derives from the ferromagnetic  $\psi^3$  Landau-Ginzburg interaction, proportional to  $J$ . It is represented by the term,



$$= -\frac{J}{3}Q_{\alpha\beta\gamma\nu}(\mathbf{k})\hat{\delta}(\tilde{\mathbf{k}} - \tilde{\mathbf{q}} - \tilde{\mathbf{p}} - \tilde{\mathbf{h}}), \quad (72)$$

The other three vertices involve one field  $\hat{s}$  and derive from the equation for the spin. The first one represents the dynamic mode-coupling interaction proportional to  $g$  with the addition of the two mode-coupling anomalous terms, with different tensorial structure,



$$= \frac{g}{2}\mathbb{I}_{\alpha\beta\rho\sigma}\mathbb{I}_{\rho\tau\gamma\nu}\left[\left(p^2 - h^2\right)\delta_{\sigma\tau} + \Phi_1 p_\sigma^{(+)}p_\tau^{(-)} + \Phi_2 p_\sigma^{(-)}p_\tau^{(+)}\right]\hat{\delta}(\tilde{\mathbf{k}} - \tilde{\mathbf{h}} - \tilde{\mathbf{p}}), \quad (73)$$

where  $\mathbf{p}^{(+)} = \mathbf{p} + \mathbf{h}$  while  $\mathbf{p}^{(-)} = \mathbf{p} - \mathbf{h}$ . This vertex vanishes when  $\mathbf{h} = \mathbf{p}$ , guaranteeing that this interaction does not contribute to the dynamics of the total spin  $S(t) = s(\mathbf{k} = 0, t)$ . The anomalous mode coupling terms are those proportional to  $\Phi_{1,2}$ . From a technical point of view, it is essential to note that this vertex can be rewritten in an

alternative form; by using the delta function, together with a symmetric distribution of the momenta, one has,

$$= g \mathbb{I}_{\alpha\beta\rho\sigma} \mathbb{I}_{\rho\tau\gamma\nu} [\mathbf{k} \cdot \mathbf{q} \delta_{\sigma\tau} + \Phi_1 k_\sigma q_\tau + \Phi_2 q_\sigma k_\tau] . \quad (74)$$

This second form is convenient for two reasons: first, it has a simpler structure, which makes it easier to recognize corrections to the coupling constant  $g$ ; secondly, in this form, it is more transparent to demonstrate the diagrammatic origin of the anomalous terms, a derivation that we will see later on in SI-Section IC 4. On the other hand, the first form of this same vertex, equation (73), is handier when calculating diagrams in which  $\hat{s}_{\alpha\beta}$  appears as an internal leg.

The second vertex involving  $\hat{\mathbf{s}}$  is the self-propulsion interaction, coming from the fact that  $\mathbf{s}$  is advected by the velocity  $v_0\boldsymbol{\psi}$ , and it is proportional to  $v_0\gamma_s$ . Graphically, this interaction is represented by,

$$= -v_0 \frac{i\gamma_s}{2} \mathbb{I}_{\alpha\beta\rho\sigma} \mathbb{I}_{\rho\tau\gamma\nu} [k_\eta \delta_{\sigma\tau} + 2\mu_1 k_\tau \delta_{\sigma\eta} + 2\mu_2 k_\sigma \delta_{\tau\eta}] \hat{\delta}(\tilde{\mathbf{k}} - \tilde{\mathbf{q}} - \tilde{\mathbf{p}}) , \quad (75)$$

Also this interaction vanishes when  $\mathbf{q} = \mathbf{p}$ , and therefore does not contribute to the dynamics of the total spin either. This vertex takes into account also the anomalous advection of  $\mathbf{s}$  through the terms proportional to  $\mu_{1,2}$ .

The last interaction term is the DYNAMIC-Static (DYS) vertex [12]. This interaction mixes the ferromagnetic-like interaction and the mode-coupling dynamic term, as a consequence of the presence of incompressibility. It represents the effects of the Landau confining potential on the dynamics of  $\mathbf{s}$ , mediated by the mode-coupling dynamic interaction. It takes the following form,

$$= \frac{\kappa}{12} K_{\alpha\beta\gamma\nu\sigma\tau}(\mathbf{k}, \mathbf{p}_1, \mathbf{p}_2, \mathbf{p}_3, \mathbf{p}_4) \hat{\delta}(\tilde{\mathbf{k}} - \tilde{\mathbf{p}}_1 - \tilde{\mathbf{p}}_2 - \tilde{\mathbf{p}}_3 - \tilde{\mathbf{p}}_4) . \quad (76)$$

This interaction does not vanish when  $\mathbf{k} = 0$ , and thus it contributes to the dynamics of the total spin. However, we shall be careful not to confuse the absence of conservation with the presence of dissipation. If the spin was largely dissipated, it would become a non-hydrodynamic variable whose behaviour does not affect that of the order parameter. As shown in [12], where the fixed network approximation of the incompressible theory developed here is analyzed, even though the spin may not be globally conserved due to the DYS interaction, it represents still an hydrodynamic slow mode. This is because the DYS vertex does not involve the spin, and thus represents the effects of the slow-mode  $\boldsymbol{\psi}$ . Even if this effect remains finite as  $\mathbf{k} \rightarrow 0$ , it may only be responsible for slow variations of the total spin  $\mathbf{s}$ . Hence, although the total spin is not conserved, it is not even dissipated and thus it undergoes a generalized precession caused by the DYS vertex [12].

### C. The diagrammatic expansion

#### 1. Dynamical RG in momentum shell: general procedure

The momentum shell RG scheme [28–32] provides an explicit method to calculate critical exponents. By integrating out the short-wavelength modes iteratively, the RG generates a flow in the parameter space that eventually converges

towards a fixed point. The study of the linearized flow equations near an attractive fixed point allows computing explicitly the critical exponents of the theory. Universality, in this RG context, consists of the fact that one single fixed point rules the long-wavelength behaviour of a large class of theories, each one identified by a different initial point in the parameter space. The RG flow is defined by a set of recursive relations, obtained by iterating a RG transformation of the effective action of the field theory. The RG transformation consists of two steps: *i*) the probability distribution of the fields is marginalized by integrating short-wavelength modes on the shell  $b^{-1}\Lambda < k < \Lambda$ , with  $b > 1$ , hence effectively decreasing the cutoff in momentum space; *ii*) space and time are rescaled, so to formally restore the same cutoff as the original theory. The action obtained after one RG transformation has different parameters and it describes the system when it is observed on a larger scale. However, since the partition function remains the same up to a multiplicative constant, the physical observables are left unchanged. The flow equations are obtained under the form of recursive relations, describing how the parameters at the iteration  $(l + 1)$  can be obtained starting from those at step  $l$ .

In the gaussian theory, namely when all interaction terms vanish, the shell integration is harmless since modes at different wavelengths are independent [29], and thus the RG flow is trivial: essentially each parameter rescales according to naive dimensional analysis. However, when non-gaussian interactions are present, the shell integration couples long and short wavelength modes, generating nontrivial corrections to the bare action. These corrections can be computed within a perturbative expansion in powers of  $\epsilon = d_c - d$ , where  $d_c$  is the upper critical dimension, namely the dimension above which mean-field theory is exact, while  $d$  is the spatial dimension. This expansion method to compute the critical exponents, known as  $\epsilon$ -expansion, was proposed by K.G. Wilson in the seminal paper “*Critical exponents in 3.99 dimensions*” [33], in honour of which we chose the title of the present work.

In order to perform the shell integration, it is convenient to split the fields in their Infra-Red (IR) and Ultra-Violet (UV) modes [29], and write the partition function as,

$$\mathcal{Z} = \int \mathcal{D}\phi e^{-\mathcal{S}[\phi]} = \int \mathcal{D}\phi^{<} \mathcal{D}\phi^{>} e^{-\mathcal{S}[\phi^{<} + \phi^{>}]} \quad (77)$$

where  $\phi$  stands for all the fields of the theory, while superscripts  $<$  and  $>$  indicate whether the field has momenta lower (IR modes) or higher (UV modes) than  $\Lambda/b$  respectively. The action  $\mathcal{S}$  can then be written in the following form,

$$\mathcal{S}[\phi^{<} + \phi^{>}] = \mathcal{S}[\phi^{<}] + \mathcal{S}_0[\phi^{>}] - \mathcal{V}[\phi^{<}, \phi^{>}] \quad (78)$$

where  $\mathcal{S}_0$  is the gaussian part of the action while  $\mathcal{V}$  represents all the interactions between UV and IR modes. Integrating out short wavelength details, namely performing the integration over the UV modes  $\phi^{>}$  with wavevector on the shell, leads to,

$$\mathcal{Z} = \mathcal{Z}_0^{>} \int \mathcal{D}\phi^{<} e^{-\mathcal{S}[\phi^{<}] - \Delta\mathcal{S}[\phi^{<}]} \quad (79)$$

where,

$$e^{-\Delta\mathcal{S}[\phi^{<}]} = \frac{1}{\mathcal{Z}_0^{>}} \int \mathcal{D}\phi^{>} e^{-\mathcal{S}_0[\phi^{>}]} e^{\mathcal{V}[\phi^{<}, \phi^{>}]} \quad (80)$$

is the gaussian average of  $e^{\mathcal{V}[\phi^{<}, \phi^{>}]}$  over the UV fields with on-shell momentum, and  $\Delta\mathcal{S}[\phi^{<}]$  represents the corrections to the bare action  $\mathcal{S}$  due to the shell integration. By assuming the interaction couplings *small* – assumption that will be verified *a posteriori* at the stable fixed point – it is possible to expand  $e^{\mathcal{V}}$  in powers of the couplings. The expansion of  $\Delta\mathcal{S}$  can be graphically represented as an expansion in Feynman diagrams, composed only by connected diagrams [29]. This shell integration is usually performed under a thin-shell approximation, namely taking  $b \sim 1$ : in this limit  $\Delta\mathcal{S}$  is proportional to the shell thickness  $1 - b^{-1} \simeq \ln b$ . The final result after the integration over the UV modes  $\phi^{>}$  is an effective action with a new cutoff  $\Lambda/b$  and modified parameters, namely,

$$\mathcal{P}_0 \rightarrow \mathcal{P}_0 + \mathcal{P}_0 \delta\mathcal{P} \ln b = \mathcal{P}_0 (1 + \delta\mathcal{P} \ln b) \simeq \mathcal{P}_0 b^{\delta\mathcal{P}} \quad (81)$$

where we used the relation  $b^a \simeq 1 + a \ln b$  when  $b$  is close to 1. The aim of the perturbative theory is to calculate the corrections to the parameters, namely the values of the  $\delta\mathcal{P}$ .

To recover a renormalized theory with the same cutoff  $\Lambda$  of the bare theory, the space must be rescaled as  $\mathbf{x}_b = b^{-1}\mathbf{x}$ , or equivalently momenta must be rescaled as  $\mathbf{k}_b = b\mathbf{k}$ . According to the static and dynamic scaling hypothesis [34–37], correlation functions and thus fields obey scaling relations of the form

$$\phi(\mathbf{k}, \omega) = b^{x_\phi} \phi(b\mathbf{k}, b^z \omega) \quad (82)$$

Therefore, in order to fully restore the same form of the original action, also fields and frequencies must be properly rescaled,

$$\mathbf{k} = b^{-1} \mathbf{k}_b \quad \omega = b^{-z} \omega_b \quad \phi(\mathbf{k}, \omega) = b^{\chi_\phi} \phi(\mathbf{k}_b, \omega_b) \quad (83)$$

where  $z$  is the dynamical critical exponent and  $\chi_\phi$  is the scaling dimension of the field. Once this rescaling is done, the action takes the same form as the bare one, but with new renormalized parameters and couplings, which will be denoted with a subscript  $b$ . These new values of the parameters, defined in order to absorb all the powers of  $b$  in front of them, can be expressed as functions of the bare parameters,

$$\mathcal{P}_b = b^{-\chi_{\mathcal{P}}} \mathcal{P}_0 \quad (84)$$

where  $\chi_{\mathcal{P}}$  is the total scaling dimension of  $\mathcal{P}$ . This total scaling takes into account both naive scaling, coming from dimensional analysis, and the anomalous scaling due to the RG coupling of IR and UV modes. We may therefore write  $\chi_{\mathcal{P}}$  as  $\chi_{\mathcal{P}} = d_{\mathcal{P}} - \delta\mathcal{P}$ , where  $d_{\mathcal{P}}$  is the naive dimension of  $\mathcal{P}$  while  $\delta\mathcal{P}$  is the anomalous scaling, as defined in Eq (81). Thanks to this transformation, the partition function can be written as,

$$\mathcal{Z} \propto \int \mathcal{D}\phi^< e^{-(S[\phi^<] + \Delta S[\phi^<])} \propto \int \mathcal{D}\phi e^{-S_b[\phi]} \quad (85)$$

where  $S_b[\phi]$  is the *renormalized action*, obtained after integration over a shell of thickness  $\ln b$  and rescaling.

## 2. Self-energies and vertex corrections

Following the RG scheme introduced in the previous Section we now derive the recursive relations for the parameters and coupling constants. As a consequence of the shell integration, the bare gaussian action  $\mathcal{S}_0$  of (54) and (55) acquires some corrections, that it is customary to write in the following way [9],

$$\begin{aligned} \Delta\mathcal{S}_0 = & \int \hat{\psi}_\alpha(-\tilde{\mathbf{k}}) \Sigma_{\alpha\beta}(\tilde{\mathbf{k}}) \psi_\beta(\tilde{\mathbf{k}}) - \hat{\psi}_\alpha(-\tilde{\mathbf{k}}) \tilde{\Sigma}_{\alpha\beta}(\tilde{\mathbf{k}}) \hat{\psi}_\beta(\tilde{\mathbf{k}}) + \\ & + \int \hat{s}_{\alpha\beta}(-\tilde{\mathbf{k}}) \Pi_{\alpha\beta\gamma\nu}(\tilde{\mathbf{k}}) s_{\gamma\nu}(\tilde{\mathbf{k}}) - \hat{s}_{\alpha\beta}(-\tilde{\mathbf{k}}) \tilde{\Pi}_{\alpha\beta\gamma\nu}(\tilde{\mathbf{k}}) \hat{s}_{\gamma\nu}(\tilde{\mathbf{k}}) , \end{aligned} \quad (86)$$

where all momenta are integrated off-shell,  $k < \Lambda/b$ , while frequency integrals still run from  $-\infty$  to  $\infty$ . The new quantities  $\Sigma$ ,  $\tilde{\Sigma}$ ,  $\Pi$  and  $\tilde{\Pi}$  are the *self-energies*, which contribute to the perturbative corrections of the gaussian parameters of the original action. On the other hand, the interacting part of the action (56) acquires the corrections,

$$\begin{aligned} \Delta\mathcal{S}_I = & \int \hat{\psi}_\alpha(-\tilde{\mathbf{k}}) V_{\alpha\beta\gamma\nu}^{\hat{\psi}\psi s}(\tilde{\mathbf{k}}, \tilde{\mathbf{q}}) \psi_\beta(\tilde{\mathbf{k}} - \tilde{\mathbf{q}}) s_{\gamma\nu}(\tilde{\mathbf{q}}) + \\ & + \int \hat{s}_{\alpha\beta}(-\tilde{\mathbf{k}}) V_{\alpha\beta\gamma\nu}^{\hat{s}\psi\psi}(\tilde{\mathbf{k}}, \tilde{\mathbf{q}}) \psi_\gamma(-\tilde{\mathbf{q}} + \tilde{\mathbf{k}}/2) \psi_\nu(\tilde{\mathbf{q}} + \tilde{\mathbf{k}}/2) + \\ & + \int \hat{\psi}_\alpha(-\tilde{\mathbf{k}}) V_{\alpha\beta\gamma}^{\hat{\psi}\psi\psi}(\tilde{\mathbf{k}}, \tilde{\mathbf{q}}) \psi_\beta(\tilde{\mathbf{q}}) \psi_\gamma(\tilde{\mathbf{k}} - \tilde{\mathbf{q}}) + \\ & + \int \hat{s}_{\alpha\beta}(-\tilde{\mathbf{k}}) V_{\alpha\beta\gamma\nu\eta}^{\hat{s}s\psi}(\tilde{\mathbf{k}}, \tilde{\mathbf{q}}) s_{\gamma\nu}(\tilde{\mathbf{q}}) \psi_\eta(\tilde{\mathbf{k}} - \tilde{\mathbf{q}}) + \\ & + \int \hat{\psi}_\alpha(-\tilde{\mathbf{k}}) V_{\alpha\beta\gamma\nu}^{\hat{\psi}\psi\psi\psi}(\tilde{\mathbf{k}}, \tilde{\mathbf{q}}, \tilde{\mathbf{h}}) \psi_\beta(\tilde{\mathbf{q}}) \psi_\gamma(\tilde{\mathbf{h}}) \psi_\nu(\tilde{\mathbf{k}} - \tilde{\mathbf{q}} - \tilde{\mathbf{h}}) + \\ & + \int \hat{s}_{\alpha\beta}(-\tilde{\mathbf{k}}) V_{\alpha\beta\gamma\nu\sigma\tau}^{\hat{s}\psi\psi\psi\psi}(\tilde{\mathbf{k}}, \tilde{\mathbf{q}}, \tilde{\mathbf{h}}, \tilde{\mathbf{p}}) \psi_\gamma(\tilde{\mathbf{q}}) \psi_\nu(\tilde{\mathbf{h}}) \psi_\sigma(\tilde{\mathbf{p}}) \psi_\tau(\tilde{\mathbf{k}} - \tilde{\mathbf{q}} - \tilde{\mathbf{h}} - \tilde{\mathbf{p}}) , \end{aligned} \quad (87)$$

where the various vertex-functions  $V$ s give perturbative corrections to the coupling constants of the non-linear interactions. We notice that all the corrections are proportional to the volume of the momentum shell, which is given by  $1 - b^{-1} \simeq \ln b$ . In what follows, we will compute the self-energies and the vertex functions by using perturbation theory. Evaluation of perturbative corrections is done using a Feynman diagram expansion and considering only the first order in  $\epsilon$ . Since we are interested in the dynamic behaviour near criticality, the mass  $m$  is set to 0 in all diagrams contributing to self-energies and vertex functions [29].

As mentioned earlier, the self-energies represent the perturbative corrections to the gaussian part of the effective action. We distinguish four different self energies, one for each combination of fields appearing in  $\mathcal{S}_0$ , namely  $\hat{\psi}\psi$ ,  $\hat{\psi}\hat{\psi}$ ,  $\hat{s}s$  and  $\hat{s}\hat{s}$ . This means that, from a diagrammatic point of view, the self-energies can be represented as follows

$$\Sigma_{\alpha\beta}(\tilde{\mathbf{k}}) = \hat{\psi}_\alpha(-\tilde{\mathbf{k}}) \longrightarrow \text{blob} \longrightarrow \psi_\beta(\tilde{\mathbf{k}}) \quad (88)$$

$$\tilde{\Sigma}_{\alpha\beta}(\tilde{\mathbf{k}}) = \hat{\psi}_\alpha(-\tilde{\mathbf{k}}) \longrightarrow \text{blob} \longleftarrow \hat{\psi}_\beta(\tilde{\mathbf{k}}) \quad (89)$$

$$\Pi_{\alpha\beta\gamma\nu}(\tilde{\mathbf{k}}) = \hat{s}_{\alpha\beta}(-\tilde{\mathbf{k}}) \rightsquigarrow \text{blob} \rightsquigarrow s_{\gamma\nu}(\tilde{\mathbf{k}}) \quad (90)$$

$$\tilde{\Pi}_{\alpha\beta\gamma\nu}(\tilde{\mathbf{k}}) = \hat{s}_{\alpha\beta}(-\tilde{\mathbf{k}}) \rightsquigarrow \text{blob} \longleftarrow \hat{s}_{\gamma\nu}(\tilde{\mathbf{k}}) \quad (91)$$

where the blob stands for the sum of all amputated 1-particle irreducible diagrams compatible with the given external fields. Each self-energy gives perturbative corrections to the gaussian parameters present in  $\mathcal{S}_0$ , namely  $\Gamma$ ,  $m$ ,  $\tilde{\Gamma}$ ,  $\lambda^{\perp/\parallel}$  and  $\tilde{\lambda}^{\perp/\parallel}$ . Moreover, the self-energy  $\Sigma$  contains perturbative corrections proportional to  $-i\omega\hat{\psi}\psi$ ; because this term is not multiplied by any parameter in the original bare action, the only way to reabsorb these corrections is through a modification of the scaling dimension of the field  $\psi$  (i.e. by generating an anomalous dimension). On the other hand, analogous perturbative terms do not arise in the self-energy  $\Pi$ , because all one-loop diagrams are at least of order  $\mathbf{k}$  as a consequence of the particular properties of the vertices (73) and (75), which vanish at  $\mathbf{k} = 0$ , so that the term  $-i\omega\hat{s}s$  acquires only  $\mathbf{k}$ -dependent perturbative corrections that vanish when  $\mathbf{k} = 0$ . For this reason, the spin does not acquire an anomalous dimension. To identify perturbative corrections of the gaussian parameters, we need to expand the self energies in  $\omega$  and  $\mathbf{k}$  and keep only the leading terms. By comparing the form of  $\mathcal{S}_0$  in Eq. (54)-(55) with the correction  $\Delta\mathcal{S}_0$  in Eq. (86), we define the perturbative corrections to the gaussian parameters through the relations,

$$\Sigma_{\alpha\beta}(\tilde{\mathbf{k}}) = \left[ -i\omega \delta\omega_\psi + m_0 \delta m + k^2 \Gamma_0 \delta\Gamma \right] \ln b P_{\alpha\beta}^\perp(\mathbf{k}) + \dots \quad (92)$$

$$\tilde{\Sigma}_{\alpha\beta}(\tilde{\mathbf{k}}) = \tilde{\Gamma}_0 \delta\tilde{\Gamma} \ln b P_{\alpha\beta}^\perp(\mathbf{k}) + \dots \quad (93)$$

$$\Pi_{\alpha\beta\gamma\nu}(\tilde{\mathbf{k}}) = \frac{1}{2} k^2 \lambda_0^\perp \delta\lambda^\perp \ln b \mathbb{P}_{\alpha\beta\gamma\nu}^\perp(\mathbf{k}) + \frac{1}{2} k^2 \lambda_0^\parallel \delta\lambda^\parallel \ln b (\mathbb{I} - \mathbb{P}^\perp)_{\alpha\beta\gamma\nu}(\mathbf{k}) + \dots \quad (94)$$

$$\tilde{\Pi}_{\alpha\beta\gamma\nu}(\tilde{\mathbf{k}}) = \frac{1}{2} k^2 \tilde{\lambda}_0^\perp \delta\tilde{\lambda}^\perp \ln b \mathbb{P}_{\alpha\beta\gamma\nu}^\perp(\mathbf{k}) + \frac{1}{2} k^2 \tilde{\lambda}_0^\parallel \delta\tilde{\lambda}^\parallel \ln b (\mathbb{I} - \mathbb{P}^\perp)_{\alpha\beta\gamma\nu}(\mathbf{k}) + \dots \quad (95)$$

where we denoted the bare parameters with the subscript 0 and where the ellipses stand for higher orders terms in  $\omega$  and  $\mathbf{k}$ , which are irrelevant in determining the critical behaviour at first order in  $\epsilon$ . The  $\ln b$  factors present in all terms reflect the fact that perturbative corrections are proportional to the volume of the momentum shell. After the shell integration, the gaussian action takes the following form,

$$\begin{aligned} \mathcal{S}_{\Lambda/b} = & \int \hat{\psi} \left[ -i\omega (1 + \delta\omega_\psi \ln b) + \Gamma_0 (1 + \delta\Gamma \ln b) k^2 + m_0 (1 + \delta m \ln b) \right] \psi - \hat{\psi} \tilde{\Gamma}_0 \left( 1 + \delta\tilde{\Gamma} \ln b \right) \hat{\psi} + \\ & + \frac{1}{2} \int \hat{s} \left[ -i\omega + \lambda_0^\perp (1 + \delta\lambda^\perp \ln b) k^2 + \lambda_0^\parallel (1 + \delta\lambda^\parallel \ln b) k^2 \right] s - \hat{s} \left[ \tilde{\lambda}_0^\perp (1 + \delta\tilde{\lambda}^\perp \ln b) k^2 + \tilde{\lambda}_0^\parallel (1 + \delta\tilde{\lambda}^\parallel \ln b) k^2 \right] \hat{s} \end{aligned} \quad (96)$$

where we omitted the tensorial structure of the action to facilitate the reading. The standard way to explicitly perform this task, and to compute the corrections to the bare parameters of the model, is using perturbation theory. The corrections  $\delta\mathcal{P}$  are thus computed using a Feynman diagram expansion. At order  $\epsilon$ , the non-vanishing diagrams contributing the self-energies are listed in SI-Section III.

Once the shell integration is performed, we are left with an effective action with a cutoff of  $\Lambda/b$ , a coefficient different from 1 in front of the  $-i\omega\hat{\psi}\psi$  term and modified parameters, namely

$$\mathcal{P}_0 \rightarrow \mathcal{P}_0 (1 + \delta\mathcal{P} \ln b) \simeq \mathcal{P}_0 b^{\delta\mathcal{P}} \quad (97)$$

Following SI-Section IC 1, we perform the following rescalings

$$\mathbf{k} = b \mathbf{k}_b \quad \omega = b^z \omega_b \quad (98)$$

$$\psi(\mathbf{k}, \omega) = b^{-\chi_\psi} \psi(\mathbf{k}_b, \omega_b) \quad \hat{\psi}(\mathbf{k}, \omega) = b^{-\chi_{\hat{\psi}}} \hat{\psi}(\mathbf{k}_b, \omega_b) \quad (99)$$

$$\mathbf{s}(\mathbf{k}, \omega) = b^{-\chi_s} \mathbf{s}(\mathbf{k}_b, \omega_b) \quad \hat{\mathbf{s}}(\mathbf{k}, \omega) = b^{-\chi_{\hat{s}}} \hat{\mathbf{s}}(\mathbf{k}_b, \omega_b) \quad (100)$$

After this rescaling, we end up with an action with the same cutoff  $\Lambda$  but with new renormalized parameters and couplings, which will be denoted with a subscript  $b$ . These new values of the parameters, defined to absorb all the powers of  $b$  in front of them, can be expressed as functions of the bare parameters, the dynamic exponent  $z$  and the scaling exponents  $\chi$  of the fields. Scaling exponents for time and fields are not known *a priori*, but can be determined by imposing additional conditions. For what concerns the gaussian action, the renormalized parameters are given by

$$\Gamma_b = \Gamma_0 b^{-\chi_\Gamma} \quad \chi_\Gamma = -\chi_{\hat{\psi}} - \chi_\psi + d + 2 + z - \delta\Gamma \quad (101)$$

$$\lambda_b^{\perp/\parallel} = \lambda_0^{\perp/\parallel} b^{-\chi_{\lambda^{\perp/\parallel}}} \quad \chi_{\lambda^{\perp/\parallel}} = -\chi_{\hat{s}} - \chi_s + d + 2 + z - \delta\lambda^{\perp/\parallel} \quad (102)$$

$$\tilde{\Gamma}_b = \tilde{\Gamma}_0 b^{-\chi_{\tilde{\Gamma}}} \quad \chi_{\tilde{\Gamma}} = -2\chi_{\hat{\psi}} + d + z - \delta\tilde{\Gamma} \quad (103)$$

$$\tilde{\lambda}_b^{\perp/\parallel} = \tilde{\lambda}_0^{\perp/\parallel} b^{-\chi_{\tilde{\lambda}^{\perp/\parallel}}} \quad \chi_{\tilde{\lambda}^{\perp/\parallel}} = -2\chi_{\hat{s}} + d + 2 + z - \delta\tilde{\lambda}^{\perp/\parallel} \quad (104)$$

$$(105)$$

The scaling dimensions of the response fields are chosen in order to absorb the powers of  $b$  in front of the terms proportional to  $-i\omega_b$  which lack of a coupling constant to redefine, thus meaning that

$$\chi_{\hat{\psi}} = -\chi_\psi + d + 2z - \delta\omega_\psi \quad \chi_{\hat{s}} = -\chi_s + d + 2z \quad (106)$$

It is furthermore possible to write all the scaling dimensions in terms of the scaling dimensions of the frequency and physical fields, namely  $z$ ,  $\chi_\psi$  and  $\chi_s$ :

$$\chi_{\hat{\psi}} = -\chi_\psi + d + 2z - \delta\omega_\psi \quad \chi_{\hat{s}} = -\chi_s + d + 2z \quad (107)$$

$$\chi_\Gamma = 2 - z - \delta\Gamma + \delta\omega_\psi \quad \chi_{\lambda^{\perp/\parallel}} = 2 - z - \delta\lambda^{\perp/\parallel} \quad (108)$$

$$\chi_{\tilde{\Gamma}} = 2\chi_\psi - d - 3z - \delta\tilde{\Gamma} + 2\delta\omega_\psi \quad \chi_{\tilde{\lambda}^{\perp/\parallel}} = 2\chi_s - d - 3z + 2 - \delta\tilde{\lambda}^{\perp/\parallel} \quad (109)$$

Now that we have defined the perturbative corrections to the gaussian parameters, we shall switch our attention to the coupling constants of the non-linear interactions. Perturbative corrections to the interactions are known as vertex functions. The six vertex functions of our theory, one for each bare vertex, are given by

$$V_{\alpha\beta\gamma\nu}^{\hat{\psi}\psi s}(\tilde{\mathbf{k}}, \tilde{\mathbf{q}}) = \hat{\psi}_\alpha(-\tilde{\mathbf{k}}) \rightarrow \begin{array}{c} \psi_\beta(\tilde{\mathbf{k}} - \tilde{\mathbf{q}}) \\ \text{blob} \\ s_{\gamma\nu}(\tilde{\mathbf{q}}) \end{array} \quad V_{\alpha\beta\gamma\nu}^{\hat{s}\psi\psi}(\tilde{\mathbf{k}}, \tilde{\mathbf{q}}) = \hat{s}_{\alpha\beta}(-\tilde{\mathbf{k}}) \rightsquigarrow \begin{array}{c} \psi_\gamma(\tilde{\mathbf{k}}/2 - \tilde{\mathbf{q}}) \\ \text{blob} \\ \psi_\nu(\tilde{\mathbf{k}}/2 + \tilde{\mathbf{q}}) \\ s_{\gamma\nu}(\tilde{\mathbf{k}}/2 - \tilde{\mathbf{q}}) \end{array} \quad (110)$$

$$V_{\alpha\beta\gamma}^{\hat{\psi}\psi\psi}(\tilde{\mathbf{k}}, \tilde{\mathbf{q}}) = \hat{\psi}_\alpha(-\tilde{\mathbf{k}}) \rightarrow \begin{array}{c} \psi_\beta(\tilde{\mathbf{q}}) \\ \text{blob} \\ \psi_\gamma(\tilde{\mathbf{k}} - \tilde{\mathbf{q}}) \end{array} \quad V_{\alpha\beta\gamma\nu\eta}^{\hat{s}s\psi}(\tilde{\mathbf{k}}, \tilde{\mathbf{q}}) = \hat{s}_{\alpha\beta}(-\tilde{\mathbf{k}}) \rightsquigarrow \begin{array}{c} \psi_\nu(\tilde{\mathbf{k}}/2 + \tilde{\mathbf{q}}) \\ \text{blob} \\ \psi_\eta(\tilde{\mathbf{k}}/2 + \tilde{\mathbf{q}}) \end{array} \quad (111)$$

$$V_{\alpha\beta\gamma\nu}^{\hat{\psi}\psi\psi\psi}(\tilde{\mathbf{k}}, \tilde{\mathbf{q}}, \tilde{\mathbf{h}}) = \hat{\psi}_\alpha(-\tilde{\mathbf{k}}) \rightarrow \begin{array}{c} \psi_\beta(\tilde{\mathbf{q}}) \\ \text{blob} \\ \psi_\gamma(\tilde{\mathbf{h}}) \\ \psi_\gamma(\tilde{\mathbf{k}} - \tilde{\mathbf{q}} - \tilde{\mathbf{h}}) \end{array} \quad V_{\alpha\beta\gamma\nu\sigma\tau}^{\hat{s}\psi\psi\psi\psi}(\tilde{\mathbf{k}}, \tilde{\mathbf{q}}, \tilde{\mathbf{h}}, \tilde{\mathbf{p}}) = \hat{s}_{\alpha\beta}(-\tilde{\mathbf{k}}) \rightsquigarrow \begin{array}{c} \psi_\gamma(\tilde{\mathbf{q}}) \\ \text{blob} \\ \psi_\nu(\tilde{\mathbf{h}}) \\ \psi_\sigma(\tilde{\mathbf{p}}) \\ \psi_\tau(\tilde{\mathbf{k}} - \tilde{\mathbf{q}} - \tilde{\mathbf{h}} - \tilde{\mathbf{p}}) \end{array} \quad (112)$$

where, as in the self-energies, the blob represents the sum of all amputated 1-particle irreducible diagrams compatible with the given external fields. At order  $\epsilon$ , the non-vanishing diagrams contributing to the vertices are listed in SI-Section

III. Each vertex function contributes to the corrections of couplings and parameters of Eqs. (70)-(76) in the following way,

$$V_{\alpha\beta\gamma\nu}^{\hat{\psi}\psi s}(\tilde{\mathbf{k}}, \tilde{\mathbf{q}}) = g \delta g_{\psi} P_{\alpha\rho}^{\perp}(\mathbf{k}) \mathbb{I}_{\rho\beta\gamma\nu} \quad (113)$$

$$V_{\alpha\beta\gamma}^{\hat{\psi}\psi\psi}(\tilde{\mathbf{k}}, \tilde{\mathbf{q}}) = -v_0 \frac{i\gamma_v}{2} \delta\gamma_v P_{\alpha\beta\nu}(\mathbf{k}) \quad (114)$$

$$V_{\alpha\beta\gamma\nu}^{\hat{\psi}\psi\psi\psi}(\tilde{\mathbf{k}}, \tilde{\mathbf{q}}, \tilde{\mathbf{h}}) = -\frac{J}{3} \delta J Q_{\alpha\beta\gamma\nu}(\mathbf{k}) \quad (115)$$

$$V_{\alpha\beta\gamma\nu}^{\hat{s}\psi\psi}(\tilde{\mathbf{k}}, \tilde{\mathbf{q}}) = g \mathbb{I}_{\alpha\beta\rho\sigma} \mathbb{I}_{\rho\tau\gamma\nu} [\delta g_s \mathbf{k} \cdot \mathbf{q} \delta_{\sigma\tau} + \Phi_1 \delta g_{s1} k_{\sigma} q_{\tau} + \Phi_2 \delta g_{s2} q_{\sigma} k_{\tau}] \quad (116)$$

$$V_{\alpha\beta\gamma\nu\eta}^{\hat{s}s\psi}(\tilde{\mathbf{k}}, \tilde{\mathbf{q}}) = -v_0 \frac{i\gamma_s}{2} \mathbb{I}_{\alpha\beta\rho\sigma} \mathbb{I}_{\rho\tau\gamma\nu} [\delta\gamma_s k_{\eta} \delta_{\sigma\tau} + 2\mu_1 \delta\gamma_{s1} k_{\tau} \delta_{\sigma\eta} + 2\mu_2 \delta\gamma_{s2} k_{\sigma} \delta_{\tau\eta}] \quad (117)$$

$$V_{\alpha\beta\gamma\nu\sigma\tau}^{\hat{s}\psi\psi\psi\psi}(\tilde{\mathbf{k}}, \tilde{\mathbf{q}}, \tilde{\mathbf{h}}, \tilde{\mathbf{p}}) = \frac{\kappa}{12} \delta\kappa K_{\alpha\beta\gamma\nu\sigma\tau}(\mathbf{k}, \mathbf{q}, \mathbf{h}, \mathbf{p}, \mathbf{k} - \mathbf{q} - \mathbf{h} - \mathbf{p}) \quad (118)$$

Higher orders in  $\omega$  and  $\mathbf{k}$  turn out to be irrelevant in determining the critical behaviour at first order in  $\epsilon$ . When also the rescaling of momenta, frequency and fields is performed, we obtain the following RG transformations,

$$\gamma_{\psi b} = \gamma_{\psi 0} b^{-\chi_{\gamma\psi}} \quad \chi_{\gamma\psi} = -\chi_{\hat{\psi}} - 2\chi_{\psi} + 2d + 1 + 2z - \delta\gamma_{\psi} \quad (119)$$

$$\gamma_{sb} = \gamma_{s0} b^{-\chi_{\gamma s}} \quad \chi_{\gamma s} = -\chi_{\hat{s}} - \chi_s - \chi_{\psi} + 2d + 1 + 2z - \delta\gamma_s \quad (120)$$

$$\mu_{1b} = \mu_{10} b^{-\chi_{\mu_1}} \quad \chi_{\mu_1} = \delta\gamma_s - \delta\gamma_{s1} \quad (121)$$

$$\mu_{2b} = \mu_{20} b^{-\chi_{\mu_2}} \quad \chi_{\mu_2} = \delta\gamma_s - \delta\gamma_{s2} \quad (122)$$

$$g_b^{(\psi)} = g_0 b^{-\chi_{g^{(\psi)}}} \quad \chi_{g^{(\psi)}} = -\chi_{\hat{\psi}} - \chi_{\psi} - \chi_s + 2d + 2z - \delta g_{\psi} \quad (123)$$

$$g_b^{(s)} = g_0 b^{-\chi_{g^{(s)}}} \quad \chi_{g^{(s)}} = -\chi_{\hat{s}} - 2\chi_{\psi} + 2d + 2 + 2z - \delta g_s \quad (124)$$

$$\Phi_{1b} = \Phi_{10} b^{-\chi_{\Phi_1}} \quad \chi_{\Phi_1} = \delta g_s - \delta g_{s1} \quad (125)$$

$$\Phi_{2b} = \Phi_{20} b^{-\chi_{\Phi_2}} \quad \chi_{\Phi_2} = \delta g_s - \delta g_{s2} \quad (126)$$

$$J_b = J_0 b^{-\chi_J} \quad \chi_J = -\chi_{\hat{\psi}} - 3\chi_{\psi} + 3d + 3z - \delta J \quad (127)$$

$$\kappa_b = \kappa_0 b^{-\chi_{\kappa}} \quad \chi_{\kappa} = -\chi_{\hat{s}} - 4\chi_{\psi} + 4d + 4z - \delta\kappa \quad (128)$$

By using Eq. (106) we can write all the scaling dimensions of the interaction couplings in terms of the scaling dimensions of the frequency and physical fields, namely  $z$ ,  $\chi_{\psi}$  and  $\chi_s$ :

$$\chi_{\gamma\psi} = -\chi_{\psi} + d + 1 - \delta\gamma_{\psi} + \delta\omega_{\psi} \quad \chi_{\gamma s} = -\chi_{\psi} + d + 1 - \delta\gamma_s \quad (129)$$

$$\chi_{\mu_1} = \delta\gamma_s - \delta\gamma_{s1} \quad \chi_{\mu_2} = \delta\gamma_s - \delta\gamma_{s2} \quad (130)$$

$$\chi_{g^{(\psi)}} = -\chi_s + d - \delta g_{\psi} + \delta\omega_{\psi} \quad \chi_{g^{(s)}} = \chi_s - 2\chi_{\psi} + d + 2 - \delta g_s \quad (131)$$

$$\chi_{\Phi_1} = \delta g_s - \delta g_{s1} \quad \chi_{\Phi_2} = \delta g_s - \delta g_{s2} \quad (132)$$

$$\chi_J = -2\chi_{\psi} + 2d + z - \delta J + \delta\omega_{\psi} \quad \chi_{\kappa} = \chi_s - 4\chi_{\psi} + 3d + 2z - \delta\kappa \quad (133)$$

By looking at Eqs. (123) and (124) it may seem that we have *two* different mode-coupling constants; however, this is not the case. We defined two different renormalized coupling constants  $g^{(\psi)}$  and  $g^{(s)}$  only because the perturbative corrections  $\delta g_{\psi}$  and  $\delta g_s$  arising in Eqs. (113) and (116) are completely independent from each other, but this does not mean that there are two different *physical* constants. In fact, there must be only one mode-coupling constant, because  $g$  arises in the derivation of the equations of motion as the consequence of a symmetry, encoded by the Poisson-bracket relation  $\{s, \psi\} \propto g\psi$ , stating that  $s$  is the generator of the rotations of  $\psi$ . The mode-coupling terms in both the equations of motion derive from this one Poisson-bracket relation; therefore, the existence of two different couplings would mean losing the connection with the underlying symmetry and Poisson structure. As we mentioned before, the scaling behaviour of the physical fields  $\psi$  and  $s$  is arbitrary, which allows a certain freedom in determining the scaling dimensions  $\chi_{\psi}$  and  $\chi_s$ , which enter Eqs. (123) and (124). Hence, it is possible to use this freedom to restore the identity of the two mode-coupling constants,

$$g_b^{(\psi)} = g_b^{(s)} = g_b \quad (134)$$

by simply asking that  $\chi_s$  is chosen in such a way that,

$$\chi_{g^{(\psi)}} = \chi_{g^{(s)}} \quad (135)$$

Essentially, we are requiring the field  $s$  to scale in such a way that the coupling regulating the symmetry has one unique scaling behaviour.

### 3. A primer of the diagrammatic expansion

The one-loop Feynman diagrams generated by the action's expansion, and necessary to calculate all the corrections  $\delta\mathcal{P}$  to the parameters and coupling constants, are listed in SI-Section III; not only they are many, but they are also quite complicated due to the tensorial structure of the theory. Hence, we will perform in this Section the explicit calculation of one diagram, hoping that this may help the interested reader in picking up the general technique. The diagram we calculate is a contribution to the self-energy  $\Sigma$  defined in (88),

$$D_{\alpha\beta}(\mathbf{k}, \omega_k) = \begin{array}{c} \begin{array}{ccc} & \mathbf{k}/2 - \mathbf{p}, \omega_k/2 - \omega_p & \\ & \curvearrowright & \\ \alpha & & \beta \\ \begin{array}{c} \text{---} \mathbf{k}, -\omega_k \text{---} \end{array} & \bullet & \bullet & \begin{array}{c} \text{---} \mathbf{k}, \omega_k \text{---} \end{array} \\ & \curvearrowleft & \\ & \mathbf{k}/2 + \mathbf{p}, \omega_k/2 + \omega_p & \end{array} \end{array} \quad (136)$$

The integral expression corresponding to this diagram can be written following the definitions of lines and vertices given in Appendices IB2 and IB3,

$$D_{\alpha\beta}(\mathbf{k}, \omega_k) = g^2 \int \frac{d^d p}{(2\pi)^d} \frac{d\omega_p}{2\pi} P_{\alpha\theta}(\mathbf{k}) \mathbb{I}_{\theta\gamma\rho\sigma} \mathbb{G}_{\gamma\nu}^{0,\psi} \left( \frac{\mathbf{k}}{2} - \mathbf{p}, \frac{\omega_k}{2} - \omega_p \right) \mathbb{C}_{\rho\sigma\mu\lambda}^{0,s} \left( \frac{\mathbf{k}}{2} + \mathbf{p}, \frac{\omega_k}{2} + \omega_p \right) P_{\nu\eta} \left( \frac{\mathbf{k}}{2} - \mathbf{p} \right) \mathbb{I}_{\eta\beta\mu\lambda} \quad (137)$$

While the momentum integral is restricted to the momentum shell,  $\Lambda/b < p < \Lambda$ , the frequency integral is extended over the whole spectrum  $(-\infty, +\infty)$ . Furthermore, we notice that the integrand (137) depends on the frequency  $\omega_p$  only through the correlation functions  $\mathbb{G}^{0,\psi}$  and  $\mathbb{C}^{0,s}$  defined in SI-Section IB2; this is in general true for any Feynman diagram present in this work. All the correlation functions (61)-(64) have at most two poles in the complex plane, and it is always possible to compute the frequency integral using the residue theorem. In the case of this diagram the integration over  $\omega_p$  yields,

$$D_{\alpha\beta}(\mathbf{k}, \omega_k) = g^2 \int \frac{d^d p}{(2\pi)^d} P_{\alpha\theta}(\mathbf{k}) \mathbb{I}_{\theta\gamma\rho\sigma} P_{\nu\eta}(\mathbf{k}/2 - \mathbf{p}) \mathbb{I}_{\eta\beta\mu\lambda} \left[ \frac{2\tilde{\lambda}^\perp \delta_{\gamma\nu} \mathbb{P}_{\rho\sigma\mu\lambda}^\perp(\mathbf{k}/2 - \mathbf{p})}{\lambda^\perp [\Gamma(\mathbf{k}/2 - \mathbf{p})^2 + \lambda^\perp (\mathbf{k}/2 + \mathbf{p})^2 - i\omega_k + m]} \right. \\ \left. + \frac{2\tilde{\lambda}^\parallel \delta_{\gamma\nu} (\mathbb{P}_{\rho\sigma\mu\lambda}^\perp(\mathbf{k}/2 - \mathbf{p}) - \mathbb{I}_{\rho\sigma\mu\lambda})}{\lambda^\parallel [\Gamma(\mathbf{k}/2 - \mathbf{p})^2 + \lambda^\parallel (\mathbf{k}/2 + \mathbf{p})^2 - i\omega_k + m]} \right] \quad (138)$$

Since we are going to work at first order in  $\epsilon = 4 - d$  (one loop), we can drop the  $m$  dependence in the Feynman diagrams, because this would lead to higher order corrections. Hence we set  $m = 0$  in the following. The integral over the modulus of the momentum becomes trivial if we assume that the RG transformation is infinitesimal, namely if  $b \simeq 1$ ; this means that the thickness of the momentum shell is infinitesimal and it is possible to approximate the integral of a generic function  $f(\mathbf{p})$  as follows,

$$\int_{\Lambda/b}^{\Lambda} d^d p f(\mathbf{p}) = \int f(\mathbf{p}) d\Omega_d p^{d-1} dp = \ln b \Lambda^d \int f(\mathbf{p}) \Big|_{|p|=\Lambda} d\Omega_d \quad (139)$$

which corresponds to approximating the integral as the value of the function at  $|p| = \Lambda$  times the volume of the momentum shell  $\Lambda^d(1 - 1/b) \simeq \ln b$ . After this step, the integrand may still depend on the direction of the momentum  $\hat{\mathbf{p}} = \mathbf{p}/|p|$ , which is a unit versor. Applying this procedure to equation (138) leads to,

$$D_{\alpha\beta}(\mathbf{k}, \omega_k) = g^2 \int \frac{d\Omega_d}{(2\pi)^d} \Lambda^d \ln b P_{\alpha\theta}(\mathbf{k}) \mathbb{I}_{\theta\gamma\rho\sigma} P_{\nu\eta}(\mathbf{k}/2 - \Lambda\hat{\mathbf{p}}) \mathbb{I}_{\eta\beta\mu\lambda} \left[ \frac{2\tilde{\lambda}^\perp \delta_{\gamma\nu} \mathbb{P}_{\rho\sigma\mu\lambda}^\perp(\mathbf{k}/2 - \Lambda\hat{\mathbf{p}})}{\lambda^\perp [\Gamma(\mathbf{k}/2 - \Lambda\hat{\mathbf{p}})^2 + \lambda^\perp (\mathbf{k}/2 + \Lambda\hat{\mathbf{p}})^2 - i\omega_k]} \right. \\ \left. + \frac{2\tilde{\lambda}^\parallel \delta_{\gamma\nu} (\mathbb{P}_{\rho\sigma\mu\lambda}^\perp(\mathbf{k}/2 - \Lambda\hat{\mathbf{p}}) - \mathbb{I}_{\rho\sigma\mu\lambda})}{\lambda^\parallel [\Gamma(\mathbf{k}/2 - \Lambda\hat{\mathbf{p}})^2 + \lambda^\parallel (\mathbf{k}/2 + \Lambda\hat{\mathbf{p}})^2 - i\omega_k]} \right] \quad (140)$$

where the versor  $\hat{\mathbf{p}}$  is integrated over the  $d$ -dimensional sphere  $\Omega_d$ . The main advantage of having an expression of this kind is that all the dependence on the cut-off  $\Lambda$  is made explicit.

In order to recognize within this diagram the corrections to the various parameters of the original action, one has to expand in small external momenta and frequency, as we did in (92). The order at which it is convenient to perform

this expansion depends on the particular Feynman diagram we are considering and the specific parameters or coupling constants that it corrects. For example, the diagram we are studying here gives rise to perturbative corrections to the  $\hat{\psi}\psi$  term in the Gaussian action (54); hence we must expand it up to the second order in the external momentum  $\mathbf{k}$  and up to the first order in the external frequency  $\omega_k$ . In this example we will calculate explicitly only the contribution of order  $\omega_k$  of this diagram, even though the diagram gives also contributions of  $\mathcal{O}(1)$  and of  $\mathcal{O}(k^2)$ . The diagram at order  $\omega_k$  is,

$$D_{\alpha\beta}(\mathbf{k}, \omega_k) = i\omega_k g^2 \Lambda^{d-4} \ln b \int \frac{d\Omega_d}{(2\pi)^d} P_{\alpha\theta}(\mathbf{k}) \mathbb{I}_{\theta\gamma\rho\sigma} P_{\nu\eta}(\hat{\mathbf{p}}) \mathbb{I}_{\eta\beta\mu\lambda} \delta_{\gamma\nu} \left[ 2\tilde{\lambda}^\perp \frac{\mathbb{P}_{\rho\sigma\mu\lambda}^\perp(\hat{\mathbf{p}})}{\lambda^\perp(\Gamma + \lambda^\perp)^2} + 2\tilde{\lambda}^\parallel \frac{\mathbb{P}_{\rho\sigma\mu\lambda}^\parallel(\hat{\mathbf{p}}) - \mathbb{I}_{\rho\sigma\mu\lambda}}{\lambda^\parallel(\Gamma + \lambda^\parallel)^2} \right] \quad (141)$$

Expanding all the tensors in equation (141), using the definitions (31), (37) and (38), we obtain,

$$D_{\alpha\beta}(\mathbf{k}, \omega_k) = i\omega_k g^2 \Lambda^{d-4} \ln b P_{\alpha\theta}(\mathbf{k}) \int \frac{d\Omega_d}{(2\pi)^d} \left[ \frac{\tilde{\lambda}^\perp}{\lambda^\perp(\Gamma + \lambda^\perp)^2} (1-d) \hat{p}_\beta \hat{p}_\theta + \frac{\tilde{\lambda}^\parallel}{\lambda^\parallel(\Gamma + \lambda^\parallel)^2} (d-2) (\hat{p}_\beta \hat{p}_\theta - \delta_{\alpha\beta}) \right] \quad (142)$$

We can now perform the integral over the  $d$ -dimensional sphere  $d\Omega_d$ , which can be done using the following two relations,

$$\langle \hat{p}_\alpha \hat{p}_\beta \rangle_{\hat{\mathbf{p}}} = \frac{1}{d} \delta_{\alpha\beta}, \quad \langle \hat{p}_\alpha \hat{p}_\beta \hat{p}_\gamma \hat{p}_\nu \rangle_{\hat{\mathbf{p}}} = \frac{1}{d(d+2)} (\delta_{\alpha\beta} \delta_{\gamma\nu} + \delta_{\alpha\gamma} \delta_{\beta\nu} + \delta_{\alpha\nu} \delta_{\beta\gamma}), \quad (143)$$

where the brackets indicate the average over the  $d$ -dimensional sphere,

$$\langle \cdot \rangle = \frac{1}{\Omega_d} \int \cdot d\Omega_d \quad (144)$$

While the average of an even number of versors  $\hat{\mathbf{p}}$  is nonzero, the angular average of an odd number of momenta vanishes by symmetry. This leads to the following expression for the diagram (136),

$$D_{\alpha\beta}(\mathbf{k}, \omega_k) = -i\omega_k g^2 \Lambda^{d-4} \left[ \frac{\tilde{\lambda}^\perp}{\lambda^\perp(\Gamma + \lambda^\perp)^2} \frac{d-1}{d} + \frac{\tilde{\lambda}^\parallel}{\lambda^\parallel(\Gamma + \lambda^\parallel)^2} (d-2) \frac{d-1}{d} \right] \ln b P_{\alpha\beta}^\perp(\mathbf{k}) \quad (145)$$

Since we are performing an  $\epsilon$ -expansion around the upper critical dimension  $d_c = 4$ , we can set  $d = 4$  in all the Feynman diagrams. In the end, by comparing this expression to the expansion of the self-energy in (92), we can finally read the correction to the scaling dimension of the field coming from this one diagram, namely,

$$\delta\omega_\psi = \Lambda^{d-4} g^2 \left[ \frac{3}{4} \frac{\tilde{\lambda}^\perp}{\lambda^\perp(\Gamma + \lambda^\perp)^2} + \frac{3}{2} \frac{\tilde{\lambda}^\parallel}{\lambda^\parallel(\Gamma + \lambda^\parallel)^2} \right] + \dots \quad (146)$$

where the dots indicates the corrections from *all* other diagrams contributing to the self-energy  $\Sigma$ , which are listed in SI-Section III.

#### 4. Generation of the anomalous terms

The equations of motion proposed initially in (18), (19), in which the anomalous terms proportional to  $\mu_1$ ,  $\mu_2$ ,  $\Phi_1$  or  $\Phi_2$  do not appear, are of clear physical interpretation. However, as previously pointed out, in the absence of some additional terms, to which we referred to as *anomalous*, the equations of motion are not RG-invariant; basically, what happens is that the RG generates some terms that were not present in the original action. To see how this happens, we perform here a shell integration starting from a theory with bare coefficients  $\Phi_{10} = \Phi_{20} = \mu_{10} = \mu_{20} = 0$ , and we show that these anomalous terms are spontaneously generated by the renormalization group transformation. We also hope that this further direct analysis of some highly nontrivial diagrams may provide the reader with a more robust technique to perform the entire calculation.

\*\*\* Anomalous Mode-Coupling terms

Without anomalies, the non Gaussian action (56) has only one term proportional to  $\hat{s}\psi\psi$ , corresponding to the following vertex,

$$\begin{array}{c}
 \psi_\gamma(\tilde{\mathbf{k}}/2 - \tilde{\mathbf{q}}) \\
 \swarrow \\
 \hat{s}_{\alpha\beta}(-\tilde{\mathbf{k}}) \text{ --- } \circ \\
 \searrow \\
 \psi_\nu(\tilde{\mathbf{k}}/2 + \tilde{\mathbf{q}})
 \end{array}
 = g \mathbb{I}_{\alpha\beta\gamma\nu} \mathbf{k} \cdot \mathbf{q} \quad (147)$$

which is the same mode coupling vertex as (74), but without the anomalous terms. To compute the perturbative corrections to this vertex we must consider all the diagrams with an incoming  $\hat{s}$  line and two outgoing  $\psi$  lines; these are 12 diagrams, listed in Fig.(12) of SI-Section III, most of which produce anomalous corrections. Here, as an example, we limit ourselves to consider only the first *two* of all these diagrams namely,

$$\begin{array}{c}
 \tilde{\mathbf{k}}/2 - \tilde{\mathbf{q}}, \gamma \\
 \swarrow \\
 \tilde{\mathbf{k}}/2 + \tilde{\mathbf{q}} + \tilde{\mathbf{p}} \text{ --- } \circ \\
 \searrow \\
 \tilde{\mathbf{p}} - \tilde{\mathbf{q}}/2 \\
 \downarrow \\
 \tilde{\mathbf{k}}/2 + \tilde{\mathbf{q}}, \nu
 \end{array}
 , \quad
 \begin{array}{c}
 \tilde{\mathbf{k}}/2 - \tilde{\mathbf{q}}, \gamma \\
 \swarrow \\
 \tilde{\mathbf{k}}/2 + \tilde{\mathbf{q}} + \tilde{\mathbf{p}} \text{ --- } \circ \\
 \searrow \\
 \tilde{\mathbf{p}} - \tilde{\mathbf{q}}/2 \\
 \downarrow \\
 \tilde{\mathbf{k}}/2 + \tilde{\mathbf{q}}, \nu
 \end{array}
 , \quad (148)$$

where we explicitly write also the momenta of internal field lines. These diagrams can be converted into integral expressions following the usual Feynman rules. It is important to note, though, that this is exactly one of the cases in which it is more convenient to write the spin mode-coupling vertex as in (73) (but of course with  $\Phi_1 = \Phi_2 = 0$ ), rather than as in (74). The result is,

$$\begin{aligned}
 D_{\alpha\beta\gamma\nu}^{\text{mc},1} = & g^3 \int_{\Lambda/b < |\mathbf{p}| < \Lambda} \frac{d^d p}{(2\pi)^d} \left[ \left( \mathbf{p} + \frac{\mathbf{k}}{2} + \frac{\mathbf{q}}{2} \right)^2 - \left( \mathbf{p} - \frac{\mathbf{k}}{2} + \frac{\mathbf{q}}{2} \right)^2 \right] \left[ \left( \mathbf{q} + \frac{\mathbf{k}}{2} \right)^2 - \left( \mathbf{p} - \frac{\mathbf{k}}{2} + \frac{\mathbf{q}}{2} \right)^2 \right] \times \\
 & \times \mathbb{I}_{\alpha\beta\sigma\rho} P_{\mu,\eta}^\perp \left( \mathbf{p} + \frac{\mathbf{k}}{2} + \frac{\mathbf{q}}{2} \right) \mathbb{I}_{\eta\gamma\xi\zeta} \mathbb{I}_{\phi\chi\tau\nu} \int_{-\infty}^{\infty} \frac{d\omega_p}{2\pi} \mathbb{G}_{\rho\mu}^{0,\psi} \left( \tilde{\mathbf{p}} + \frac{\tilde{\mathbf{k}}}{2} + \frac{\tilde{\mathbf{q}}}{2} \right) \mathbb{G}_{\xi\zeta\phi\chi}^{0,s} \left( \tilde{\mathbf{p}} - \frac{\tilde{\mathbf{q}}}{2} \right) \mathbb{C}_{\sigma\tau}^{0,\psi} \left( \tilde{\mathbf{p}} - \frac{\tilde{\mathbf{k}}}{2} + \frac{\tilde{\mathbf{q}}}{2} \right) , \quad (149)
 \end{aligned}$$

$$\begin{aligned}
 D_{\alpha\beta\gamma\nu}^{\text{mc},2} = & g^3 \int_{\Lambda/b < |\mathbf{p}| < \Lambda} \frac{d^d p}{(2\pi)^d} \left[ \left( \mathbf{p} + \frac{\mathbf{k}}{2} + \frac{\mathbf{q}}{2} \right)^2 - \left( \mathbf{p} - \frac{\mathbf{k}}{2} + \frac{\mathbf{q}}{2} \right)^2 \right] \mathbb{I}_{\alpha\beta\sigma\rho} P_{\mu,\eta}^\perp \left( \mathbf{p} + \frac{\mathbf{k}}{2} + \frac{\mathbf{q}}{2} \right) \mathbb{I}_{\eta\gamma\xi\zeta} P_{\sigma,\delta}^\perp \left( \mathbf{p} - \frac{\mathbf{k}}{2} + \frac{\mathbf{q}}{2} \right) \mathbb{I}_{\phi\chi\tau\nu} \times \\
 & \times \int_{-\infty}^{\infty} \frac{d\omega_p}{2\pi} \mathbb{G}_{\rho\mu}^{0,\psi} \left( \tilde{\mathbf{p}} + \frac{\tilde{\mathbf{k}}}{2} + \frac{\tilde{\mathbf{q}}}{2} \right) \mathbb{C}_{\xi\zeta\phi\chi}^{0,s} \left( \tilde{\mathbf{p}} - \frac{\tilde{\mathbf{q}}}{2} \right) \mathbb{G}_{\delta\tau}^{0,\psi} \left( -\tilde{\mathbf{p}} + \frac{\tilde{\mathbf{k}}}{2} - \frac{\tilde{\mathbf{q}}}{2} \right) . \quad (150)
 \end{aligned}$$

Their sum is given by,

$$D_{\alpha\beta\gamma\nu}^{\text{mc},1} + D_{\alpha\beta\gamma\nu}^{\text{mc},2} = g[\delta g_s \mathbb{I}_{\alpha\beta\gamma\nu} \mathbf{k} \cdot \mathbf{q} + A \mathbb{I}_{\alpha\beta\rho\sigma} k_\sigma q_\tau \mathbb{I}_{\rho\tau\gamma\nu} + B \mathbb{I}_{\alpha\beta\rho\sigma} q_\sigma k_\tau \mathbb{I}_{\rho\tau\gamma\nu}] , \quad (151)$$

where the constants  $\delta g_s$ ,  $A$  and  $B$  are,

$$\begin{aligned}
\delta g_s &= g^2 w \frac{\tilde{\lambda}^\perp w(w+1)^2 + \tilde{\Gamma} x(w(x-5) - 3x - 1) - \tilde{\lambda}^\parallel (w-3)wx(w+x)}{12\Gamma^3(w+1)^2x(w+x)} \ln b \\
A &= -g^2 w \frac{-3\tilde{\lambda}^\perp w(w+1)^2 + \tilde{\Gamma} x(w(6w+3x+11) + 5x+3) - \tilde{\lambda}^\parallel w(3w+5)x(w+x)}{12\Gamma^3(w+1)^2x(w+x)} \ln b \\
B &= g^2 w \frac{-5\tilde{\lambda}^\perp w(w+1)^2 + \tilde{\Gamma} x(w(7-5x) - 3x+5) + \tilde{\lambda}^\parallel w(5w+3)x(w+x)}{12\Gamma^3(w+1)^2x(w+x)} \ln b
\end{aligned} \tag{152}$$

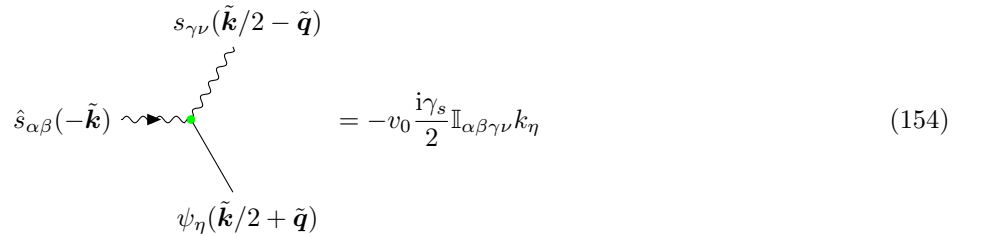
with  $w = \Gamma/\lambda^\parallel$  and  $x = \lambda^\perp/\lambda^\parallel$ . These two Feynman diagrams correct the interacting part of the action relative to the mode-coupling of the spin as follows,

$$\Delta \mathcal{S}_{\text{mc}} = \int_0^{\Lambda/b} d\tilde{\mathbf{k}} d\tilde{\mathbf{q}} g \hat{s}_{\alpha\beta}(-\tilde{\mathbf{k}}) \left[ \underbrace{\delta g_s \mathbb{I}_{\alpha\beta\gamma\nu} \mathbf{k} \cdot \mathbf{q}}_{\text{bare structure}} + \underbrace{A \mathbb{I}_{\alpha\beta\rho\sigma} k_\sigma q_\tau \mathbb{I}_{\rho\tau\gamma\nu} + B \mathbb{I}_{\alpha\beta\rho\sigma} q_\sigma k_\tau \mathbb{I}_{\rho\tau\gamma\nu}}_{\text{absent in the bare theory}} \right] \psi_\gamma(\tilde{\mathbf{k}}/2 - \tilde{\mathbf{q}}) \psi_\nu(\tilde{\mathbf{k}}/2 + \tilde{\mathbf{q}}) \quad , \tag{153}$$

The core idea of the renormalization group is that the perturbative contributions generated by Feynman diagrams can be reabsorbed into a redefinition of the model's parameters. Comparing equations (147) and (153) it is evident that the first term, proportional to  $\mathbb{I}_{\alpha\beta\gamma\nu} \mathbf{k} \cdot \mathbf{q}$ , has the same form as the bare vertex, hence it can be reabsorbed in the coupling,  $g \rightarrow g(1 + \Delta g_s)$ . However, we cannot reabsorb the second and third terms of equation (153) as correction of any pre-existing parameters, because of the different tensorial structure. For this reason two novel terms, proportional to  $\mathbb{I}_{\alpha\beta\rho\sigma} k_\sigma q_\tau \mathbb{I}_{\rho\tau\gamma\nu}$  and  $\mathbb{I}_{\alpha\beta\rho\sigma} q_\sigma k_\tau \mathbb{I}_{\rho\tau\gamma\nu}$  respectively, must be included in the action. These two terms coincide with the two *anomalous* terms  $\Phi_1$  and  $\Phi_2$  in equations (56). We remind that most of the diagrams listed in Fig.(12) of SI-Section III *generate* the same anomalous terms with different coefficients  $A$  and  $B$ . It is crucial to note that, if the model is at equilibrium,  $v_0 = 0$ ,  $\tilde{\Gamma} = \Gamma$  and  $\tilde{\lambda}^{\perp,\parallel} = \lambda^{\perp,\parallel}$ , all these perturbative contributions vanish:  $A = B = \delta g_s = 0$ , so that no anomalous terms are generated by any diagram.

### \*\*\* Anomalous Advection terms

The same procedure can be used to prove that the two anomalous advection terms, proportional to  $\mu_1$  and  $\mu_2$ , are fundamental to guarantee the closure of the theory under the RG transformation. We use the same strategy: we assume that the anomalous terms are zero in the bare theory,  $\mu_1 = \mu_2 = 0$ , then they are spontaneously generated by the renormalization group transformation. If we assume that  $\mu_1 = \mu_2 = 0$ , there is only one term proportional to  $\hat{s}s\psi$  in the non Gaussian action (56), corresponding to the advective derivative. In the diagrammatic expansion, this corresponds to modifying the vertex,



$$\hat{s}_{\alpha\beta}(-\tilde{\mathbf{k}}) \begin{array}{c} \nearrow s_{\gamma\nu}(\tilde{\mathbf{k}}/2 - \tilde{\mathbf{q}}) \\ \searrow \psi_\eta(\tilde{\mathbf{k}}/2 + \tilde{\mathbf{q}}) \end{array} = -v_0 \frac{i\gamma_s}{2} \mathbb{I}_{\alpha\beta\gamma\nu} k_\eta \tag{154}$$

The term proportional to  $\hat{s}s\psi$  in the action is corrected by the Feynman diagrams with an incoming  $\hat{s}$ , one outgoing  $s$  and  $\psi$  line. These are only 3 diagrams, listed in Fig.(14) of SI-Section III, so we calculate here all the three of them,

namely,

$$D^{\text{adv},1} = -\tilde{k}, \alpha\beta, \alpha\beta, \tilde{k}/2 - \tilde{q}, \gamma\nu, \tilde{k}/2 + \tilde{q}, \eta, \tilde{k}/2 + \tilde{q}/2 + \tilde{p}, \tilde{p} - \tilde{q}/2, \tilde{k}/2 - \tilde{q}/2 - \tilde{p}, \quad , \quad D^{\text{adv},2} = -\tilde{k}, \alpha\beta, \alpha\beta, \tilde{k}/2 - \tilde{q}, \gamma\nu, \tilde{k}/2 + \tilde{q}, \eta, \tilde{k}/2 + \tilde{q}/2 + \tilde{p}, \tilde{p} - \tilde{q}/2, \tilde{k}/2 - \tilde{q}/2 - \tilde{p}, \quad , \quad (155)$$

$$D^{\text{adv},3} = -\tilde{k}, \alpha\beta, \alpha\beta, \tilde{k}/2 - \tilde{q}, \gamma\nu, \tilde{k}/2 + \tilde{q}, \eta, \tilde{k}/2 + \tilde{q}/2 + \tilde{p}, \tilde{p} - \tilde{q}/2, \tilde{k}/2 - \tilde{q}/2 - \tilde{p} .$$

The integral expressions of these Feynman diagrams are:

$$D^{\text{adv},1} = -iv_0 \frac{\gamma_s g^2}{2} \int_{\Lambda/b < |\mathbf{p}| < \Lambda} \frac{d^d p}{(2\pi)^d} \mathbb{I}_{\alpha\beta\xi\zeta} k_\rho P_{\mu}^\perp \left( \mathbf{p} + \frac{\mathbf{k}}{2} + \frac{\mathbf{q}}{2} \right) \mathbb{I}_{\iota\sigma\gamma\nu} P_{\tau}^\perp \left( \mathbf{p} - \frac{\mathbf{q}}{2} \right) \mathbb{I}_{\delta\eta\phi\chi} \times \\ \times \int_{-\infty}^{\infty} \frac{d\omega_p}{2\pi} \mathbb{G}_{\rho\mu}^{0,\psi} \left( \tilde{\mathbf{p}} + \frac{\tilde{\mathbf{k}}}{2} + \frac{\tilde{\mathbf{q}}}{2} \right) \mathbb{G}_{\sigma\tau}^{0,\psi} \left( \tilde{\mathbf{p}} - \frac{\tilde{\mathbf{q}}}{2} \right) \mathbb{C}_{\xi\zeta\phi\chi}^{0,s} \left( \tilde{\mathbf{p}} - \frac{\tilde{\mathbf{k}}}{2} + \frac{\tilde{\mathbf{q}}}{2} \right), \quad (156)$$

$$D^{\text{adv},2} = -iv_0 \frac{\gamma_s g^2}{2} \int_{\Lambda/b < |\mathbf{p}| < \Lambda} \frac{d^d p}{(2\pi)^d} \mathbb{I}_{\alpha\beta\xi\zeta} k_\rho P_{\mu}^\perp \left( \mathbf{p} + \frac{\mathbf{k}}{2} + \frac{\mathbf{q}}{2} \right) \mathbb{I}_{\iota\sigma\gamma\nu} \left[ \left( \mathbf{q} + \frac{\mathbf{k}}{2} \right)^2 - \left( \mathbf{p} - \frac{\mathbf{q}}{2} \right)^2 \right] \mathbb{I}_{\phi\chi\tau\eta} \times \\ \times \int_{-\infty}^{\infty} \frac{d\omega_p}{2\pi} \mathbb{G}_{\rho\mu}^{0,\psi} \left( \tilde{\mathbf{p}} + \frac{\tilde{\mathbf{k}}}{2} + \frac{\tilde{\mathbf{q}}}{2} \right) \mathbb{C}_{\sigma\tau}^{0,\psi} \left( \tilde{\mathbf{p}} - \frac{\tilde{\mathbf{q}}}{2} \right) \mathbb{G}_{\xi\zeta\phi\chi}^{0,s} \left( -\tilde{\mathbf{p}} + \frac{\tilde{\mathbf{k}}}{2} - \frac{\tilde{\mathbf{q}}}{2} \right), \quad (157)$$

$$D^{\text{adv},3} = -iv_0 \frac{\gamma_s g^2}{2} \int_{\Lambda/b < |\mathbf{p}| < \Lambda} \frac{d^d p}{(2\pi)^d} \mathbb{I}_{\alpha\beta\xi\zeta} k_\rho P_{\sigma}^\perp \left( -\mathbf{p} + \frac{\mathbf{q}}{2} \right) \mathbb{I}_{\iota\mu\gamma\nu} \left[ \left( \mathbf{q} + \frac{\mathbf{k}}{2} \right)^2 - \left( \mathbf{p} - \frac{\mathbf{q}}{2} \right)^2 \right] \mathbb{I}_{\phi\chi\tau\eta} \times \\ \times \int_{-\infty}^{\infty} \frac{d\omega_p}{2\pi} \mathbb{C}_{\rho\mu}^{0,\psi} \left( \tilde{\mathbf{p}} + \frac{\tilde{\mathbf{k}}}{2} + \frac{\tilde{\mathbf{q}}}{2} \right) \mathbb{G}_{\sigma\tau}^{0,\psi} \left( -\tilde{\mathbf{p}} + \frac{\tilde{\mathbf{q}}}{2} \right) \mathbb{G}_{\xi\zeta\phi\chi}^{0,s} \left( -\tilde{\mathbf{p}} + \frac{\tilde{\mathbf{k}}}{2} - \frac{\tilde{\mathbf{q}}}{2} \right), \quad (158)$$

their sum is,

$$D^{\text{adv},1} + D^{\text{adv},2} + D^{\text{adv},3} = \gamma_s [\delta\gamma_s \mathbb{I}_{\alpha\beta\gamma\nu} k_\eta + C \mathbb{I}_{\alpha\beta\rho\eta} k_\tau \mathbb{I}_{\rho\tau\gamma\nu} + D \mathbb{I}_{\alpha\beta\rho\sigma} k_\sigma \mathbb{I}_{\rho\eta\gamma\nu}] \quad (159)$$

with the constants  $\delta\gamma_s$ ,  $C$  and  $D$ , given by,

$$\delta\gamma_s = ig^2 \frac{-x(x-1)(1+2w+x)\tilde{\Gamma} + wx(w+x)^2\tilde{\lambda}^\parallel - w(1+w)^2\tilde{\lambda}^\perp}{24\Gamma^3(1+w)^2x(w+x)^2} \mathbb{I}_{\alpha\beta\gamma\nu} k_\eta \\ C = ig^2 \frac{-x(5+10w+12w^2+14wx+7x^2)\tilde{\Gamma} + 7wx(w+x)^2\tilde{\lambda}^\parallel + 5w(1+w)^2\tilde{\lambda}^\perp}{24\Gamma^3(1+w)^2x(w+x)^2} \mathbb{I}_{\alpha\beta\rho\eta} k_\tau \mathbb{I}_{\rho\tau\gamma\nu} \\ D = ig^2 \frac{-x(x-1)(1+2w+x)\tilde{\Gamma} + wx(w+x)^2\tilde{\lambda}^\parallel - w(1+w)^2\tilde{\lambda}^\perp}{24\Gamma^3(1+w)^2x(w+x)^2} \mathbb{I}_{\alpha\beta\rho\sigma} k_\sigma \mathbb{I}_{\rho\eta\gamma\nu}, \quad (160)$$

These three Feynman diagrams correct the interacting part of the action relative to the advection of the spin as follows,

$$\Delta\mathcal{S}_{\text{adv}} = \int_0^{\Lambda/b} d\tilde{\mathbf{k}} d\tilde{\mathbf{q}} v_0 \gamma_s \hat{s}_{\alpha\beta}(-\tilde{\mathbf{k}}) \left[ \underbrace{\delta\gamma_s \mathbb{I}_{\alpha\beta\gamma\nu} k_\eta}_{\text{bare structure}} + \underbrace{C \mathbb{I}_{\alpha\beta\rho\eta} k_\tau \mathbb{I}_{\rho\tau\gamma\nu} + D \mathbb{I}_{\alpha\beta\rho\sigma} k_\sigma \mathbb{I}_{\rho\eta\gamma\nu}}_{\text{absent in the bare theory}} \right] s_{\gamma\nu}(\tilde{\mathbf{q}}) \psi_\eta(\tilde{\mathbf{k}} - \tilde{\mathbf{q}}) \quad , \quad (161)$$

Comparing equations (161) and (154) it is evident that the term proportional to  $\mathbb{I}_{\alpha\beta\gamma\nu} k_\eta$  is the same as in the bare case and it can be reabsorbed as a correction of the advection coupling,  $\gamma_s$ . On the other hand, the two terms proportional to  $\mathbb{I}_{\alpha\beta\rho\eta} k_\tau \mathbb{I}_{\rho\tau\gamma\nu}$  and  $\mathbb{I}_{\alpha\beta\rho\sigma} k_\sigma \mathbb{I}_{\rho\eta\gamma\nu}$  have tensorial structure different from the bare action, so that they require the addition of two new anomalous advection terms, which are exactly the ones proportional to  $\mu_1$  and  $\mu_2$  in equation (56).

\*\*\* *Summary of the anomalous terms*

We have shown explicitly that some vertex correction diagrams generate the following mode-coupling and advective anomalous terms in the equation of motion for the spin,

$$\text{MC} \quad \left\{ \begin{array}{l} \psi_\gamma(\tilde{\mathbf{k}}/2 - \tilde{\mathbf{q}}) \psi_\nu(\tilde{\mathbf{k}}/2 + \tilde{\mathbf{q}}) \mathbb{I}_{\alpha\beta\rho\sigma} k_\sigma q_\tau \mathbb{I}_{\rho\tau\gamma\nu} \\ \psi_\gamma(\tilde{\mathbf{k}}/2 - \tilde{\mathbf{q}}) \psi_\nu(\tilde{\mathbf{k}}/2 + \tilde{\mathbf{q}}) \mathbb{I}_{\alpha\beta\rho\sigma} q_\sigma k_\tau \mathbb{I}_{\rho\tau\gamma\nu} \end{array} \right\} \longrightarrow \left\{ \begin{array}{l} \left[ \partial_\alpha (\psi_\nu \partial_\nu \psi_\beta) - \partial_\beta (\psi_\nu \partial_\nu \psi_\alpha) \right] \\ \partial_\nu \left[ \psi_\nu (\partial_\alpha \psi_\beta - \partial_\beta \psi_\alpha) \right] \end{array} \right\} \quad , \quad (162)$$

$$\text{ADV} \quad \left\{ \begin{array}{l} s_{\gamma\nu}(\tilde{\mathbf{k}}/2 - \tilde{\mathbf{q}}) \psi_\eta(\tilde{\mathbf{k}}/2 + \tilde{\mathbf{q}}) \mathbb{I}_{\alpha\beta\rho\eta} k_\tau \mathbb{I}_{\rho\tau\gamma\nu} \\ s_{\gamma\nu}(\tilde{\mathbf{k}}/2 - \tilde{\mathbf{q}}) \psi_\eta(\tilde{\mathbf{k}}/2 + \tilde{\mathbf{q}}) \mathbb{I}_{\alpha\beta\rho\sigma} k_\sigma \mathbb{I}_{\rho\eta\gamma\nu} \end{array} \right\} \longrightarrow \left\{ \begin{array}{l} \partial_\nu (s_{\alpha\nu} \psi_\beta - s_{\beta\nu} \psi_\alpha) \\ \left[ \partial_\alpha (\psi_\nu s_{\nu\beta}) - \partial_\beta (\psi_\nu s_{\nu\alpha}) \right] \end{array} \right\} \quad . \quad (163)$$

which we have summarized here together with the real-space form that we anticipated in (21) and (23). Notice a complication: while each one of the two advection terms in  $k$  space gives rise to one term in  $x$  space, both mode-coupling anomalous terms in  $k$  space give contribute to both terms in  $x$  space. For this same reason the couplings of the MC anomalous terms in momentum space,  $\Phi_1, \Phi_2$  are a linear combination of those in real space,  $\phi_1, \phi_2$  (see equations (46) and (47)).

The crucial result of the diagrammatic calculation is that *all* diagrams generating anomalous terms (including all diagrams that we have not explicitly analyzed in this Section), generate *only* terms with one of these four tensorial structures. In this sense, the RG calculation is closed once we include these four vertices in the action. However, notice that the total perturbative amplitudes of these terms are *not* simply given by the coefficients  $A, B, C, D$  calculated here, indeed because anomalous corrections with the same tensorial structure arise in *many* more diagrams than the five computed in this Section.

## 5. Effective couplings and beta functions

The presence of the scaling exponents  $z, \chi_\psi$  and  $\chi_s$  in the definition of the scaling dimension of all the parameters of the theory seems to suggest that fixing a set of conditions on these exponents is necessary to study the RG flow. In fact, it is possible to define a set of effective parameters whose scaling behaviour does not depend on  $z, \chi_\psi$  and  $\chi_s$ ; moreover, all physical quantities turn out to depend on the parameters of the theory only via these effective couplings. The effective couplings can be found by looking at the scaling dimensions of the parameters of the theory, given in Eqs. (108), (109), (129)-(133). By recalling that the scaling dimension of the product of two couplings is given by the sum of the respective scaling dimensions, namely,

$$\mathcal{C}_b = \mathcal{A}_b \mathcal{B}_b = b^{-\chi_A - \chi_B} \mathcal{A}_0 \mathcal{B}_0 = b^{-\chi_C} \mathcal{C}_0 \quad \longrightarrow \quad \chi_C = \chi_A + \chi_B \quad (164)$$

it is always possible to find a set of combinations of coupling constants and parameters of the theory that have a scaling behaviour which is independent from  $z, \chi_\psi$  and  $\chi_s$  [18]. For example, let us consider the coupling constant  $J$ : its scaling, given by Eq. (133), depends on  $\chi_\psi$  and  $z$ . To compensate the dependence on  $\chi_\psi$  we can multiply it by the noise strength  $\tilde{\Gamma}$ , which also has a  $\chi_\psi$  scaling dependence; thus, the product  $\tilde{\Gamma}J$  does not depend anymore on  $\chi_\psi$ . Similarly, the dependence on  $z$  can be compensated by dividing by  $\Gamma^2$ , making the scaling behaviour of the combination  $\tilde{\Gamma}J/\Gamma^2$  depending only on  $d$  and perturbative corrections, which are computed through Feynman diagrams. A similar procedure can be applied at any other constant; multiplying it by appropriate powers of  $\tilde{\lambda}^{\pm/\parallel}$  or  $\tilde{\Gamma}$  to compensate the dependence on  $\chi_s$  or  $\chi_\psi$  respectively, and by appropriate powers of  $\Gamma, \lambda^{\pm/\parallel}$  to compensate the dependence on  $z$ . There is an ambiguity on the choice of whether to use  $\tilde{\lambda}^\perp$  or  $\tilde{\lambda}^\parallel$  to compensate  $\chi_s$  and whether to use  $\Gamma, \lambda^\perp$  or  $\lambda^\parallel$  to compensate  $z$ . However, as long as these parameters are not singular (and they will not be at the fixed point), this choice is irrelevant.

The effective parameters for (24)-(25) are,

$$w = \frac{\Gamma}{\lambda^{\parallel}}, \quad x = \frac{\lambda^{\perp}}{\lambda^{\parallel}}, \quad \theta^{\perp} = \frac{\tilde{\Gamma}\lambda^{\perp}g^{(s)}}{\Gamma\tilde{\lambda}^{\perp}g^{(\psi)}}, \quad \theta^{\parallel} = \frac{\tilde{\Gamma}\lambda^{\parallel}g^{(s)}}{\Gamma\tilde{\lambda}^{\parallel}g^{(\psi)}}, \quad (165)$$

where  $\theta^{\perp,\parallel} \neq 1$  if the system is out-of-equilibrium. Although the technical definition of  $\theta^{\perp/\parallel}$  contains the ratio  $g^{(s)}/g^{(\psi)}$ , in the physical case we expect  $g^{(s)} = g^{(\psi)}$ , as argued in SI-Section IC 2 . Hence, the physical meaning of  $\theta^{\perp/\parallel}$  is that of the ratio between the effective temperatures of the two fields,  $T_{\psi} = \tilde{\Gamma}/\Gamma$  and  $T_s^{\perp/\parallel} = \tilde{\lambda}^{\perp/\parallel}/\lambda^{\perp/\parallel}$ , namely

$$\theta^{\perp} = \frac{T_{\psi}}{T_s^{\perp}} = \frac{\tilde{\Gamma}\lambda^{\perp}}{\Gamma\tilde{\lambda}^{\perp}}, \quad \theta^{\parallel} = \frac{T_{\psi}}{T_s^{\parallel}} = \frac{\tilde{\Gamma}\lambda^{\parallel}}{\Gamma\tilde{\lambda}^{\parallel}}. \quad (166)$$

The effective coupling constants regulating activity are,

$$c_v = v_0 \frac{\gamma_v}{\Gamma} \sqrt{\frac{\tilde{\Gamma}}{\Gamma}} \sqrt{K_d \Lambda^{d-4}}, \quad c_s = v_0 \frac{\gamma_s}{\lambda^{\parallel}} \sqrt{\frac{\tilde{\Gamma}}{\Gamma}} \sqrt{K_d \Lambda^{d-4}}, \quad (167)$$

while the mode-coupling, the ferromagnetic and the DYS effective coupling constants respectively are,

$$f = \frac{\tilde{\lambda}^{\parallel}}{\lambda^{\parallel}} \frac{g^2}{\lambda^{\parallel}\Gamma} K_d \Lambda^{d-4}, \quad \tilde{u} = \frac{\tilde{\Gamma}}{\Gamma} \frac{J}{\Gamma} K_d \Lambda^{d-4} = \frac{\tilde{\Gamma}}{\Gamma} u K_d \Lambda^{d-4}, \quad \tilde{u}_{\kappa} = \frac{\tilde{\Gamma}}{\Gamma} \frac{\kappa}{g} K_d \Lambda^{d-4}; \quad (168)$$

where  $\Lambda$  is the cutoff of the theory and  $K_d$  is the surface of the unitary sphere in  $d$  dimensions. The presence of  $\Lambda$  to the power  $4 - d$  in all effective couplings suggests that the upper critical dimension of the theory is  $d_c = 4$ , which means that all couplings are relevant in  $d < 4$ , while mean-field behaviour is recovered for  $d \geq 4$ . At equilibrium, where  $v_0 = 0$  and  $\tilde{\Gamma} = \Gamma, \tilde{\lambda} = \lambda, \kappa = ug$ , all the effective couplings become identical to their standard equilibrium counterpart [9], with the equilibrium result  $\tilde{u} = \tilde{u}_{\kappa}$  [12] being recovered.

The flow of the effective couplings can be obtained by iterating the infinitesimal RG transformation, thus defining a set of recursive relations. After  $l$  iterations, the new parameters will take the form,

$$\mathcal{P}_{l+1} = b^{-\chi_{\mathcal{P}}} \mathcal{P}_l \quad (169)$$

where  $\chi_{\mathcal{P}}$  is evaluated using the values of the parameters at step  $l$ . The values  $\mathcal{P}^*$  to which the flow of  $\mathcal{P}$  approaches when  $l \rightarrow \infty$  are called fixed points, and play a crucial role in determining the critical behaviour of the theory [29]. To search these fixed points, we shall switch our attention to the derivative of  $\mathcal{P}$  with respect to  $\ln b$ , known as  $\beta$ -functions. The zeros of  $\beta_{\mathcal{P}} = \partial\mathcal{P}/\partial(\ln b)$  represent those values of  $\mathcal{P}$  which are fixed points of the flow, meaning that any further iteration of an RG step will leave the values unchanged. Since the  $\beta$ -function of the generic parameter  $\mathcal{P}$  is given by

$\beta_{\mathcal{P}} = -\mathcal{P}\chi_{\mathcal{P}}$ , for the parameters defined in Eqs. (165)-(168) the beta functions take the following form,

$$\beta_w = w \left( \delta\Gamma - \delta\lambda^{\parallel} \right) \quad (170)$$

$$\beta_x = x \left( \delta\lambda^{\perp} - \delta\lambda^{\parallel} \right) \quad (171)$$

$$\beta_{\theta^{\perp}} = \theta^{\perp} \left( \delta\tilde{\Gamma} - \delta\Gamma + \delta\lambda^{\perp} - \delta\tilde{\lambda}^{\perp} + \delta g_s - \delta g_{\psi} \right) \quad (172)$$

$$\beta_{\theta^{\parallel}} = \theta^{\perp} \left( \delta\tilde{\Gamma} - \delta\Gamma + \delta\lambda^{\parallel} - \delta\tilde{\lambda}^{\parallel} + \delta g_s - \delta g_{\psi} \right) \quad (173)$$

$$\beta_{c_v} = \frac{1}{2}c_v \left( \epsilon + \delta\tilde{\Gamma} + 2\delta\gamma_{\psi} - 3\delta\Gamma - \delta\omega_{\psi} \right) \quad (174)$$

$$\beta_{c_s} = \frac{1}{2}c_s \left( \epsilon + \delta\tilde{\Gamma} + 2\delta\gamma_s - \delta\Gamma - 2\delta\lambda^{\parallel} - \delta\omega_{\psi} \right) \quad (175)$$

$$\beta_f = f \left( \epsilon + \delta\tilde{\lambda}^{\parallel} + 2\delta g_{\psi} - 2\delta\tilde{\lambda}^{\parallel} - \delta\Gamma - \delta\omega_{\psi} \right) \quad (176)$$

$$\beta_{\tilde{u}} = \tilde{u} \left( \epsilon + \delta\tilde{\Gamma} + \delta J - 2\delta\Gamma - \delta\omega_{\psi} \right) \quad (177)$$

$$\beta_{\tilde{u}_{\kappa}} = \tilde{u}_{\kappa} \left( \epsilon + \delta\tilde{\Gamma} + \delta\kappa - \delta\Gamma - \delta g_s - \delta\omega_{\psi} \right) \quad (178)$$

$$\beta_{\mu_1} = \mu_1 \left( \delta\gamma_{s1} - \delta\gamma_s \right) \quad (179)$$

$$\beta_{\mu_2} = \mu_2 \left( \delta\gamma_{s2} - \delta\gamma_s \right) \quad (180)$$

$$\beta_{\Phi_1} = \Phi_1 \left( \delta g_{s1} - \delta g \right) \quad (181)$$

$$\beta_{\Phi_2} = \Phi_2 \left( \delta g_{s2} - \delta g \right) \quad (182)$$

where all the perturbative corrections  $\delta\mathcal{P}$  are obtained from the Feynman diagram expansion. The explicit expressions of these beta functions are given in the Mathematica attached notebook (*beta\_functions.nb*).

## D. Properties of the new RG solution

### 1. Flow and fixed points

The fixed points of the RG flow are given by the zeros of the  $\beta$ -functions, which in simpler field theories are usually found analytically. Here we tackle this problem by integrating numerically the set of partial differential equations defining the RG flow, namely

$$\dot{\mathcal{P}} = \beta_{\mathcal{P}} \quad (183)$$

and looking at what values of the parameters the flow converges. If the flow does converge, the point to which it will converge is a fixed point of the theory. This procedure does not allow us to find unstable fixed points, but only the IR-stable ones. To perform this numerical integration, we have to take great care in the choice of initial conditions of the parameters and couplings, as we expect a large portion of this 13-dimensional space to be just unphysical. The set of parameters  $v_0 = 0$  (and thus  $c_v = c_s = 0$ ),  $\theta^{\perp/\parallel} = 1$ ,  $\Phi_1 = \Phi_2 = 0$  and  $\tilde{u} = \tilde{u}_{\kappa} \neq 0$  identifies Solenoidal Model G [12], which represents the equilibrium limit of our theory – Eq. (24) (25). We expect a system with *small*, but non-vanishing activity  $v_0$  to belong to the neighbourhood of the equilibrium limit, and thus to be physical in the RG space. If activity is relevant, and indeed we will see it is, the corresponding coupling constants  $c_v$  and  $c_s$  should grow along with the RG flow and drive the system towards an out-of-equilibrium active fixed point, if it exists. We remark that we do not start close to equilibrium because we expect activity to be weak in swarms; in fact, quite the opposite: as we show in the main text, activity in natural swarms is strong. We start close to the equilibrium fixed point for a mere technical need: we need a safe path through a very dangerous parameter space in which it is far too easy for the RG flow to go bonkers if one deviates too much from a physical initial condition.

The constants  $\mu_1$  and  $\mu_2$  have undefined values in the equilibrium limit, since they are both multiplied by  $v_0\gamma_s$  in the equations of motion and thus we have no *a priori* argument to fix their value near equilibrium. However, we find

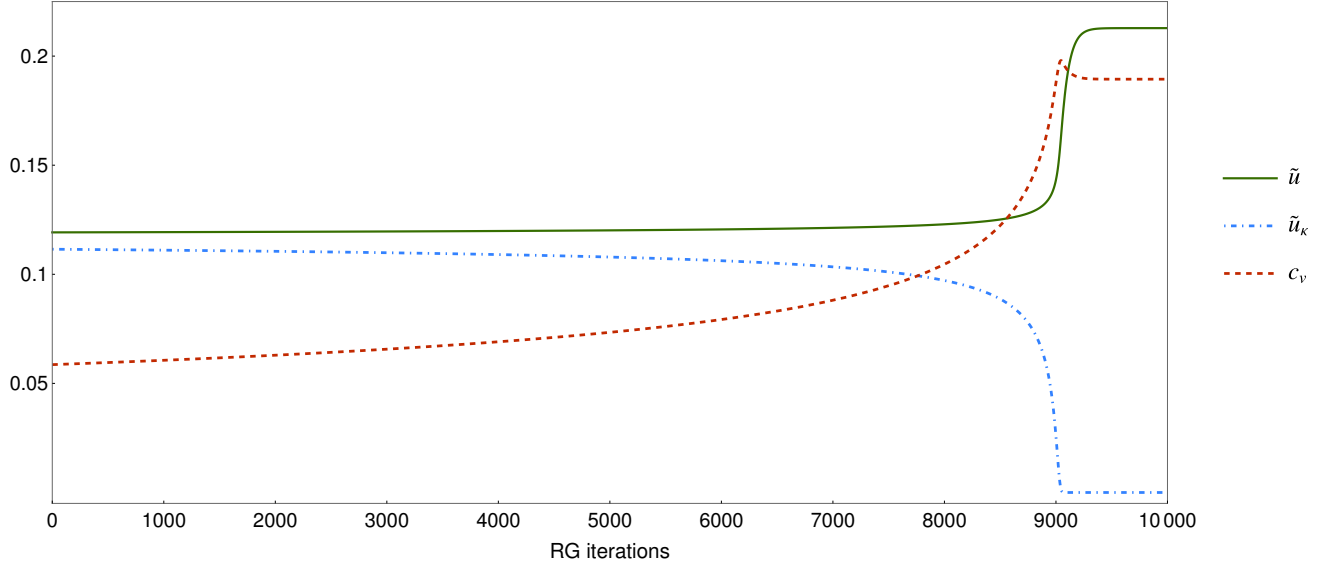


FIG. 4. **RG flow of  $\tilde{u}$ ,  $\tilde{u}_\kappa$  and  $c_v$ .** As an example, we show a portion of the RG flow of the couplings  $\tilde{u}$ ,  $\tilde{u}_\kappa$  and  $c_v$  from the unstable equilibrium fixed point towards the stable off-equilibrium fixed point. From the plot we can clearly see that as activity increases,  $\tilde{u}$  and  $\tilde{u}_\kappa$  become different one from the other. As the fixed point is approached, the value of  $\tilde{u}_\kappa$  drops to 0.

that the  $\beta$ -functions of these two parameters, namely  $\beta_{\mu_1}$  and  $\beta_{\mu_2}$ , vanish when  $\mu_1$  and  $\mu_2$  take the following values

$$\mu_1 = \frac{1}{2} \quad , \quad \mu_2 = -\frac{1}{2} \quad (184)$$

$$\mu_1 = -1 \quad , \quad \mu_2 = 0 \quad (185)$$

independently of the values of all other parameters. This means that both these combinations of  $\mu_{1,2}$  remain constant along with the RG flow, whatever the other couplings and parameters are doing. The first solution of  $\mu_{1,2}$  turns out to be unstable for small perturbations of their values, at least near the equilibrium fixed point, while the second solution is stable. Hence, we fix from the beginning  $\mu_1 = -1$  and  $\mu_2 = 0$  and check the consistency of this choice by looking in the aftermath the stability of the RG flow with respect to perturbations in  $\mu_1$  and  $\mu_2$ , thus reducing our problem to 11 coupled equations instead of 13.

We simulate the RG flow starting from various initial conditions close to equilibrium by using the built-in *NDSolve* function of the software *Mathematica*, and we always find the same attractive fixed point,

$$\tilde{u}^* = 0.213\epsilon \quad \tilde{u}_\kappa^* = 0 \quad c_v^* = 0.189\sqrt{\epsilon} \quad (186)$$

$$f^* = 1.68\epsilon \quad \Phi_1 = -0.762 \quad \Phi_2^* = -0.137 \quad (187)$$

$$c_s^* = 0.882\sqrt{\epsilon} \quad \mu_1 = -1 \quad \mu_2 = 0 \quad (188)$$

$$x^* = 0.369 \quad w^* = 3.95 \quad (189)$$

$$\theta_\perp^* = 1.34 \quad \theta_\parallel^* = 0.920 \quad (190)$$

A typical RG flow of a selected number of couplings is represented in Fig. 4. Since  $c_v$ ,  $c_s$  and  $f$  have a finite fixed point value, both activity and mode-coupling are relevant at this fixed point, making it the ideal candidate to describe incompressible inertial active matter. The stability of the novel fixed point is analyzed by looking at the Jacobian matrix of the beta functions

$$J_\beta = \frac{\partial \vec{\beta}}{\partial \vec{\mathcal{P}}} \quad (191)$$

The eigenvalues of  $J_\beta$  at the new fixed point are given by

$$-2.26\epsilon, \quad -1.66\epsilon, \quad -1.00\epsilon, \quad (-0.724 + 0.107i)\epsilon, \quad (-0.724 - 0.107i)\epsilon \quad (192)$$

$$-0.562\epsilon, \quad -0.498\epsilon, \quad -0.315\epsilon, \quad (-0.247 + 0.00185i)\epsilon, \quad (-0.247 - 0.00185i)\epsilon \quad (193)$$

$$-0.0584\epsilon, \quad -0.0532\epsilon, \quad -0.0167\epsilon \quad (194)$$

A negative (positive) real part of an eigenvalue indicates that the flow near the fixed point converges (diverges) exponentially in the number of RG-steps in the direction of the associated eigenvector. On the other side, the presence of an imaginary part of the eigenvalues stems from a spiralling convergence or divergence of the flow in the direction of the eigenvalue. Since the real part of all the eigenvalues of  $J_\beta$  is negative when  $\epsilon > 0$ , we can conclude that this new fixed point is stable in  $d < 4$  and thus it rules the long-wavelength behaviour of the system in the physical case of  $d = 3$ .

## 2. The dynamical critical exponent

The spatio-temporal behaviour of a collective system is described by the two-point connected correlation function of the order parameter,  $C(\mathbf{x}, t)$ . In general, the correlation function encodes a very complicated relation between time and space and depends on a set of control parameters  $\mathcal{P}$  defining the state of the system. In the case of critical systems, the control parameters enter the correlation function only through the correlation length  $\xi(\mathcal{P})$ . This property is known as *dynamic scaling* [36, 37], and it states that the correlation function  $C$ , when expressed as a function of wave-vector and frequency, obeys the following scaling form,

$$C(\mathbf{k}, \omega; \mathcal{P}) = C_0(\mathbf{k}; \xi) F\left(\frac{\omega}{\omega_k(\mathcal{P})}, k\xi\right) \quad (195)$$

where  $\xi = \xi(\mathcal{P})$  is the correlation length and where the static correlation function  $C_0$  has in turns the scaling form,

$$C_0(k, \xi) = k^{2-\eta} F_0(k\xi) \quad (196)$$

while the characteristic frequency at scale  $k$  is given by,

$$\omega_k(\mathcal{P}) = k^z \Omega(k\xi(\mathcal{P})) \quad (197)$$

In the relations above,  $\Omega$ ,  $F_0$  and  $F$  are well-behaved scaling functions, whose explicit form is not relevant for our purposes;  $\eta$  is the critical exponent for the static correlation function (normally called anomalous dimension of the order parameter [38]). What dynamic scaling asserts is that the divergence of space correlations and time correlations are not independent near the critical point, but they are connected by the dynamic critical exponent  $z$ . To find the critical exponent  $z$ , following a standard procedure [9, 32] we require that the kinetic coefficient of the velocity field is not singular at the RG stable fixed point, namely,

$$\Gamma^* = O(1) \quad \rightarrow \quad \chi_\Gamma = 0 \quad (198)$$

By rearranging the condition  $\chi_\Gamma = 0$  from Eq. (108), one easily finds the expression of  $z$ ,

$$z = 2 - \delta\Gamma + \delta\omega_\psi \quad (199)$$

Once we substitute the diagrammatic results for  $\delta\Gamma$  and  $\delta\omega_\psi$  in the equation for  $z$ , we finally obtain the following expression for the dynamic critical exponent,

$$\begin{aligned} z = 2 & - \frac{3f(3w+2x+1)}{4(w+1)(w+x)} - \frac{c_v^2}{4} + \frac{f(\theta^\perp - 1)(13w^2 + 12wx + 5x^2)}{12\theta^\perp(w+x)^3} - \\ & - \frac{f(\theta^\parallel - 1)(13w^3 + w^2(4x+75) + w(48x+51) + 24x+9)}{12(w+1)^3(w+x)} \\ & - \frac{f(\theta^\parallel - 1)(\theta^\perp - 1)(13w^2 + 12wx + 5x^2)}{12\theta^\perp(w+x)^3} - \frac{f\theta^\parallel\Phi_1x(3w+2x)}{4(w+x)^3} \\ & - \frac{f\theta^\parallel\Phi_2(9w^3x + 2w^2(4x^2 + 9x - 1) + wx(2x^2 + 16x + 3) + 2x^2(2x + 1))}{12(w+1)^2(w+x)^3} \end{aligned} \quad (200)$$

The value of  $z$  is then simply obtained by plugging into (200) the fixed point values of the parameters, which gives,

$$z = 2 - 0.7\epsilon \quad (201)$$

in a first digit approximation. For  $d = 3$  ( $\epsilon = 1$ ), we finally obtain the RG prediction for the dynamic critical exponents of natural swarms,

$$z = 1.3 . \quad (202)$$

The correction of  $0.7\epsilon$  with respect to the free value  $z = 2$  might seem large for a first-order term in a perturbative expansion, which is true if we consider the overdamped free theory of Model A, the theory around which we are doing the expansion. In fact, the new fixed point has been found by adding nonlinear activity to Model G [9], which has a *non-perturbative* dynamic critical exponent  $z = \frac{d}{2} = 2 - \frac{\epsilon}{2}$  [18]. Thus, our result should be considered as a  $0.2\epsilon$  departure from Model G's non-perturbative exponent, rather than a  $0.7\epsilon$  correction to Model A. To compare our result with previous ones in a similar context, the incompressible Toner and Tu theory has a dynamic critical exponent of  $z = 2 - 0.3\epsilon$  [2], with a perturbative departure of  $0.3\epsilon$  from equilibrium Model A's exponent, which is its natural expansion point. Numerical simulations of Vicsek Model in  $d = 3$  found a dynamic exponent of  $z \approx 1.7$  [3], showing that the dynamic exponent found in [2] holds with remarkable accuracy also in  $d = 3$ , namely when  $\epsilon = 1$ .

### 3. Non-conservative dissipation and the crossover to overdamped dynamics

Up to now, the field theory we analyzed was fully conservative, since the order parameter was coupled to a globally conserved quantity, namely the spin. This coupling has been proposed in the Inertial Spin Model [6] to provide a theoretical explanation for information propagation in flocks [4], by making the spin responsible to carry information giving rise to the observed second-sound propagation. The presence of second-sound modes even close to the ordering transition (called 'paramagnons' in condensed matter) was also found experimentally in natural swarms [5], supporting the idea that spin-velocity mode-coupling is an essential mechanism also of these systems. However, in real biological systems, information is not expected to be propagated forever with zero dissipation, as damping effects must become relevant over longer and longer distances. Thus, a small spin dissipation is always expected in real biological systems.

In order to introduce dissipation, a  $k$ -independent term must be added to the kinetic coefficient of the spin,  $\Lambda_{\alpha\beta\gamma\nu} \rightarrow \Lambda_{\alpha\beta\gamma\nu} + \eta \mathbb{I}_{\alpha\beta\gamma\nu}$  where  $\eta$  is the dissipative friction (not to be confused with the anomalous dimension of the correlation function). The new form of  $\Lambda_{\alpha\beta\gamma\nu}$  is therefore given by

$$\Lambda_{\alpha\beta\gamma\nu} = \eta \mathbb{I}_{\alpha\beta\gamma\nu} + \lambda^\perp k^2 \mathbb{P}_{\alpha\beta\gamma\nu}^\perp + \lambda^\parallel k^2 (\mathbb{I} - \mathbb{P}^\perp)_{\alpha\beta\gamma\nu} . \quad (203)$$

This addition leads to the presence of a new linear term in the equation of motion for the spin, namely  $\partial_t \mathbf{s} \sim -\eta \mathbf{s}$ , giving to all  $\mathbf{s}$  modes, including the  $k = 0$  mode, a finite relaxation time  $\eta^{-1}$ . The scaling dimension of this new parameter  $\eta$  is given by

$$\chi_\eta = -z - \delta\eta \quad (204)$$

where  $-z$  is the naive dimension of  $\eta$ , coming from the fact that  $\eta$  is the inverse of a time-scale, while  $\delta\eta$  represents the perturbative correction given by the coupling between IR and UV modes during the RG transformation.

The finite relaxation time for the spin  $\eta^{-1}$  will become, close to criticality, much smaller than the velocity relaxation time  $\tau = \xi^z$ , making the spin  $\mathbf{s}$  a *fast mode*. Hence, the presence of dissipation strongly modifies the asymptotic critical behaviour, since near criticality only the modes fluctuating on the same scales of the order parameter may affect universal quantities [9]. Therefore, when dissipation is present, the *asymptotic* critical dynamics in the *thermodynamic limit* is unaffected by the presence of the spin-velocity coupling, making the theory equivalent to the overdamped incompressible Toner and Tu theory [2]. However, swarms are very much finite-size systems, not even close to the thermodynamic limit; moreover, we are interested in their dynamics over finite time-scales, much larger than the microscopic ones, but certainly not infinitely long. Hence, while inertial dynamics may not be relevant over infinitely large length-scales and infinitely long times, it turns out to be relevant over realistic biological scales, whose size depends on the relative value of dissipation and inertia [10, 11].

At the theoretical level, this crossover between a finite-size physics influenced by inertia, and an asymptotic physics completely overdamped manifests itself as a crossover between different RG fixed points. Hence, following [10, 11], we will investigate the crossover between the conservative dynamic behaviour, ruled by our novel fixed point with  $z = 1.3$ , and the dissipative dynamics of the incompressible Toner and Tu theory, investigated by Chen *et al.* in [2] with  $z = 1.7$ . The starting point of this analysis is the observation that the ratio between non-conservative friction  $\eta$  and conservative kinetic coefficient  $\lambda^\parallel$  naturally defines, by simple power counting, a length-scale  $\mathcal{R}$  given by [10, 11],

$$\mathcal{R} = \sqrt{\frac{\lambda^\parallel}{\eta}} \quad (205)$$

We could define a second length-scale:  $\sqrt{\lambda^\perp/\eta}$ . However, it turns out this second length-scale has the same scaling behaviour as  $\mathcal{R}$ , hence it makes no difference what definition we use.

The parameter  $\mathcal{R}$  plays the role of a conservation length-scale, in the sense that fluctuations occurring on length-scales smaller than  $\mathcal{R}$  obey a conservative dynamics, while beyond  $\mathcal{R}$  fluctuations are insensitive to inertia and conservation

laws. The scaling dimension of  $\mathcal{R}$  is that of a length, but only at the naive (non-interacting) level; in fact, we know that the RG coupling between the UV and IR degrees of freedom generates non-trivial modifications of naive scaling dimensions of  $\lambda^\parallel$  and in principle also of  $\eta$ . The RG flow of  $\mathcal{R}$  can be written as (see Eq. (169)),

$$\mathcal{R}_{l+1} = b^{-\chi_{\mathcal{R}}} \mathcal{R}_l \quad (206)$$

and its scaling dimension is given by,

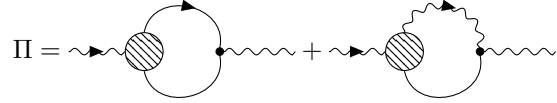
$$\chi_{\mathcal{R}} = \frac{1}{2}(\chi_{\lambda^\parallel} - \chi_\eta) = 1 + \frac{1}{2}\delta\eta - \frac{1}{2}\delta\lambda^\parallel \quad (207)$$

where 1 is the naive dimension of  $\mathcal{R}$ , which allowed us to naively identify it as a length-scale, while  $\delta\eta$  is the perturbative correction to the friction  $\eta$  and  $\delta\lambda^\parallel$  the correction to the kinetic coefficient  $\lambda^\parallel$ .

As it happens in the equilibrium case [11], also in the present theory the dissipation  $\eta$  is not corrected by shell integration, hence we have,

$$\delta\eta = 0 . \quad (208)$$

The physical origin of this fact is that all diagrams contributing to the self energy  $\Pi$  (which contains corrections to both  $\eta$  and  $\lambda^\parallel$ ) vanish at  $k = 0$  as a consequence of the form of the mode-coupling and the self-propulsion vertices for  $\mathbf{s}$ . This has been verified in our calculation at first order in perturbation theory, where higher order effects of diagrams containing the DYS vertex on  $\Pi$  are not taken into account; however, if the result  $\kappa^* = 0$  is exact to all orders, the DYS vertex is always irrelevant and thus no diagrams could ever generate dissipation. This is what we expect, as  $\kappa^* = 0$  implies a global conservation of the spin (at  $\eta = 0$ ), which does not seem a perturbative accident (see next Section). But even in the unlikely case in which the result  $\kappa^* = 0$  were an accident of first order perturbation theory, we prove here that the dissipation of the spin still can *never* receive any perturbative corrections. In general, the self-energy  $\Pi$  takes contributions only from the following two distinct classes of diagrams,



$$\Pi = \text{diagram 1} + \text{diagram 2} \quad (209)$$

where the blobs represent the renormalized mode-coupling and self-propulsion vertices respectively, in which all the possible diagrammatic corrections (at all orders in  $\mathbf{k}$  and  $\mathbf{q}$ ) are taken into account. Because the renormalized spin mode-coupling and self-propulsion vertices vanish at zero external momentum  $\mathbf{k}$ , then these diagrams are zero at  $k = 0$ , implying that no dissipation is generated. Therefore, as long as the structure of the equations of motion (24) and (25) is preserved under the RG, no spin dissipation can be generated.

To work out the correction  $\delta\lambda^\parallel$  we need a different argument. As we have seen, the ratio  $w = \Gamma/\lambda^\parallel$  is finite at the novel fixed point,  $w^* = 3.95$  (equation (190)); moreover, the kinetic coefficient of the primary field is also finite at the fixed point,  $\Gamma^* = O(1)$  (this is how one works out the dynamic exponent  $z$ ), implying that also the kinetic coefficient of the spin is finite,  $\lambda^{\parallel*} = O(1)$ , and thus that  $\chi_{\lambda^\parallel} = 0$ . From (108) we conclude,

$$\delta\lambda^\parallel = 2 - z . \quad (210)$$

From equations (207), (208) and (210), we finally obtain the scaling dimension of  $\mathcal{R}$  near the active conservative fixed point,

$$\chi_{\mathcal{R}} = \frac{z}{2} . \quad (211)$$

The fact that the scaling dimension of  $\mathcal{R}$  is positive implies (through (206)) that it *decreases* along with the RG flow, making the length-scale within which critical dynamics is underdamped shorter and shorter; this is another way to see that dissipation eventually takes over in the hydrodynamic limit. However, thanks to (211), we can now quantitatively describe the RG crossover from the conservative active fixed point to the dissipative one, or – more precisely – describe the departure of the RG flow from the conservative active fixed point when we start close to it. Close to criticality, the correlation length-scales as  $\xi_l = b^{-l}\xi_{l-1} = b^{-l}\xi_0$ , where  $\xi_0$  is its physical value in the original system under study. The RG flow stops when the system is far from the critical manifold, namely when the correlation length becomes of the same size of the microscopic scale  $\Lambda^{-1}$ , giving  $l^{\text{stop}} = \xi_0\Lambda$  [9, 32]. Let us consider a system with small bare dissipation,  $\eta_0$ , and therefore with a large conservation length-scale  $\mathcal{R}_0$  (the subscript zero indicates the bare values of the parameter, namely the starting values of the RG flow or the parameters that are those of the equations of motion).

The RG flow will rapidly approach the conservative fixed point, remaining in its neighborhood for a large number of RG iterations and eventually flowing towards the dissipative fixed point [11]. Whether the system is ruled by the conservative or dissipative fixed point depends on how large  $\mathcal{R}_{l_{\text{stop}}}$  is when the RG flow leaves the critical region: if when the flow stops  $\mathcal{R}_{l_{\text{stop}}} \gg \Lambda^{-1}$ , the critical behaviour is ruled by the conservative fixed point; this is equivalent to the condition,

$$\mathcal{R}_0(b^{-\chi\mathcal{R}})^{l_{\text{stop}}} = \mathcal{R}_0(\xi_0\Lambda)^{-\chi\mathcal{R}} \gg \Lambda^{-1} \quad (212)$$

that is,

$$\xi_0 \ll (\mathcal{R}_0\Lambda)^{\frac{1}{\chi\mathcal{R}}} \Lambda^{-1} . \quad (213)$$

By using equation (211) and by measuring all lengths in units of the microscopic scale  $\Lambda^{-1}$  (which is equivalent to simply set  $\Lambda = 1$  in all equations), we obtain the following condition for active underdamped dynamics,

$$\xi_0 \ll (\mathcal{R}_0)^{2/z} \quad (214)$$

while beyond this scale the overdamped fixed point with  $z = 1.7$  takes over. In Fig. 5 we show the regions corresponding to the two dynamical behaviours. In the case of finite-size systems as natural swarms, the size of the system  $L$  is a physical upper bound to the correlation length  $\xi_0$ . Therefore, if the dissipation  $\eta_0$  is small enough to have  $L \ll (\mathcal{R}_0)^{2/z}$ , the ruling fixed point is the underdamped active one. By recalling the definition of  $\mathcal{R}$ , equation (205), we finally get,

$$L \ll \left( \frac{\lambda_0^{\parallel}}{\eta_0} \right)^{1/z} \rightarrow z = 1.3 . \quad (215)$$

The crossover exponent  $\phi = 2/z$  determines how slowly the dissipative dynamics becomes relevant. The larger this exponent is, the larger the system must be before crossing over to the dissipative fixed point. Since the non-equilibrium dynamic critical exponent  $z = 1.3$  is smaller than its equilibrium counterpart  $z_{eq} = 1.5$ , this means that the crossover exponent will be larger in the non-equilibrium scenario, implying that the conservative fixed point rules the dynamic behaviour up to larger scales with respect to the equilibrium scenario (see Fig. (5)).

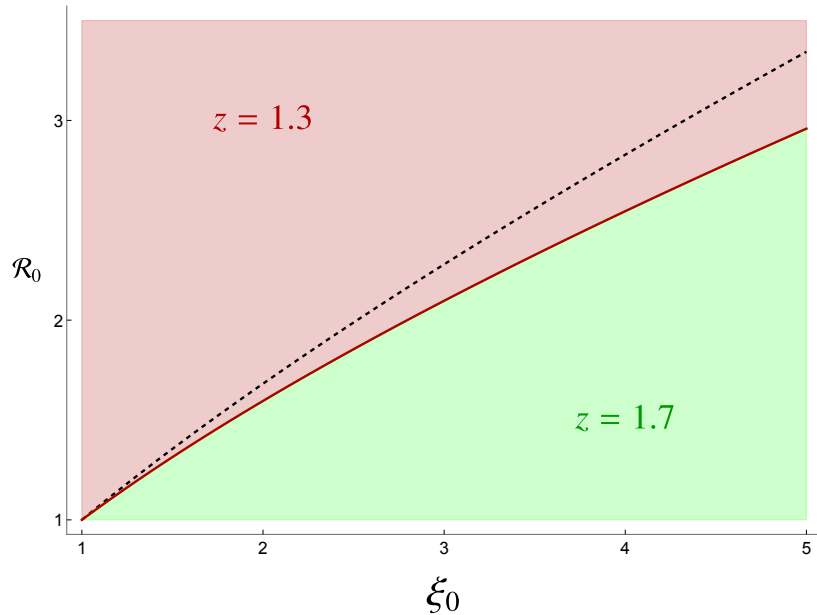


FIG. 5. **Crossover between different critical regions.** Different values of  $\mathcal{R}_0$  lead to different critical behaviour, depending on the correlation length  $\xi$ . We restrict ourselves to the physical range  $\xi_0 > \Lambda^{-1}$ , and measure lengths in units of  $\Lambda^{-1}$ . The figure refers to the  $d = 3$  case. The dark red region is where dissipation is weak enough that conservative dynamics still holds, thus leading to  $z = 1.3$ , while in the light green dissipation overcomes and the dynamic behaviour is controlled by  $z = 1.7$ . The red line represents  $L_c$ , the threshold between the two behaviour in the active case. The black dashed line represents instead the threshold between conservative and dissipative dynamics at equilibrium: since the conservative region is lower here, we conclude that activity protects conservative behaviour up to high scales.

#### 4. Off-equilibrium activity restores the conservation of the spin

One of the most intriguing features of the novel active inertial fixed point - we remind  $\eta = 0$  here - is the vanishing of the DYS vertex effective coupling constant, namely  $\tilde{u}_\kappa^* = 0$  (see Eq. (186) of SI-Section ID 1). At equilibrium, the presence of the DYS vertex, with  $\tilde{u}_\kappa = \tilde{u}$ , had such a crucial role in keeping the dynamics of  $\mathbf{s}$  consistent with the solenoidal constraint on  $\boldsymbol{\psi}$  [12] that it seems surprising to find that this vertex disappears out of equilibrium. Moreover, the couplings  $\tilde{u}$  and  $\tilde{u}_\kappa$  both derive from derivatives of the  $u\psi^4$  term in the free energy functional  $\mathcal{H}$ , and thus one would expect a deep connection between the two. However, the fact that the DYS vertex vanishes at this novel fixed point avoids the odd scenario of having two different ferromagnetic couplings; both at equilibrium and off-equilibrium, the RG suggests that only *one* ferromagnetic coupling should exist, by requiring in the former case that  $\tilde{u} = \tilde{u}_\kappa$  and in the latter  $\tilde{u}_\kappa = 0$ .

But by far the most surprising consequence of the off-equilibrium vanishing of the DYS vertex is that when  $\tilde{u}_\kappa = 0$  the global spin turns out to be conserved! As mentioned in SI-Section IB 3 and discussed in [12], the DYS vertex is the only interaction that contributes to the dynamics of the spin at  $k = 0$  when  $\eta = 0$ , thus violating the spin conservation (although it does not violate it strongly, e.g. through dissipation). Since  $\tilde{u}_\kappa$  is the effective coupling associated with the DYS interaction, the fact that it vanishes means that this vertex is irrelevant at the novel fixed point and thus the spin becomes globally conserved. The restored spin conservation in the active off-equilibrium case is surprising, and it can hardly be a mere accident of the RG calculation. To try to understand its meaning we have to go back to the underlying symmetry and conservation law in the theory.

At equilibrium, and in absence of any constraint on the field, the presence of an exact rotational symmetry guarantees that the spin is globally conserved since it is the generator of the symmetry. This is exactly what happens in Model G, described in SI-Section IA 2. Now we add the solenoidal constraint, which is the equilibrium version of incompressibility: as it is clear from Fig.6-left, the solenoidal constraint breaks the rotational invariance: if we start from a solenoidal configuration of the field and rotate each vector by the same constant amount, we obtain a new field configuration which violates the solenoidal constraint. At the field-theoretical level, this manifests itself by the RG generation of the DYS vertex that indeed breaks the symmetry and conservation of the spin [12]. This is what happens at equilibrium, namely in the non-active case.

According to the RG, if we now turn from the inactive solenoidal case to the active incompressible one, the presence of activity restores the full power of the rotation symmetry - at least on long wavelengths - by making the spin

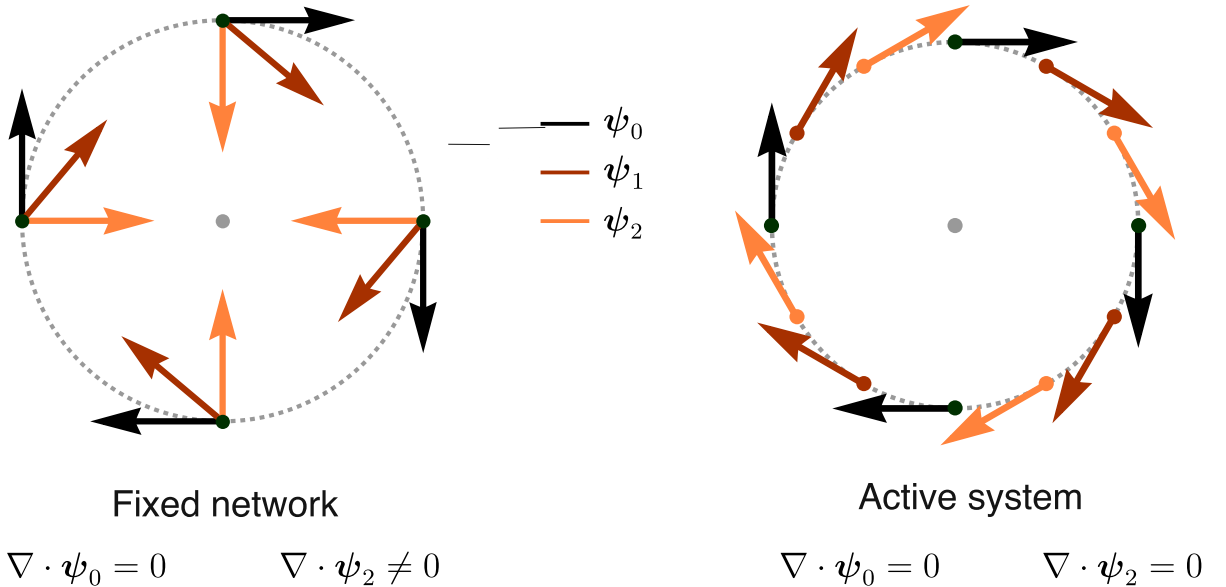


FIG. 6. **Incompressibility in the inactive vs active case.** Left: in the inactive case, if we start from a solenoidal configuration of the field ( $\boldsymbol{\psi}_0$ , black) and we let a constant uniform spin rotate the field, we obtain a non-solenoidal configuration ( $\boldsymbol{\psi}_2$ , orange). This is equivalent to saying that the solenoidal constraint breaks rotational invariance at equilibrium. Right: in the active case the particles are dragged by the field, hence the rotation generated by the spin rotates both the field *and* the position of the field, giving rise to a new configuration that is equally solenoidal (that is incompressible).

conserved once again. This suggests that - at variance with the inactive case - activity preserves incompressibility under local rotations. A qualitative cartoon of this mechanism can be seen in Fig.6-right: in the active case a local rotation generated by the spin has a twofold effect: *i*) it rotates the field (as in the inactive case); *ii*) it also rotates the positions, through the self-propelled part of the equations,  $\dot{\vec{x}} = \vec{v}$  (at variance with the inactive case). These two rotations balance each other, giving rise to a new field configuration that is still solenoidal, i.e. incompressible (Fig.6-right). We stress that this is far from being a general mathematical proof, as it is restricted to the very simple case of a purely rotational field, while one would need to generalize this argument to a generic solution of the dynamical equations. It may be that the full proof of spin conservation in the case of active incompressible dynamics is the very RG calculation that we carried out here; even though one would hope for a simpler and more direct way to prove this result, we could not find it.

In fact, when we reflect on the whole RG flow, rather than restricting ourselves to the fixed point, the situation becomes even more intriguing. As we wrote above, we found the new active incompressible mode-coupling fixed point by starting close to the inactive (equilibrium) incompressible mode-coupling fixed point. At the starting point,  $\tilde{u}_\kappa^* \neq 0$ , because - as we said - at equilibrium the DYS vertex is required to enforce incompressibility; along with the flow which goes from equilibrium to off-equilibrium, the coupling  $\tilde{u}_\kappa^*$  decreases weakly (see Fig.4) until it abruptly goes to zero right before arriving at the new fixed point. If we tried to start the flow with all parameters close to their equilibrium values, but with  $\tilde{u}_\kappa^* = 0$  from the outset, we would *not* reach the new off-equilibrium fixed point, and the RG flow would simply go bonkers. Hence, not only the symmetry-breaking coupling  $\tilde{u}_\kappa^*$  is necessary *at* equilibrium, but it is also necessary to accompany the RG flow to the off-equilibrium fixed point; only there,  $\tilde{u}_\kappa^*$  is finally allowed to vanish. Clearly, this phenomenon deserves a deeper study.

## II. ASSESSING THE RELEVANCE OF ACTIVITY IN NATURAL SWARMS

In systems of active individuals interacting via local alignment there are two distinct mechanisms allowing propagation of directional information through the group. The first consists in passing the information from neighbour to neighbour via local interaction links: this mechanism would be present even at equilibrium, i.e. for a Heisenberg model on a fixed network. The second is due to the individuals' movement, which carry the information along with their motion causing a rearrangement of the interaction network in time: this second (activity-related) mechanism would be absent in standard ferromagnets and it is a characteristic out-of-equilibrium feature. A quantitative way to assess the role of activity in determining the relaxation properties of the system is therefore to compare the typical timescales related to the rearrangement of the interaction network and the relaxation of directional observables. In order to do so, we consider the following two correlation functions.

To characterize the dynamical evolution of the network we define the network overlap function  $C_{\text{net}}(r, t)$  as

$$C_{\text{net}}(r, t) = \frac{1}{N} \sum_i \left\langle \frac{1}{n_i(t_0)} \sum_j n_{ij}(t_0) n_{ij}(t_0 + t) \right\rangle_{t_0}, \quad (216)$$

where the *connectivity* matrix  $n_{ij}(t)$  is equal to 1 if the two individuals  $i$  and  $j$  are at mutual distance  $r_{ij} < r$  at time  $t$  and zero otherwise,  $n_i(t_0)$  represents the global number of neighbors in a region of size  $r$  around individual  $i$  at time  $t_0$ , and  $\langle \dots \rangle_{t_0}$  represents a time average over  $t_0$ . The function  $C_{\text{net}}(r, t)$  measures how much on average a neighborhood of size  $r$  of a given individual remains the same in a time interval  $t$ . For systems with a metric interaction - like swarms are [24] - if we set  $r$  equal to the interaction range  $r_c$ , then  $C_{\text{net}}(r_c, t)$  measures the reshuffling of the interaction neighborhood (i.e. how many individuals interacting at time  $t_0$  are still interacting at time  $t_0 + t$ ).

To characterize the directional relaxation we consider the space-time correlation function of velocity fluctuations. In the context of the field theory described in the main text, this function would be given by the connected correlations of the field  $\psi(\mathbf{x}, t)$ . However, if we want to measure such quantity on real data, it is convenient to define it in terms of the individual velocities:

$$C(r, t) = \frac{1}{N(r)} \sum_{ij} \left\langle \frac{\delta \mathbf{v}_i(t_0)}{\sqrt{\sigma(t_0)}} \cdot \frac{\delta \mathbf{v}_j(t_0 + t)}{\sqrt{\sigma(t_0 + t)}} \delta(r_{ij}(t_0, t) - r) \right\rangle_{t_0}, \quad (217)$$

where  $\delta \mathbf{v}_i = \mathbf{v}_i - \mathbf{V}$  indicates the individual fluctuation with respect to the collective velocity of the swarm  $\mathbf{V}$  that takes into account global translation, rotation and dilation modes,  $\sigma = (1/N) \sum_i \delta \mathbf{v}_i^2$  is the variance,  $r_{ij}(t_0, t) = |\mathbf{x}_i(t_0) - \mathbf{x}_j(t_0 + t)|$  the mutual distance, and  $N(r)$  is the number of pairs at distance  $r$  (see [5] for details).

These two correlation functions can be easily computed on experimental data of natural swarms and compared with each other. Ideally, one would like to compare these two curves on the scale of the interaction range, to check whether relaxation is affected by activity even locally. For natural swarms we estimated the interaction range to be of the order of a few cm [24]. However, since this information is not precise, we looked at scales ranging from  $r = 0.05m$  up to  $r = 0.15m$ . To have a better intuition of what these numbers mean, we note that  $r = 0.05$  corresponds to a neighbourhood of approximately 3 individuals, while  $r = 0.15$  to one of 41 individuals. To be more quantitative we also computed - for any given  $r$  - the characteristic timescale  $\tau$  of both functions. To do so, we used the method outlined by Halperin and Hohenberg in [9], which provides a reliable evaluation of  $\tau$  independently of the functional form of the correlation function.

In Fig.2 in the main text we display the behaviour of both  $C_{\text{net}}(r, t)$  and  $C(r, t)$  in a swarming event from our data-set. In panel a) we can see that for both the minimal and maximal values of  $r$  considered the correlations decay approximately on the same time-scale. In panel b) we show the behaviour of  $\tau$  - for the network and the velocity correlations - as a function of  $r$ : we can see that in the entire considered range the characteristic timescale is the same in the two cases. Remembering that the correlation functions quantify, respectively, how quickly the network changes on scale  $r$ , and how quickly directional correlations decay on the same scale, we can conclude that activity is always relevant and affects the relaxation properties of the system. We note that this behaviour is different from what is observed in natural flocks, where network rearrangements on the interaction scale occur on longer timescales than orientational relaxation, a situation defined as 'local equilibrium' [39].

Finally, we notice that the characteristic timescales discussed in this section to compare activity and relaxation are different from the relaxation time displayed in Fig.3 in the main text. In Fig.3 we indeed focus on collective relaxation: the timescale  $\tau$  in that figure quantifies the decay of the velocity correlation function on spatial scales of the order of the correlation length. We investigated these correlations in [5], where we showed that they obey dynamic scaling. Each point in the insets of Fig.3 corresponds to a different swarming event, with different correlation length and different relaxation time.

EVENT LABEL	$N$	DURATION (s)	$\tau(s)$	$\xi(cm)$	$r_1(cm)$
20110511_A2	279	0.88	0.12	12.3	5.33
20110906_A3	138	2.05	0.09	4.40	2.94
20110908_A1	119	4.41	0.11	4.30	3.59
20110909_A3	312	2.73	0.10	6.53	2.59
20110930_A1	173	5.88	0.47	11.9	5.72
20110930_A2	99	5.88	0.27	12.7	6.32
20111003_A1	89	5.58	0.14	6.05	7.74
20111006_A1	88	11.76	0.18	9.37	8.28
20111011_A1	131	5.88	0.23	14.9	7.52
20120702_A1	98	2.14	0.22	8.30	6.16
20120702_A2	111	7.29	0.14	7.88	5.57
20120702_A3	80	9.99	0.11	6.06	5.97
20120703_A2	167	4.41	0.09	5.93	4.65
20120704_A1	152	9.99	0.13	7.21	4.98
20120704_A2	154	5.29	0.13	7.34	5.32
20120705_A1	188	5.88	0.15	9.19	5.54
20120828_A1	89	6.29	0.11	7.75	6.18
20120907_A1	169	3.23	0.62	21.9	6.21
20120910_A1	219	1.76	0.24	10.6	4.68
20120917_A2	212	5.88	0.35	13.2	5.15
20120917_A3	554	4.12	0.28	13.4	4.40
20120918_A2	69	15.8	0.22	8.58	6.06
20120918_A3	215	5.00	0.31	12.0	5.04
20150729_A1	110	5.87	0.32	8.61	4.63
20150910_A2	99	2.99	0.15	7.56	4.61
20150921_A1	201	4.11	0.23	9.81	4.21
20150922_A1	94	5.87	0.19	8.98	6.04
20150922_A2	126	5.87	0.29	11.4	5.29
20150924_A1	115	5.87	0.30	12.2	4.81
20150924_A2	781	2.94	0.59	19.1	4.08
20150924_A3	232	3.23	0.41	16.2	5.55
20150924_A4	107	4.38	0.32	15.0	6.38
20151008_A2	92	3.51	0.27	10.1	5.33
20151008_A3	91	5.87	0.16	7.30	4.41
20151008_A4	87	3.29	0.21	13.6	8.63
20151026_A1	85	5.87	0.19	7.37	6.67
20151030_A1	274	5.87	0.27	9.34	3.96
20151030_A2	123	5.81	0.21	9.18	4.96

TABLE I. Summary of experimental data. Swarming events are labelled according to experimental date and acquisition number.  $N$  indicates the number of insects (and reconstructed trajectories) in the swarm,  $\tau$  is the relaxation time and  $\xi$  is the correlation length. The average nearest neighbour distance  $r_1$  is calculated by averaging over all individuals in the swarm, and over the event duration.

### III. FEYNMAN DIAGRAMS

#### A. Self Energies

##### 1. Self Energy $\Sigma$

The self energy  $\Sigma_{\alpha\beta}$  corrects the inverse bare propagator of  $\psi$ , and is given by

$$\hat{\psi}_\alpha(-\tilde{\mathbf{k}}) \longrightarrow \text{[shaded circle]} \longrightarrow \psi_\beta(\tilde{\mathbf{k}}) \quad (218)$$

with the following non-vanishing diagrams contributing to it

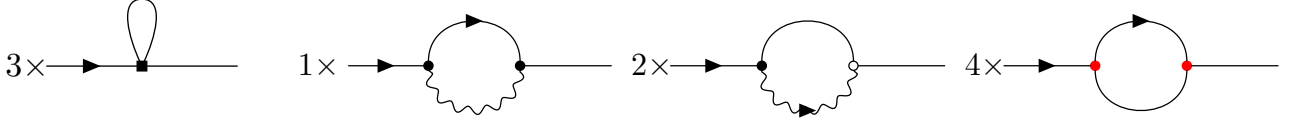


FIG. 7. Diagrams contributing to leading order of  $\Sigma$

##### 2. Self Energy $\Pi$

The self energy  $\Pi_{\alpha\beta\gamma\nu}$  corrects the inverse bare propagator of  $\mathbf{s}$ , and is given by

$$\hat{s}_{\alpha\beta}(-\tilde{\mathbf{k}}) \rightsquigarrow \text{[shaded circle]} \rightsquigarrow s_{\gamma\nu}(\tilde{\mathbf{k}}) \quad (219)$$

with the following non-vanishing diagrams contributing to it

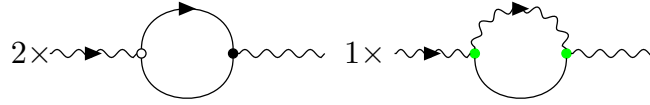


FIG. 8. Diagrams contributing to leading order of  $\Pi$

##### 3. Self Energy $\tilde{\Sigma}$

The self energy  $\tilde{\Sigma}_{\alpha\beta}$  corrects the noise variance of  $\psi$ , and is given by

$$\hat{\psi}_\alpha(-\tilde{\mathbf{k}}) \longrightarrow \text{[shaded circle]} \longleftarrow \hat{\psi}_\beta(\tilde{\mathbf{k}}) \quad (220)$$

with the following non-vanishing diagram contributing to it

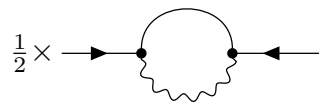


FIG. 9. Diagram contributing to leading order of  $\tilde{\Sigma}$



## B. Vertex functions

### 1. Vertex function of the Mode-Coupling vertex of $\psi$

The vertex function  $V^{\hat{\psi}\psi s}$  represents the corrections to the mode-coupling vertex in the equation of  $\psi$  and is given by

$$V_{\alpha\beta\gamma\nu}^{\hat{\psi}\psi s}(\tilde{\mathbf{k}}, \tilde{\mathbf{q}}) = \hat{\psi}_\alpha(-\tilde{\mathbf{k}}) \rightarrow \text{Diagram} \begin{matrix} \psi_\beta(\tilde{\mathbf{k}} - \tilde{\mathbf{q}}) \\ \downarrow \\ \text{Vertex} \\ \uparrow \\ s_{\gamma\nu}(\tilde{\mathbf{q}}) \end{matrix} \quad (222)$$

with the following non-vanishing diagram contributing to it

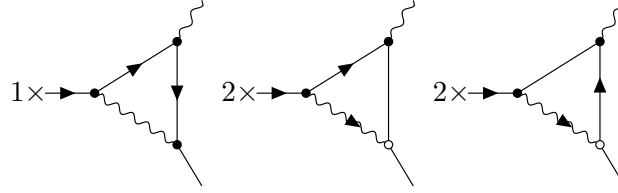


FIG. 11. Diagrams contributing to leading order of  $V^{\hat{\psi}\psi s}$



3. Vertex function of the advection vertex of  $\psi$

The vertex function  $V^{\hat{\psi}\psi\psi}$  represents the corrections to the advection vertex in the equation of  $\psi$ , and is given by

$$V_{\alpha\beta\gamma}^{\hat{\psi}\psi\psi}(\tilde{\mathbf{k}}, \tilde{\mathbf{q}}) = \hat{\psi}_\alpha(-\tilde{\mathbf{k}}) \rightarrow \text{Diagram} \begin{matrix} \psi_\beta(\tilde{\mathbf{q}}) \\ \psi_\gamma(\tilde{\mathbf{k}} - \tilde{\mathbf{q}}) \end{matrix} \quad (224)$$

with the following non-vanishing diagram contributing to it

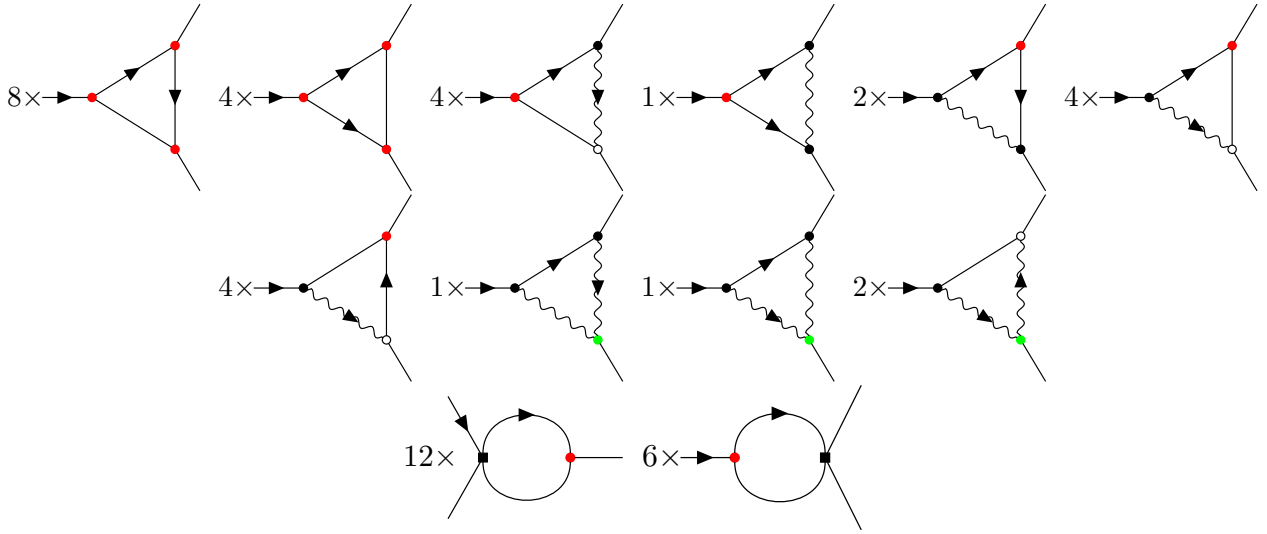


FIG. 13. Diagrams contributing to leading order of  $V^{\hat{\psi}\psi\psi}$



5. Vertex function of the ferromagnetic vertex of  $\psi$ 

The vertex function  $V^{\hat{\psi}\psi\psi\psi}$  represents the corrections to the ferromagnetic vertex in the equation of  $\psi$ , and is given by

$$V_{\alpha\beta\gamma\nu}^{\hat{\psi}\psi\psi\psi}(\tilde{\mathbf{k}}, \tilde{\mathbf{q}}, \tilde{\mathbf{h}}) = \hat{\psi}_\alpha(-\tilde{\mathbf{k}}) \rightarrow \text{diagram} \begin{matrix} \psi_\beta(\tilde{\mathbf{q}}) \\ \psi_\gamma(\tilde{\mathbf{h}}) \\ \psi_\gamma(\tilde{\mathbf{k}} - \tilde{\mathbf{q}} - \tilde{\mathbf{h}}) \end{matrix} \quad (226)$$

with the following non-vanishing diagram contributing to it

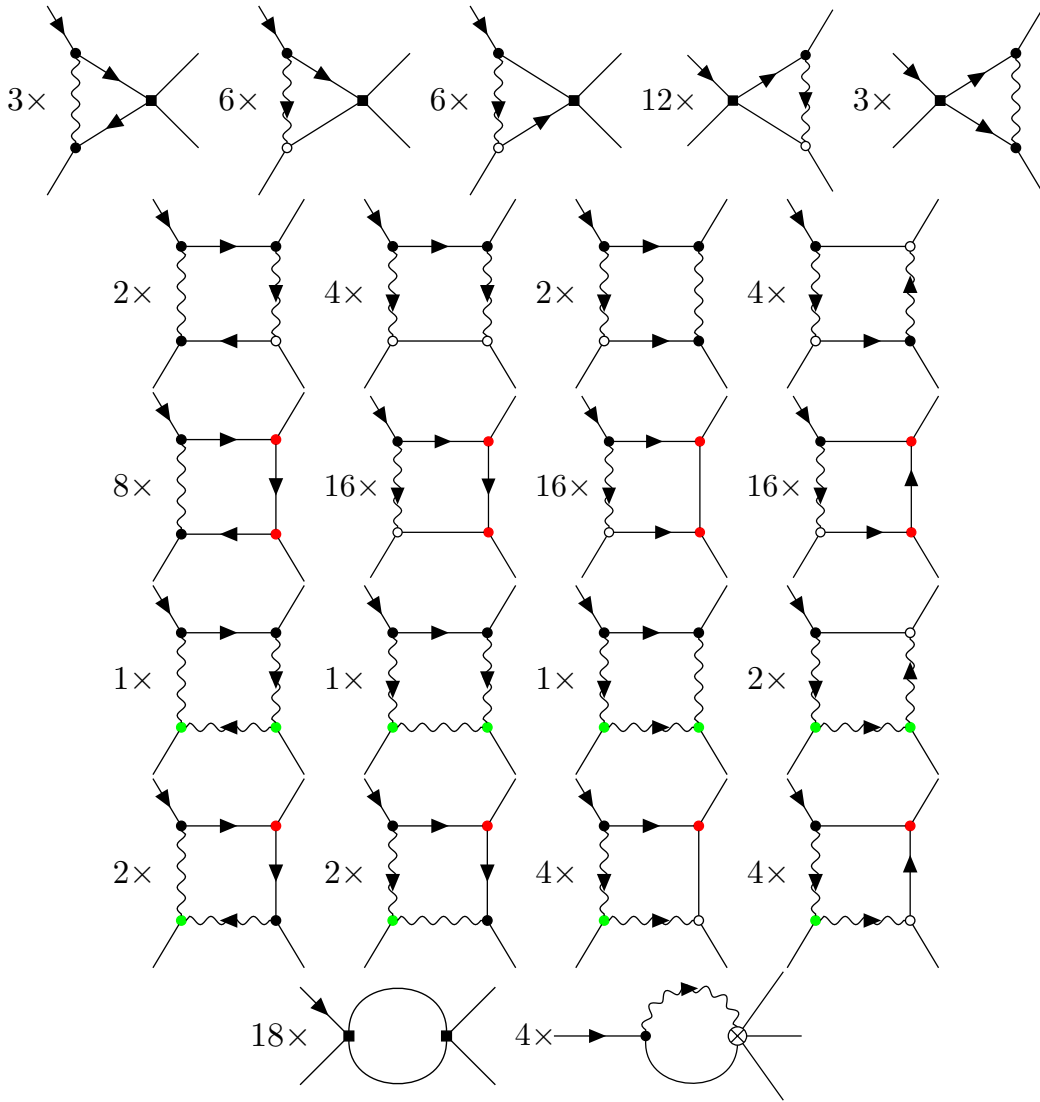


FIG. 15. Diagrams contributing to leading order of  $V^{\hat{\psi}\psi\psi\psi}$

6. Vertex function of the DYS vertex of  $s$ 

The vertex function  $V^{\hat{s}\psi\psi\psi\psi}$  represents the corrections to the DYS vertex in the equation of  $s$ , and is given by

$$V_{\alpha\beta\gamma\nu\sigma\tau}^{\hat{s}\psi\psi\psi\psi}(\tilde{\mathbf{k}}, \tilde{\mathbf{q}}, \tilde{\mathbf{h}}, \tilde{\mathbf{p}}) = \hat{s}_{\alpha\beta}(-\tilde{\mathbf{k}}) \begin{array}{c} \psi_\gamma(\tilde{\mathbf{q}}) \\ \psi_\nu(\tilde{\mathbf{h}}) \\ \psi_\sigma(\tilde{\mathbf{p}}) \\ \psi_\tau(\tilde{\mathbf{k}} - \tilde{\mathbf{q}} - \tilde{\mathbf{h}} - \tilde{\mathbf{p}}) \end{array} \quad (227)$$

with the following non-vanishing diagram contributing to it

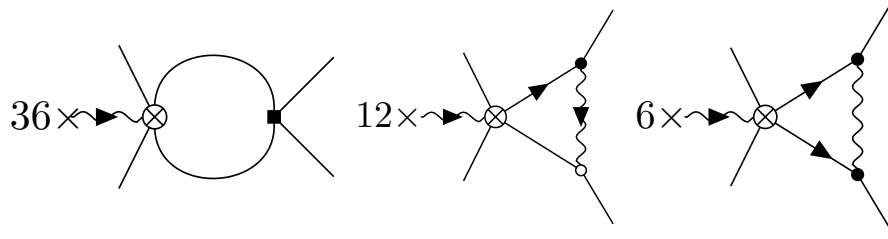


FIG. 16. Diagrams contributing to leading order of  $V^{\hat{s}\psi\psi\psi\psi}$

- 
- [1] J. Toner and Y. Tu, Phys. Rev. Lett. **75**, 4326 (1995).
  - [2] L. Chen, J. Toner, and C. F. Lee, New Journal of Physics **17**, 042002 (2015).
  - [3] A. Cavagna, L. Di Carlo, I. Giardina, T. S. Grigera, and G. Pisezna, Phys. Rev. Research **3**, 013210 (2021).
  - [4] A. Attanasi, A. Cavagna, L. Del Castello, I. Giardina, T. S. Grigera, A. Jelić, S. Melillo, L. Parisi, O. Pohl, E. Shen, and M. Viale, Nature Physics **10**, 691 (2014).
  - [5] A. Cavagna, D. Conti, C. Creato, L. Del Castello, I. Giardina, T. S. Grigera, S. Melillo, L. Parisi, and M. Viale, Nature Physics **13**, 914 (2017).
  - [6] A. Cavagna, L. Del Castello, I. Giardina, T. Grigera, A. Jelic, S. Melillo, T. Mora, L. Parisi, E. Silvestri, M. Viale, *et al.*, Journal of Statistical Physics **158**, 601 (2015).
  - [7] T. Vicsek, A. Czirók, E. Ben-Jacob, I. Cohen, and O. Shochet, Phys. Rev. Lett. **75**, 1226 (1995).
  - [8] A. Cavagna, I. Giardina, and T. S. Grigera, Physics Reports **728**, 1 (2018).
  - [9] P. C. Hohenberg and B. I. Halperin, Rev. Mod. Phys. **49**, 435 (1977).
  - [10] A. Cavagna, L. Di Carlo, I. Giardina, L. Grandinetti, T. S. Grigera, and G. Pisezna, Phys. Rev. Lett. **123**, 268001 (2019).
  - [11] A. Cavagna, L. Di Carlo, I. Giardina, L. Grandinetti, T. S. Grigera, and G. Pisezna, Phys. Rev. E **100**, 062130 (2019).
  - [12] A. Cavagna, L. D. Carlo, I. Giardina, T. Grigera, G. Pisezna, and M. Scandolo, arXiv:2103.10914 (2021).
  - [13] J. Toner and Y. Tu, Phys. Rev. E **58**, 4828 (1998).
  - [14] L. Sasvári, F. Schwabl, and P. Szépfalusy, Physica A: Statistical Mechanics and its Applications **81**, 108 (1975).
  - [15] L. Sasvári and P. Szépfalusy, Physica A: Statistical Mechanics and its Applications **87**, 1 (1977).
  - [16] H. Mori, H. Fujisaka, and H. Shigematsu, Progress of Theoretical Physics **51**, 109 (1974).
  - [17] R. Zwanzig, Phys. Rev. **124**, 983 (1961).
  - [18] C. De Dominicis and L. Peliti, Phys. Rev. B **18**, 353 (1978).
  - [19] X. Yang and M. C. Marchetti, Physical Review Letters **115**, 258101 (2015).
  - [20] D. Forster, D. R. Nelson, and M. J. Stephen, Phys. Rev. A **16**, 732 (1977).
  - [21] H. Chaté, F. Ginelli, G. Grégoire, and F. Raynaud, Phys. Rev. E **77**, 046113 (2008).
  - [22] G. Grégoire and H. Chaté, Physical review letters **92**, 025702 (2004).
  - [23] E. Bertin, M. Droz, and G. Grégoire, Phys. Rev. E **74**, 022101 (2006).
  - [24] A. Attanasi, A. Cavagna, L. Del Castello, I. Giardina, S. Melillo, L. Parisi, O. Pohl, B. Rossaro, E. Shen, E. Silvestri, and M. Viale, PLOS Computational Biology **10**, 1 (2014).
  - [25] P. C. Martin, E. Siggia, and H. Rose, Physical Review A **8**, 423 (1973).
  - [26] H.-K. Janssen, Zeitschrift für Physik B Condensed Matter **23**, 377 (1976).

- [27] De Dominicis, C., J. Phys. Colloques **37**, C1 (1976).
- [28] K. G. Wilson, Phys. Rev. B **4**, 3174 (1971).
- [29] N. Goldenfeld, *Lectures on Phase Transitions and the Renormalization Group* (Perseus Books, Reading, Massachusetts, 1992).
- [30] G. Parisi, *Statistical field theory*, Frontiers in Physics (Addison-Wesley, Redwood City, CA, 1988).
- [31] K. G. Wilson and J. Kogut, Physics Reports **12**, 75 (1974).
- [32] J. Cardy, *Scaling and renormalization in statistical physics* (Cambridge university press, 1996).
- [33] K. G. Wilson and M. E. Fisher, Phys. Rev. Lett. **28**, 240 (1972).
- [34] B. Widom, The Journal of Chemical Physics **43**, 3898 (1965).
- [35] L. P. Kadanoff, Physics Physique Fizika **2**, 263 (1966).
- [36] R. A. Ferrell, N. Menyh ard, H. Schmidt, F. Schwabl, and P. Sz epfalusy, Phys. Rev. Lett. **18**, 891 (1967).
- [37] B. I. Halperin and P. C. Hohenberg, Phys. Rev. Lett. **19**, 700 (1967).
- [38] J. J. Binney, N. J. Dowrick, A. J. Fisher, and M. E. Newman, *The theory of critical phenomena: an introduction to the renormalization group* (Oxford University Press, 1992).
- [39] T. Mora, A. M. Walczak, L. Del Castello, F. Ginelli, S. Melillo, L. Parisi, M. Viale, A. Cavagna, and I. Giardina, Nature Physics **12**, 1153 (2016).